Aus der Medizinischen Klinik und Poliklinik IV der Ludwig-Maximilians-Universität München

Direktor: Prof. Dr. med. Martin Reincke

Molecular Mechanisms of Crystal-Induced Neutrophil Cell Death

Dissertation

zum Erwerb des Doktorgrades der Humanbiologie

an der Medizinischen Fakultät der

Ludwig-Maximilians-Universität München

vorgelegt von

Jyaysi Bhagirath Desai

aus Ahmedabad, Indien

2017

Mit Genehmigung der Medizinischen Fakultät

der Ludwig-Maximilians-Universität München

Berichterstatter   : Prof. Dr. med. Hans-Joachim Anders

Mitberichterstatter   : Prof. Dr. Kirsten Lauber

Mitberichterstatter   : Priv.-Ooz. Dr. rer. nat. Gerald Schmid

Dekan   : Prof. Dr. med. dent. Reinhard Hickel

Tag der mündlichen Prüfung   : 25.04.2017

પ્રિય ભગીરથ દેસાઈ, મીલ્કા દેસાઈ અને ભુયસી દેસાઈ માટે ...

For my beloved parents and sister

Bhagirath Desai, Milka Desai & Bhuyasi Desai

TABLE OF CONTENTS

Declaration

I hereby declare that all of the present work embodied in this thesis was carried out by me from 06/2013 until 08/2016 under the supervision of Prof. Dr. Hans Joachim Anders, Nephrologisches Zentrum, Medizinische Klinik und Poliklinik IV, Innenstadt Klinikum der Universität München. This work has not been submitted in part or full to any other university or institute for any degree or diploma.

Part of the work was done by others, as mentioned below:

1. Professor Helen Liapis, Department of Pathology and Immunology,Washington University School of Medicine, Saint Louis, Missouri, USA has performed the scanning electron microscopy. The data are presented in results part I.

2. Dr. Bastian Popper, Department of Anatomy and Cell Biology, Ludwig-Maximilians Universität, Munich, Germany has performed the transmission electron microscopy. The data are presented in results part I, part II and Part III.

Part of the work has been published in *Eur J Immunol. 2016 Jan;46(1):223-9.*

Part of the work is published as a review in *Cell Mol Life Sci. 2016 Jun;73(11-12):2211-9.*

Part of the work has been published for publication in *Nat Commun. 2016 Jan 28;7:10274.*

Part of the work is published as a review in *Semin Nephrol. 2016 May;36(3):162-73.*

Part of the work is submitted for a patent at the *European patent office. EU prov. patent appl. 14192043.9-1412, 06.11.2014.*

Date: …………… Signature: ……………..

Place: Munich, Germany (Jyaysi Bhagirath Desai)

Zusammenfassung

Sowohl verschiedene Kristalle als auch feste Nano- und Mikropartikel verursachen viele akute und chronische physiologische Störungen (Kristallopathien) wie Gicht, Pseudogicht, Atherosklerose, Silikose, Asbestose, Rhabdomyolyse, verschiedene Formen kristalliner Nephropathie, sowie Nephro-/Urolithiasis. Die meisten Kristall-induzierten Schädigungen gehen oft mit einer starken Entzündungsreaktion einher. Zusammen mit der Entzündung verursachen Kristalle auch Zelltod; die genauen molekularen Mechanismen der kristallinen Zelltoxizität sind aber bisher noch ungeklärt. Wir untersuchten den Kristall-induzierten Zelltod von Neutrophilen Granulozyten. Dabei beobachteten wir das viele verschiedene Kristalle wie z.B. Calcium Oxalat (CaOx), Mononatrium-Urat (MSU), Calciumphosphat (CaP), Calciumpyrophsphat-Dihydrat (CPPD), Cystein, Cholesterol, Alaun, Asbest, Siliziumdioxid und Titan-Dioxid (TiO2)-Nanopartikel Neutrophil Extracellular Trap (NET) Formation und den damit verbundenen Zelltod der Neutrophilen, der NETose genannt wird, induzieren. Der genaue molekulare Mechanismus, der die NET-Formation verursacht, ist allerdings noch nicht bekannt.

Nekrose wurde traditionell immer als nicht programmierter Zelltod angesehen, dem überhaupt keine biochemischen Mechanismen zugrunde liegen. Im Zusammenhang mit nekrotischem Zelltod wurden jedoch mittlerweile viele verschiedene biochemische Signalwege entdeckt die unter dem Begriff der regulierten Nekrose zusammengefasst sind. Deswegen gingen wir in unserer Hypothese davon aus dass NETose nur eine andere Art Zelltod mit bestimmten molekularen Mechansimen sein könnte. Wir fanden heraus dass MSU-Kristall-induzierter Zelltod von Neutrophilen die Signalkaskade der receptor-interacting protein kinase (RIPK) 1-RIPK3-MLKL vermittelten Nekroptose auslöst. Außerdem konnten wir zeigen, dass die RIPK-1-Stabilisatoren Necrostatin-1 oder Necrostatin-1s und der MLKL-Inhibitor Necrosulfamid die NET-Formation von menschlichen und murinen Neutrophilen bei der MSU- oder PMA-induzierten Produktion von reaktiven Sauerstoffspezies (ROS) verhindern konnten. Diese Präparate haben jedoch keinen Einfluss auf die MSU- oder PMA-induzierte Produktion von reaktiven Sauerstoffspezies (ROS). Desweiteren konnte bei Neutrophilen von Patienten mit septischer Granulomatose (CGD) ein Mangel an PMA-induzierter MLKL-Phosphorylierung gezeigt werden. Ferner verhinderte der genetisch bedingte Mangel von RIPK3 bei Mäusen die MSU-induzierte NET-Formation *in vitro* und *in vivo*. Folglich könnten bei der NET-Formation und dem Zelltod der Neutrophilen der ROS-induzierte Signalweg der Nekroptose beteiligt sein.

Außerdem beobachteten wir dass die Kristalle von CaOx, MSU, CPPD und Cystein *in vitro* bei verschiedenen Nicht-Immunzelltypen, wie z.B. murinen und humanen Tubulusepithelzellen, humanen Nieren-Progenitorzellen, murinen embryonalen Fibroblasten und humanen synovialen Fibroblasten, eine caspase-unabhängige Form des Zelltods verursachen, die aber durch den RIPK1-Stabilisator Necrostatin-1 inhibiert wurde. Zusammengefasst zeigen diese Daten, dass RIPK1, RIPK3 und MLKL neue therapeutische Ziele bei der Therapie von Gicht und anderen Kristallopathien darstellen könnten.

Summary

Various crystals as well as solid nano- and micro- particles cause injury in a wide range of acute and chronic physiological disorders (crystallopathies) including gout, pseudogout, atherosclerosis, silicosis, asbestosis, rhabdomyolysis, and diverse forms of crystalline nephropathy or nephro-/urolithiasis. Most of the crystal-induced injuries are associated with strong inflammatory responses. Together with inflammation, crystals also induce cell death; however the molecular mechanisms of crystal cytotoxicity remain elusive till date. We studied the crystal induced cell death in neutrophils. We observed that a wide range of crystals e.g. calcium oxalate (CaOx), monosodium urate (MSU), calcium phosphate (CaP), calcium pyrophosphate dihydrate (CPPD), cysteine, cholesterol, alum, asbestos, silica and titanium dioxide (TiO_2) nanoparticles (20nm and 80nm) induce Neutrophil Extracellular Trap (NET) formation, and associated neutrophil cell death that is referred to as NETosis. However, the outside-in signaling pathway triggering NET formation is yet unknown.

Traditionally, necrosis was always considered a non-programmed cell death, which does not involve any biochemical signaling mechanism. However, meanwhile many biochemical pathways have been discovered to be associated with necrotic cell death, known as regulated necrosis. Therefore, we hypothesized that NETosis might be just another form of cell death involving distinct molecular mechanism. We found that MSU crystal-induced neutrophil cell death triggers the signaling cascade of regulated necrosis pathway of receptor-interacting protein kinase (RIPK) 1-RIPK3- MLKL mediated necroptosis. We show that the (RIPK)-1-stabilizers necrostatin-1 or necrostatin-1s and the MLKL-inhibitor necrosulfonamide prevent MSU- or PMA-induced NET formation in human and mouse neutrophils. These compounds do not affect MSU- or PMA-induced production of reactive oxygen species (ROS). Moreover, neutrophils of chronic granulomatous disease (CGD) patients are shown to lack PMA-induced MLKL phosphorylation. Further, genetic deficiency of RIPK3 in mice prevented MSU-induced NET formation *in vitro* and *in vivo*. Thus, NET formation and neutrophil death may involve the signaling pathway defining necroptosis downstream of ROS production.

Furthermore, we found that crystals of CaOx, MSU, CPPD, and cystine trigger a caspase-independent cell death *in vitro* in different non-immune cell types e.g. mouse and human tubular epithelial cells, human renal progenitor cells types, mouse embryonic fibroblasts (L929) as well as human synovial fibroblasts, which was inhibited by a RIPK1 stabilizer necrostatin-1. Taken together, these data imply that RIPK1, RIPK3, and MLKL may represent novel molecular targets in gout or other crystallopathies.

1. Introduction

1.1 Crystallopathies

Crystals as well as crystal-like solid nano- and microparticles (for simplicity referred to as crystals) cause diverse acute and chronic medical disorders, which have not been considered a common disease entity (figure 1)[1]. These crystals interact with different cell types in the physiological setting, leading to specific pathophysiological mechanisms that lead to a disease condition. Crystals can form from intrinsic sources or enter the body from outside. Crystallization inside the body mostly involves local supersaturation of minerals, dietary metabolites or drug overdose. Such crystal deposits often affect excretory organs such as the biliary and urinary tract where concentration and supersaturation is a common initiator of the crystallization process and stone formation (Table 1). Also, endogenous proteins can undergo self-assembly to polycrystalline structures. The process of beta-sheet fibrils self-perpetuating fibrillation to plaque-like amyloid deposits in amyloidosis or Alzheimer disease resembles mineral crystallization around a nucleus. Particulate matter that enters the body from the outside mostly include occupational, environmental or cigarette smoking-related dust, mainly affect the lungs. Other sources of extrinsic particles are metallic, plastic or silicone implants, cosmetics or nanocarriers used for drugs. All of these can evoke similar responses as crystals. Particle size is a critical determinant of the tissue response. Macrophages and other phagocytes are usually the first to engulf particles for phagocytosis, which is possible for nanoparticles and microparticles of few micrometers in diameter. Phagosomes fuse with lysosomes that contain numerous lytic proteases. The inability of phagolysosomes to digest the nano- or microparticle cargo induces cell stress, autophagy, and eventually leakage of lysosomal content into the cytoplasm. Crystal needles and other larger particles that exceed the size of macrophages may induce giant cell formation as a way to internalize larger particles[2]. Calculi and implants of a much larger size are subjects of frustrated phagocytosis. Various crystal or crystal-like particle related diseases are listed in Table 1.

Table 1: Crystal- or crystal-like particulate-related diseases

Crystal/particle	Disorder	Major disease manifestation
Intrinsic inorganic crystals		
Brushite	Nephro-/urolithiasis	Renal colic
Ca^{++} carbonate	Cholecysto-/docholithiasis	Biliary colic
	Nephro-/urolithiasis	Renal colic
Ca^{++} oxalate	Nephro-/urolithiasis	Renal colic
	Acute oxalate nephropathy	Acute kidney injury
	Polyethelene glycol poisoning	Acute kidney injury
	Dietary oxalosis: Black tea, star fruit, rhubarb, vitamin C, nuts, …	Acute kidney injury, renal colic
	Bariatric surgery-/short bowl-related	Acute kidney injury, renal colic
	Chronic oxalate nephropathy	Chronic kidney disease
	Primary hyperoxaluria	CKD, organ oxalosis
Ca^{++}pyrophosphate /Ca^{++}phosphate	Pseudogout, chondrocalcinosis, hemochromatosis, hyperparathyroidism	Acute monarthritis, periarthritis, bursitis
	Vascular calcification, calciphylaxis	Tissue ischemia, ischemic necrosis
	Warfarin calcification	Tissue ischemia, ischemic necrosis
	Dent`s disease, Nephrocalcinosis	Chronic kidney disease
Intrinsic organic crystals or microparticles		
Adenine	Adenine phosphoribosyl transferase deficiency	Nephro-/urolithiasis, renal colic, chronic kidney disease
Amyloid	Amyloid-β in Alzheimer disease	Dementia
	Amylin in diabetes	Hyperglycemia
Bile pigment	Cholecysto-/docholithiasis	Biliary colic, pancreatitis
	Bile cast nephropathy	Acute kidney injury
Cholesterol	Atherosclerosis	Tissue ischemia, ischemic necrosis
	Cholesterol embolism	Ischemic necrosis
	Nonalcoholic steatohepatitis	Acute lipotoxic liver disease
	Cholesteryl ester storage disease	Chronic lipotoxic live disease
	Cholesterol granuloma	Bone lesions
	Cholecysto-/docholithiasis	Biliary colic
Cystine	Cystinosis	CKD, urolithiasis, extrarenal

Light chains	Myeloma cast nephropathy	Acute kidney injury
	Crystalloglobulinemia	Thrombotic microangiopathy
	Light chain Fanconi syndrome	Renal tubulopathy, CKD
	Crystal-storing histiocytosis	Renal tubulopathy, CKD
	Fibrillary glomerulonephritis	Proteinuria, CKD
	Immunotactoid glomerulopathy	Proteinuria, CKD
Monosodium urate	Gout	Acute monarthritis, bursitis
		Chronic tophous gout
	Nephro-/urolithiasis	Renal colic
	Urate nephropathy	Acute kidney injury
Myoglobin	Myoglobin cast nephropathy	Acute kidney injury
Fibrillar α-synuclein	Parkinson disease	Motor symptoms (parkinsonism)
Uromodulin	Cast nephropathies	Acute kidney injury
Extrinsic crystals or particulates		
Asbestos	Lung asbestosis, malignancy	Pulmonary fibrosis, mesothelioma
Drugs: Aciclovir,MTX, Indinavir,sulfadiazine	Drug-related kidney injury	Acute kidney injury, renal colic
Hemozoin	Malaria	Hemolysis, SIRS
Implants, implant debris particles	Implant-related injury	Monarthritis, aseptic osteolysis, foreign body reactions
Occupational dusts: silica, asbestos, cotton, charcoal…	Acute dust-induced lung injury Pneumoconiosis (silicosis, asbestosis, anthracosis, …)	Dust-induced respiratory failure Lung fibrosis
Tobacco smoke particulates	Smoking-related COPD, emphysema	Chronic respiratory distress
Air pollutants	Smog-related asthma, pneumonitis, COPD	Acute respiratory distress

Ca^{++}: calcium, CKD: chronic kidney disease, SIRS: systemic inflammatory response syndrome, COPD: chronic obstructive pulmonary disease. Adapted from *Mulay et. al.* 2016[1]

1.2 Gouty arthritis

Gout is one of the most relevant crystallopathies. It is one of the most severe and frequent inflammatory rheumatic diseases. The pathology and symptoms visceral and chronic gout are less well-defined[3] as gout is most commonly presented as acute episodic arthritis event. Gouty arthritis, like all other clinical manifestations of gout, is triggered by the formation of needle-shaped MSU crystals. Due to the physiological conditions of uric acid overload either from excess oral uptake or massive cellular release of uric acid or from an impaired renal uric acid, MSU crystals are formed and deposited within joints. The final product of purine metabolism, uric acid when in excess, circulates as urate anion and combines with sodium ions to make MSU. Though hyperuricemia is one of the most important factors of gout onset, other factors such as temperature, pH, mechanical stress, cartilage components, and other synovial and serum factors may also contribute to the pathophysiological mechanisms[3,4]. MSU crystals are deposited in the form of tophi. Tophi resemble granulomas and cause trafficking of immune cells such as neutrophils, consistent with a role of inflammation in promoting tophus formation and remodeling[5]. These tophi usually develop in osteoarthritic toes and hand joints, suggesting a role of trauma, altered hydration (swelling), and connective tissue matrix structure and turnover.

1.2.1 Onset and peak of acute gouty arthritis

Gouty arthritis is characterized by a sudden onset within 2-4 hours that starts often during nighttime so that the patient wakes up with a painful joint early in the morning. The classical feature of gouty arthritis is an excruciating pain with articular and periarticular swelling and heat. When smaller joints are affected also redness may occur. Formation of MSU crystals is considered as an onset of gout that is followed by the massive infiltration of immune cells. The infiltrated neutrophils and monocytes ingest the MSU crystals at the site of tissue injury, which triggers a strong inflammatory response.

1.2.2 Spontaneous resolution of gouty arthritis

A characteristic feature of acute gout is its self-resolving nature after a few days. This spontaneous resolution suggests that the body turns on effective mechanisms to prevent an inflammatory response. Mechanisms that are involved in shutting down gouty arthritis, such

as negative regulators of toll-like receptor (TLR) and cytokine signaling, clearance of apoptotic cells and aggregated NETs are described in more detail below.

1.2.3 Pathophysiological mechanisms underlying gout onset and resolution

MSU crystals act as a danger signal and trigger an inflammatory cascade including the activation of the NLRP3 inflammasome and the subsequent release of active interleukin (IL)-1β via cleavage of pro-IL-1β[6]. Signaling for pro-IL-1β production occurs through pattern recognition receptors (PRRs) such as TLRs. These TLRs (e.g. lipopolysaccharide (LPS)) promote MyD88 signaling for the release of IL-1β by human mononuclear cells[7] [8] [9]. Evidence suggests that negative regulators of TLRs, cytokines, clearance of apoptotic cells and aggregated Neutrophil extracellular traps (NETs), contribute to the resolution of an acute gout attack. Inflammation induced via TLRs is a systemic and protective response to microbial pathogens or injury that needs to be fine-tuned and regulated, as uncontrolled inflammation can cause morbidity and mortality[10]. Negative regulators of TLR signaling have been identified to shut down inflammation. Soluble decoy TLRs (sTLRs) including sTLR-4 have the ability to extracellularly regulate TLR signaling by competing with TLR agonists, which leads to prevention of acute inflammatory responses[11]. A study reported that sTLR-4 inhibits nuclear factor (NF)-κB activation following LPS stimulation[12]. Pro-inflammatory cytokines are controlled by a number of other mechanisms including signal transducers and activators of transcription (STATs), cytokine inducible SH2-containing protein (CIS) and suppressors of cytokine signaling (SOCS)[13,14].

Data from an air pouch model of MSU crystal-induced inflammation indicated that both TLR2/4 and the ligand CD14 are involved in driving inflammation by mediating crystal uptake and pro-IL-1β priming[15]. IL-1β production and IL-1R signaling are crucial factors in driving the inflammatory response since mice deficient in the IL-1β or IL-1 receptor (IL-1R) showed MSU crystal-induced inflammation[6].

One classical mechanism involved in the resolution of acute gouty inflammation is the non-inflammatory phagocytosis of apoptotic neutrophils by macrophages[16,17]. The mechanism of apoptotic cell clearance by both macrophages and neutrophils has been linked to the production of transforming growth factor (TGF)β1[16,18]. In patients suffering from gout, TGFβ1 has been found in high levels in the synovial fluid during the resolution phase of acute inflammation[19] [20]. Furthermore, *in vitro* studies have shown that TGFβ1 can down regulate the expression of IL-1R on hemopoietic cells[21,22] suggesting a contribution of TGFβ1 during

gout resolution by limiting IL-1β signaling. IL-1R antagonist (IL-1Ra) as an endogenous mediator can function as a competitive inhibitor of IL-1R[23,24]. This is one of the mechanisms that the immune system uses to control IL-1β signaling. *In vitro* as well as *in vivo* data demonstrated that IL-1Ra has the ability to block the pro-inflammatory activities of IL-1 cytokines, indicating a regulatory role for IL-1Ra in acute inflammation[25][26][27]. Elevated levels of IL-1Ra have been found in the synovial fluid from acute gout patients with resolving inflammation, suggesting a link between the release of IL-1Ra and the shutdown of IL-1β signaling[13]. Numerous reports have demonstrated that TGFβ1 can induce the secretion of IL-1Ra by human circulating monocytes[28][29] as well as neutrophils[30] highlighting a role for IL-1Ra in the resolution of gouty arthritis that was further confirmed by a number of clinical trials showing that the recombinant IL-1Ra Anakinra is effective at relieving acute gout attacks[31,32][33].

Furthermore, to limit the *tumor necrosis factor* (TNF) α induced inflammatory response, gout patients produce a higher level of the soluble TNF receptors (sTNFR)-I/II as well as IL-10[13]. Indeed, *in vitro* and *in vivo* studies show that the extracellular release of soluble sTNFR-I/II can act to inhibit TNFα signaling by sequestering TNFα, whereas retrovirally transfected IL-10 blocks MSU crystal-induced inflammation, including suppression of TNFα production in a murine air pouch model[34]. Serum sIL-6R levels are also increased in gout patient. However, it is not clear whether sIL-6R is pro-inflammatory due to the ability to activate cells that do not express IL-6R via trans-signaling[35] or abrogates bone damage in chronic gout[36].

NETs released by activated neutrophils during the gout episode and MSU crystal-NETs aggregate play an important role in the resolution of a gout attack[37]. The biology of generation, biochemical nature and importance of neutrophils and NETs in gout and other diseases is discussed in detail in the following section.

1.3 Neutrophils

Neutrophils are important effector cells of the immune system[38]. They are also known as polymorphonuclear leukocytes (PMNs). Neutrophils are the first responders to any kind of bacterial or fungal infection and were historically considered the nonspecific pus forming white blood cells. They have a short lifespan of around 5.4 days during which they continue a process of maturation and senescence[39]. Until the late 20th century short lived neutrophils were often ignored as immune cells compared to other long-lived immune cells like

monocytes. It was believed that neutrophils were incapable of the 'more' important functions of the immune system like antigen presentation, significant protein synthesis that contributes to the production of important immune modulating factors[40]. However, the neutrophil research over the past two decades changed these classical views and neutrophils are now considered as important immune cells involved in host defense mechanisms with their unique characteristics of chemotaxis, phagocytosis and lastly forming NETs.

1.3.1 Neutrophil generation and circulation in blood stream

In the bone marrow, neutrophils are generated from granulocyte-committed progenitors called myeloblasts[41]. Myeloblasts differentiate into promyelocytes and myelocytes following the neutrophil lineage. The cell division is restricted following the differentiation to metamyelocyte state from myelocytes. Neutrophils mature after this stage and their nuclei become segmented. After 5-6 days of maturation of the last myelocytic division, neutrophils enter the blood circulation[42]. The migration of neutrophils into the blood stream is a chemokine-regulated process. The chemokine receptor CXCR2 is upregulated in young neutrophils. The higher amounts of CXCL1 and CXCL2 (ligands for CXCR2) in bone marrow direct the neutrophils towards the blood circulation. Under physiological circumstances, the life span of neutrophils in the circulation is 6-8 hours. Neutrophil senescence involves upregulation of CXCR4 facilitating homing back to the bone marrow and other organs, where neutrophils undergo apoptosis and phagocytic clearance by macrophages[43].

1.3.2 Neutrophil migration and chemotaxis

The neutrophil infiltration rate is increased in cases of infection or inflammation. Under inflammatory condition, cytokines such as G-CSF, IL-8, TNFα etc. or danger-associated molecular patterns (DAMPs) endorse the migration of neutrophils towards the site of infection[44]. Neutrophil recruitment follows four steps known as a) tethering; initiated by binding of P-selectin and E-selectin present on endothelial surface to their ligands like P-selectin glycoprotein ligand 1 (PSGL1) on neutrophil surface, followed by, b) rolling which is mediated by selectins followed by, c) crawling and d) transmigration, which depend on integrins[38]. Chemotaxis is a special mobility property of neutrophils. It is a process in which neutrophils get activated by specific chemoattractants that are released from the site of infection. These activated neutrophils sense a gradient of chemoattractants and migrate towards them[45].

1.3.3 Neutrophil phagocytosis

Neutrophils are the first immune cells reaching the site of infection and are the primary executors of rapid response against most of the fungal and bacterial infections. The recruited neutrophils engage with opsonized microbes by means of special receptors such as FcγRs and C-type lectin receptors[46]. This leads to the formation of a phagosome; a vacuole trapping the pathogens[47]. Apart from these receptors, neutrophils express wide ranges of other PRRs like TLRs, Nod-like receptors (NLRs) etc. that can recognize and interact with pathogens directly. This process of uptaking the pathogen is known as phagocytosis. Neutrophils are very efficient and rapid (less than 20s) phagocytes[48]. The phagocytosis process of neutrophils differs from that of macrophages, the well-known phagocytes. The phagosomes in neutrophils get rapidly fused with the neutrophil granules present in the cytoplasm. This process is regulated by cytosolic-free calcium in neutrophils to ensure efficient targeting and fusion of granules with phagosomes[49]. These granules contain hydrolytic enzymes as well as NADPH oxidases that initiate pathogen-killing mechanisms. The activation of NADPH oxidases leads to the oxidative burst and generation of reactive oxygen species (ROS) that can directly or indirectly kill the pathogens[50]. Patients of chronic granulomatous disease (CGD) are prone to infectious diseases as they lack one of the subunits of NADPH oxidase[40]. Thus, NADPH oxidase is a crucial player in host defense mechanisms of neutrophils. Uncontrolled release of neutrophil granular and oxidative products leads to tissue injury in a variety of infectious and inflammatory diseases[51].

1.3.4 Neutrophil extracellular traps (NETs)

Neutrophil phagocytosis was considered as one of the major functional ability of neutrophils until 2004. The laboratory of Professor A. Zychlinsky discovered a novel property of neutrophils in 2004 that opened a new horizon in neutrophil biology research[52]. Upon bacterial infections, neutrophils release their genetic material and form web like structures made up of chromatin fibers (15-17nm diameter) decorated with granular enzymes like neutrophil elastase (NE), myeloperoxidase (MPO), cathepsin G etc. (50nm). These structures were called NETs[52].
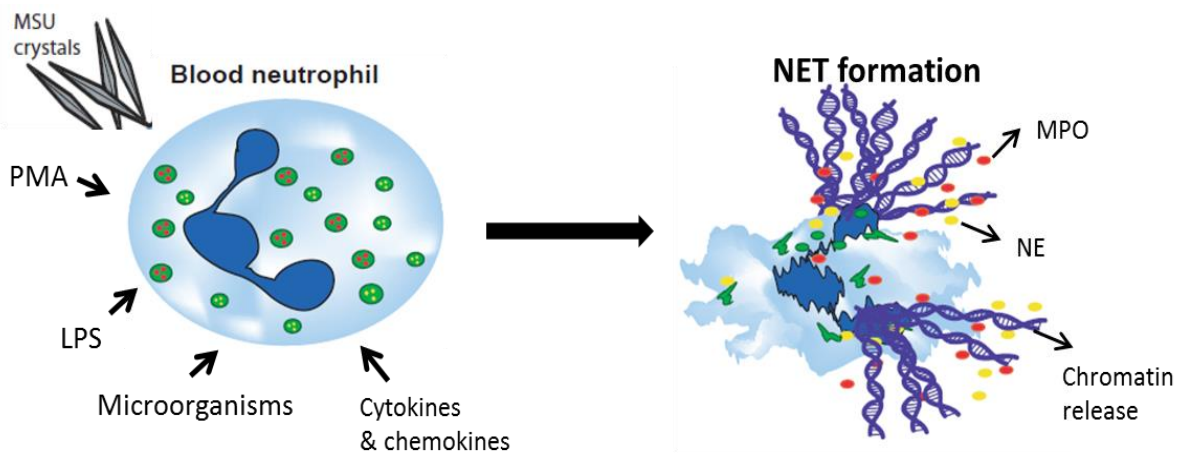
Figure 1: Induction of neutrophil extracellular traps. Neutrophils exclude their genetic material together with granular enzymes upon bacterial infection or in response to stimuli like micoorganisms, LPS, PMA, MSU crystals, cytokines or Chemokines. Adapted and modified from *Desai, et. al 2016*[53].

Over last decade, many laboratories have reported NETs in various bacterial, fungal, viral infections. In fact, extracellular trap formation is also reported in other cell types like eosinophils[54], monocytes/macrophages[55], mast cells[56] as well as in the wide range of organisms from plants to animals like mice, cattle, horses, fish, cats, rabbits, invertebrates and humans[57]. Thus, the chromatin extracellular traps on a general note are also called 'extracellular traps' (ETs)[58].

Various stimuli like phorbol myristate acetate (PMA), a wide range of bacterial pathogens (e.g. *E.coli, S.aureus* etc.), fungal pathogens (e.g. *C albicans, Aspergillus fumigatus*), LPS, complement c5a, different cytokines and chemokines like TNFα, IL-6 can induce NET formation *in vitro*. Schauer et.al recently showed that NETs can also be formed during non-infectious disease conditions like gout[37]. In this case, neutrophils rapidly form NETs because of MSU crystals accumulation within the joints. The mechanisms by which NETs are formed in response to various stimuli could be different. However, the literature is still in its primitive stage and the exact molecular pathways involved in NET formation processes remain unclear till date.

1.3.5 Signaling components in NET release

Morphologically, once activated neutrophils undergo several changes to release NETs. Neutrophils become flat and multiple lobes of the nucleus are lost within one hour after

activation. This is followed by chromatin decondensation together with the simultaneous disintegration of granules. Around two hours after stimulation *in vitro*, the plasma membrane has ruptured leading to the release of NETs in extra-cellular space[52]. Thus, NET-forming neutrophils die at the end of this process. This process of neutrophil cell death during NET formation is called 'NETosis'[59]. However, recent reports also suggest the possibility of neutrophils forming NETs without cell death[60]. Neutrophils in such cases release chromatin by forming specialized vacuoles, without plasma membrane rupture. Such NETs are named 'vital NETs' (which will be discussed later). Indeed, the literature is quite confusing when it comes to the signaling pathways that could be involved in NET formation procedures.

ROS generated during the phagocytic process plays a crucial role in NET formation. The process of NET release requires the activation of NADPH oxidase via the Raf-MEK-ERK pathway, ROS production, and upregulation of anti-apoptotic proteins[59,61]. Accordingly, neutrophils from humans or mice deficient in NADPH-oxidase cannot execute NET release[59,62,37]. But how do ROS exactly mediate NET formation? Several theories emerged to describe the involvement of ROS in "NETosis", e.g. through NE, MPO, and histone deimination etc. Upon activation of neutrophils, ROS triggers the MPO-dependent proteolytic activity of NE[63].

In the cytosol, NE degrades F-actin to arrest the actin dynamics of neutrophils before translocating to the nucleus where it degrades core histones e.g. H1 and then H4 and promotes chromatin decondensation[63,64]. MPO further synergizes with NE to induce chromatin decondensation independent of its enzymatic activity[64]. Accordingly, humans deficient in MPO as well as mice deficient in NE cannot form NETs[64,65]. However, the molecular mechanisms downstream to ROS production and upstream of NET formation are not clear. The reasons for the limited knowledge of NETs related biochemical pathways is the short life span of neutrophils, difficulties in studying NETosis *in vivo* as well as the inability to do genetic manipulations, and the lack of a neutrophil cell line that represent the physiology of primary neutrophils.

1.3.6 NETs in host defense mechanism

Entrapment by NETs. NETs can physically adhere to microbes to trap them. One possible mechanism of pathogen attachment to NETs could be the sticky nature of extracellular DNA molecules as well as electrostatic interactions. Pathogens like bacteria get trapped in NETs due to the electrostatic interactions between positively charged bacterial surfaces and negatively charged extracellular DNA present in NETs. Apart from these general

mechanisms, specifically surfactant protein D, a C-type lectin-receptor (CLR), is known to form an intermediary bridge between neutrophil and pathogen that is crucial for their binding.

Trapping bacteria. A wide range of bacteria including *Streptococcus pneumoniae*, *Staphylococcus aureus*, *Escherichia coli* are able to bind to extracellular DNA coming from NETs *in vitro*[66] [60]. There are several *in vivo* pieces of evidence of bacterial capture by NETs. For example entrapment of *Klebsiella pneumonia* in NETs during lung infection in mice is reported using an imaging approach[64]. Furthermore, intravital microscopy of liver revealed *E.coli* captured by NETs[67]. Several other laboratories have produced images of pathogen trapped in NETs using electron microscopy, immunofluorescence, spinning disc confocal microscopy as well as live-cell imaging approaches. In fact, the bacteria capture rate is increased by three to four folds after NET release independent of macrophage activities[60]. Several pathogens like *Streptococcus pyogenes, Pneumococcus* species, group A *Streptococcus* (GAS) and *Staphylococcus aureus* can synthesize endonucleases that are attached to their surfaces. These nucleases (e.g. DNase I) can cleave NETs made up of chromatin fibers and pathogens get released from the NETs[68]. Inhibiting DNase activity in infections from group A *Streptococcus* (GAS) significantly increases neutrophil-mediated pathogen clearance and reduces tissue necrosis. This could be a potential therapy for chronic diseases like sepsis.

Trapping Fungi. NETs together with phagocytosis play an important role in host defense mechanisms against fungal infections. Using similar imaging approaches of immunofluorescence, scanning electron microscopy (SEM) techniques as well as 2-photon microscopy, several laboratories have provided visual evidence of the entrapment of different fungal species like *Candida albicans, Aspergillus fumigatus* etc[69] [70].

Trapping Virus. Recent evidence suggests that apart from bacterial and fungal infections, viral infections can also be potent stimuli to release NETs from neutrophils[71]. The human immunodeficiency virus 1 (HIV-1) induces NETs *in vitro* via TLR7 and TLR8. Such studies have raised a tremendous interest in studying NETs, as they seem to have the capacity to capture a huge range of pathogens.

1.3.7 Killing mechanisms by NETs

After trapping and immobilizing pathogens, whether NETs can carry out direct pathogen killing functions or not is one of the most intriguing research question. The composition of NETs e.g. several granular proteases like NE, MPO, Cathepsin-G etc., antimicrobial peptides (the BPI protein and defensins), ion chelators (calgranulin), as well as

histones as a crucial component of the chromatin structure are well-known antimicrobial proteins[57]. Thus, it is likely that NETs can potentially carry out killing mechanisms by themselves in cases of different infections.

Microbial killing by NETs. Histones from NETs are shown to be one of the strongest bactericidal components that can kill a range of different bacteria[72]. Apart from histones, the granular enzyme NE, one of the important NET components, can inactivate virulence factors by catalyzing their splitting in different bacterial species like *Shigella flexneri*, *Salmonella typhimurium,* and *Yersinia enterocolitica*. NETs can also potentially kill *Pseudomonas* in suspension during cystic fibrosis disease[73]. Some of the NET components like MPO have the potential to carry out independent killing processes e.g. in *S. aureus* infection. However, other groups also have shown less or no significant killing by NETs upon *S. aureus* infection[74]. Several *in vitro* studies showed that PMA induced NETs could stop *C. albicans* and *Aspergillus* growth through calprotectin mediated zinc chelation[75]. However, the role of histone-mediated NET killing is debated during fungal infections[76]. Interestingly, HIV-1 virus-induced NETs could completely inactivate entrapped virions and this process was restricted by the addition of DNase leading to degradation of NETs[71].

Endothelium killing by NETs. Apart from pathogen killing mechanisms, several researchers have shown that NETs are involved in tissue injury in cases of sterile as well as non-sterile infections. LPS-activated platelets derived NETs can kill endothelial cells[67]. Especially extracellular histones coming from NETs can be cytotoxic for endothelial cells in several diseases like sepsis[77]. NETs in such cases can induce injury of the vasculature. Moreover, NETs are also important contributors to induce thrombosis as well as are associated with injury and inflammation in various autoimmune diseases like systemic lupus erythematosus (SLE) and anti-neutrophil cytoplasmic antibodies (ANCA) vasculitis. Various NET-associated diseases are discussed in detail in the following section.

1.3.8   NETs in autoimmune diseases

ANCA vasculitis and Systemic Lupus Erythematosus

Patients with an autoimmune disease or SLE possess increased levels of ANCAs, anti-nuclear antibodies against e.g. histones, DNA, and ribonucleoproteins[60]. NETs play a crucial role in the disease progression in these disorders. Infection-induced NETs are major resources

of extracellular histones and DNA, neutrophil enzymes and several antimicrobial peptides as primary antigenic components in SLE[78]. Furthermore, it is recently observed that the blood of SLE patients contains a population of low-density granulocytes, which can undergo rapid NET formation *ex vivo*[79]. Components like DNA that release from NETs activate plasmacytoid dendritic cells to secrete interferon (IFN)-α. IFN-α promotes auto reactivity and expands the SLE progression. As a positive loop, IFN-α primes neutrophils to release NETs, which can activate DCs[80]. This positive feedback loop plays an important role in the disease progression of SLE and ANCA vasculitis. Moroever, the SLE patient serum possesses elevated levels of DNase I activities, lower expression levels of DNase I inhibitors and high levels of autoantibodies that protect NETs from DNase degradation[78]. These patients may later develop kidney disorders like lupus nephritis or severe glomerulonephritis. Apart from therapies involving anti-IFN-α strategies, NETs are the potential therapeutic targets for the treatment of SLE and ANCA vasculitis[60].

Rheumatoid arthritis

Rheumatoid arthritis (RA) is a systematic autoimmune disease that primarily occurs in the synovial joints. NETs are a major inflammatory component of the disease and are primarily found in synovial fluids (SF) of joints, under the skin and in rheumatoid nodules during RA episodes[60]. NETs contain high levels of citrullinated proteins that can be adverse in RA because RA patients also have elevated levels of anti-citrullinated peptide antibodies (ACPAs) in SF[81]. Furthermore, ACPA containing SF can prime neutrophils from RA patients to induce NETs[81]. Thus, NETs play a crucial role in disease progression of RA. It is possible that within NET components, histones are the important molecules to undergo citrullination process and hence can be represented as an important source of citrullinated proteins in the joint of RA patients. In fact, RA patients exhibit increased levels of anti-PAD4 antibodies and PAD4 expression[82]. Thus, citrullinated histones may be a good diagnostic marker to study NETs in RA.

1.3.9 NETs in gout

Recent studies demonstrated that *in vitro* neutrophils form NETs following stimulation with MSU crystals, that was further confirmed after analysis of synovial fluid and tissue sections from patients suffering gout *in vivo*[83][84]. Neutrophils ingest MSU crystals leading to NETosis, whereby DNA is rapidly released into the extracellular space. The released DNA fragments form traps, which in turn cluster around MSU crystals to generate aggregated NETs

(aggNETs)[37]. These large DNA/MSU crystal structures, also known as gout tophi, can only form, when neutrophils are present in high numbers, usually at the later phase of a gout attack[85]. Functional studies have shown that aggNETs can degrade and inactivate pro-inflammatory cytokines, such as IL-1β, TNFα, IL-6, and the chemokine monocyte chemoattractant protein (MCP)-1 via neutrophil serine proteases[37]. It is known that NETosis and aggNETs are dependent on the oxidative burst in promoting inflammation and tissue damage[37]. In contrast, studies now suggest an anti-inflammatory function of ROS in facilitating the formation of aggNETs to trap and degrade inflammatory mediators in MSU crystal-induced inflammation[37] as well as other autoimmune diseases such as collagen-induced arthritis[86,87]. Moreover, human monocyte-derived macrophages from healthy volunteers efficiently ingest NETs via an immunologically silent process[88]. Together, these data underline the molecular process of aggNETs and the phagocytosis of NETs by macrophages as possible mechanisms in shutting down inflammation in gouty arthritis.

To summarize, NETs play a crucial role in most of these diseases as mentioned above. Whether neutrophils that form NETs also undergo cell death during this process is still largely unexplored.

1.4 Regulated cell death

Cell death is a crucial phenomenon in physiology to maintain the homeostasis and functionality of all tissues. To understand the mechanisms of cell death pathways has been one of the strong interests of molecular biologists and biochemists for a long time. Several biochemical pathways are now known to regulate cell death modes in different cell types in different diseases as well as under normal conditions. Typically, the cell death modes are classified in two categories: 1) programmed form of cell death, 2) non-programmed form of cell death[89]. According to the Nomenclature Committee for Cell Death, the adjective 'programmed' is thought to be involved in maintaining physiological processes such as developmental processes as well as maintenance of tissue homeostasis. Whereas the adjective 'regulated' is used to identify cell death events that rely on definite cellular and molecular mechanisms. Traditionally, apoptosis is an example of such programmed regulated form of cell death. The non-programmed form of cell death can also be called 'accidental cell death'. Typically, this mode of cell death is thought to not be dependent on specific molecular pathways like programmed cell death pathways. Necrosis was believed to be such form of cell death, which was always conceived as pharmacologically incontrollable. Necrosis was

thought to be mostly resulting due to harsh environmental conditions like severe changes in temperature, pH, osmotic pressure etc. As necrosis was always considered as an accidental cell death without involving specific molecular mechanisms, it was considered as 'non-regulated' form of cell death.

1.4.1 Apoptosis

Apoptosis is a caspase-dependent mode of programmed cell death that is regulated by two distinct biochemical pathways: i) intrinsic pathway ii) extrinsic pathway (figure 2). A wide range of injury and intracellular stress signals like DNA damage, oxidative stress, cytosolic calcium overload, endoplasmic reticulum (ER) stress promote mitochondrial outer membrane permeabilization (MOMP) that leads to the release of mitochondrial components e.g. cytochrome C, Smac, Omi/HtrA2 etc[90][91]. This leads to activation of caspase 3 dependent intrinsic pathways of apoptosis. Whereas, various extracellular stress signals e.g. different injury associated cytokine release, DAMPs, pathogen-associated molecular patterns (PAMPs) induce the extrinsic pathway of apoptosis. These danger signals associate with different transmembrane receptors viz. death receptors (DRs), TLRs or NLRs and further activate caspase 8. The proteolytic activation of caspases during apoptosis cause morphological changes in apoptotic cells that include chromatin condensation, nuclear fragmentation (karyorrhexis), plasma membrane blebbing, cellular shrinkage (pyknosis) leading to the formation of apoptotic bodies [92], which are cleared by local phagocytes without triggering immune responses due to the leakage of intracellular components.
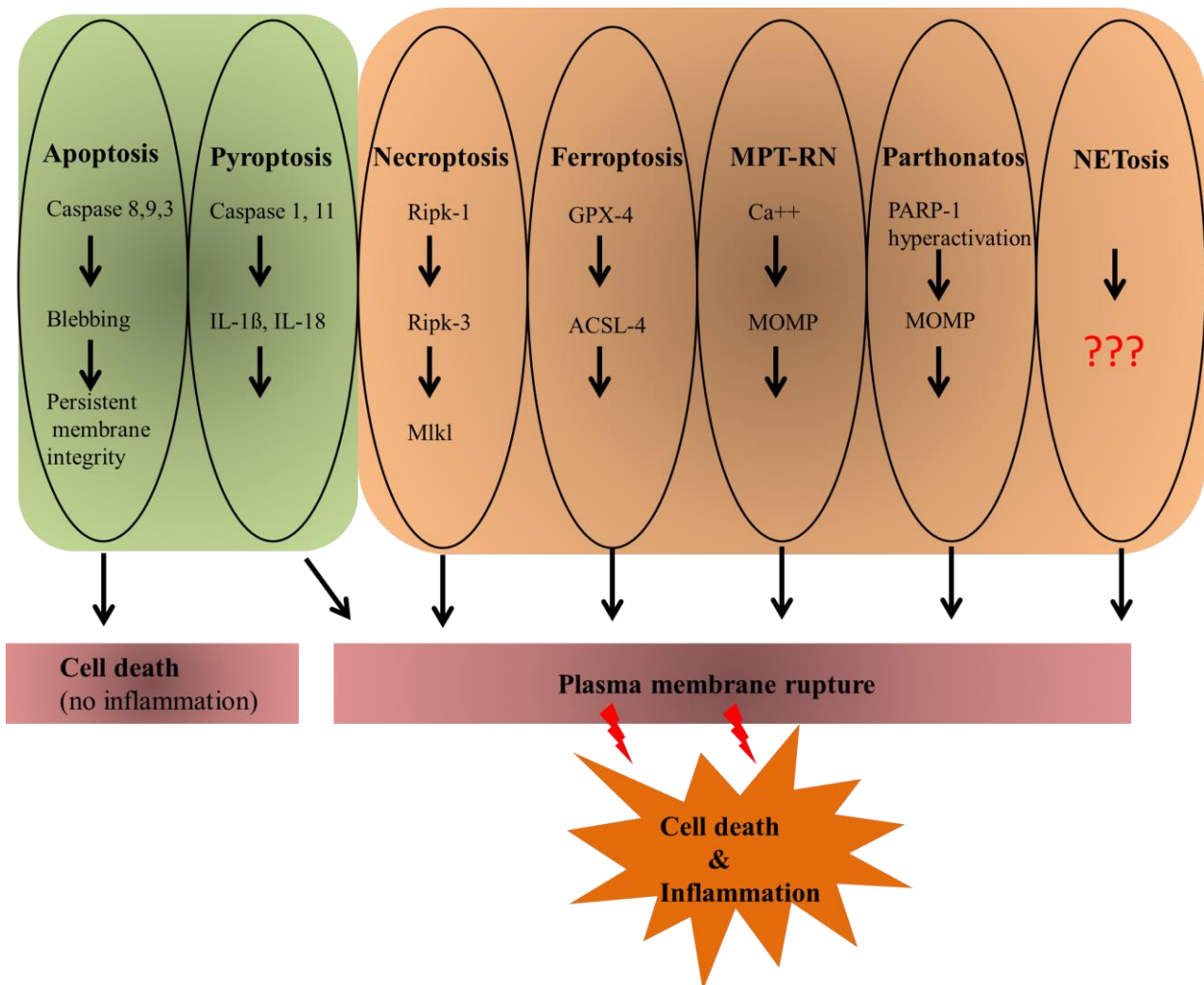
Figure 2: Different modes of regulated cell death pathways (RCD). RCD can be further divided in two categories. A) Caspase dependent RCD that includes cell death modes of apoptosis and caspase-1/caspase-11 dependent pyroptosis. B) Caspase independent RCD including necroptosis, mitochondrial permeability transport (MPT)-regulated necrosis (RN), Pathanatos, Ferroptosis and NETosis. Adapted from *Linkermann et. al 2014[93]*.

1.4.2 Regulated necrosis

In contrast to apoptosis, necrosis was traditionally considered to be a non-programmed mode of cell death occurring as a result of some physicochemical insult. However, in the last decade several genetic evidences[94] as well as pharmacological inhibitors[95] have identified the involvement of defined biochemical signaling pathways that leads to plasma membrane rupture and cellular leakage as well as cellular swelling and termed them regulated necrosis (RN)[89]. Depending on the kind of signaling pathway involved, regulated necrosis is categorized into necroptosis, ferroptosis, mitochondria permeability transition (MPT) RN pyroptosis and parthenatos (figure 2). They are described in detail in the following section.

Necroptosis

Necroptosis is a regulated mode of cell death that is driven by the protein cascade of receptor interacting protein kinase 1 (RIPK1) and RIPK3, and MLKL[96]. This cascade gets activated in response to various DAMPs, virus, DRs, and TLRs[96,97]. It is one of the most studied pathways of regulated necrosis. Upon injury, RIPK1 gets phosphorylated, which further leads to downstream events of RIPK3 and MLKL phosphorylation. The phosphorylated MLKL is translocated to the plasma membrane, where it is thought to be associated with pore formation within the plasma membrane and thus executing cell death[98]. Various chemical inhibitors like necrostatin-1[95] and necrosulfonamide (NSA)[99] are known to inhibit necroptosis in certain injury and diseases.

Ferroptosis

Ferroptosis is a form of RCD that is dependent on intracellular iron metabolism[100]. It was identified in RAS-transformed tumour cells, when treated with a lethal molecule called erastin. The small molecule erastin induces ferroptosis by inhibiting X_C^- Cystine/Glutamate antiporter that allows the exchange of extracellular L-Cystine and intracellular L-Glutamate across the plasma membrane[100]. This antiporter is required for glutathione biosynthesis. Upon depletion of intracellular glutathione, glutathione peroxidase 4 (GPX4) cannot degrade accumulating lipid peroxides, resulting in ROS-mediated lipid peroxidation and cell death[101]. Ferrostatin 1 is a chemical inhibitor of ferroptosis, however, the mechanism of action of this compound is yet unknown[100].

Mitochondrial permeability transition-related necrosis

MPT means a condition in which the permeability of the inner mitochondrial membrane is increased, which drives a massive influx of water molecules due to osmotic forces[102]. This can 1) disrupt biosynthetic and bioenergetic mitochondrial functions that depend on the transmembrane potential ($\Delta\psi_m$), 2) release various mitochondrial proteins, which can contribute to activation of both apoptotic cascade and regulated necrosis cascade (MPT-RN)[102]. MPT together with mitochondrial outer membrane permeabilization (MOMP) represents one of the crucial gateways to initiate apoptotic process in several pathophysiological conditions. During MPT-RN, the mitochondrial matrix protein called cyclophilin D (CYPD) control the MPT pore[103]. Immunosuppressive compounds, such as cyclosporine A or sanglifehrin A inhibit CYPD and thus, inhibit MPT-RN, independently of their immunosuppressive activities[104]. This mode of RCD is involved in different types of ischemia-reperfusion injury as well as acute organ failure[105].

Pyroptosis

The term pyroptosis was given for a special way of macrophage cell death upon *Salmonella enterica* infections[106]. Pyroptosis is regulated cell death that involves caspases that are different than caspases involved in apoptotic cascades. Pyroptosis depends on caspase 1 and caspase 11. It involves activation of inflammasomes and is followed by caspase-11 activation[107]. This mode of immune cell death results in a large amount of IL-1β and IL-18 secretion. In this way, pyroptotic cells are usually associated with higher inflammation rates and a highly immunogenic mode of cell death[108]. Immune cells like activated macrophages as well as dendritic cells die by switching on pyroptosis. This form of RCD was demonstrated to be associated with various bacterial and viral infections[108 109].

Parthanatos

Ted and Valina Dawson demonstrated a regulated necrosis pathway called 'parthanatos' that depends on the hyper-activation of poly (ADP-ribose) (PAR) polymerase 1 (PARP1)[110]. PARPs like PARP1 get activated upon DNA breaks induced by ultraviolet light, ROS, Ca^{2+} signalling pathway[110]. PARP1, when over-activated, can lead to parthanatos. Several preclinical pieces of evidence suggest that PARP inhibition may serve as a potential target for the treating various cancers, vascular or neurodegenerative diseases[111].

According to the new categorization, NETosis, cell deaths a result of NET formation, was also considered to be part of this RCD. However, unlike the above RCD, the molecular mechanisms involved in NETosis remain elusive.

1.5 Neutrophil death

1.5.1 NETosis: NET formation in association with cell death

NETs were first described using extensive cell imaging techniques after stimulation of human neutrophils with phorbol 12-myristate 13-acetate (PMA) or IL-8[52]. Three years later, the same group reconfirmed an observation made in 1996 that neutrophils undergo a distinct form of cell death following PMA stimulation, which is neither apoptosis nor necrosis, and named it "NETosis"[112]. "NETosis", unlike apoptosis or necrosis, was described to involve expansion of the nuclear material, chromatin decondensation, nuclear envelope disintegration, subsequent mixing of cytoplasmic and nuclear components followed by plasma membrane rupture and release of NETs[112 113]. Since then, NET release was considered to imply neutrophil death and the term "NETosis" was established in the literature. In the last decade, researchers extensively studied "NETosis" mostly using conventional bioassays, which do not

distinguish the two phenomena NET release and neutrophil death (Table 1). For example, the most widely used assays for NET release, Picogreen and Sytox assays, involve detection of cell-free DNA as the main principle. However, since these methods also detect necrosis-related passive release of chromatin, it is difficult to distinguish this process from a proactive chromatin expulsion[114] [115]. Some researchers used lactose dehydrogenase (LDH) assay to measure NET formation *in vitro*[116]. However, cells and tissues release LDH upon toxic or injury-related damage[117], making this assay highly unspecific for the distinguishing NET formation and cell death.

Furthermore, detection of histone deimination (citrullination of histones) by immunoblots or immunohistology was considered as an indicator for NET formation, since histone deimination induces chromatin decondensation, which is an essential step during NET release[59]. Several studies implicated the involvement of peptidyl-arginine deiminase 4 (PAD4) in NET formation[59] [118]. PAD4 is the enzyme required for citrullination of histones and chromatin decondensation during NET formation[59]. Accordingly, chemical inhibition of PAD4 using Cl-amidine impaired NETosis in animal models of anti-GBM disease or lupus nephritis[77] [119]. However, the requirement of PAD4 in NET formation is a debated question owing to the unspecific effects of Cl-amidine for PAD4[120,121], as well as the inconsistencies observed in NET formation in *Pad4*-deficient mice. For example, *Pad4*-deficient mice displayed impaired NET formation during necrotizing fasciitis[117] but succumbed to influenza pneumonitis, which involves influenza virus-induced NETs in the lung[122]. These disparities suggest that the involvement of PAD4 in NET formation depends on the stimulus. Indeed, it is shown that some stimuli e.g. calcium ionophores activate PKCζ, and thus PAD4, as well as PMA activate PKCα and, thus, inhibit PAD4[123], while both stimuli still induce NET release.

Another widely used technique for assaying NET formation is 'microscopy'. Researchers have used immunofluorescence (IF), confocal, as well as electron microscopy techniques to characterize either the presence of NETs, by detecting the co-localization of neutrophil-specific proteins and DNA[59], or the morphological appearances of NETs[52 59].

However, the main drawback of using these techniques is the need for cell fixation prior to microscopic examinations. Therefore, this technique cannot really distinguish the process of NET formation and cell death. Researchers also used enzyme-linked immunosorbent assay (ELISA), a technique to detect complexes of neutrophil-specific proteins and DNA, e.g. MPO-DNA or NE-DNA complexes etc[114 115 116] as an indicator of the

NET formation. However, although these assays confirm the presence of NETs, they fail to distinguish the NET formation and cell death.

Table 2. NET evaluation and bioassay characteristics

Method	Target	Identify NETs	Distinguish NET release and Cell death	Ref.
PicoGreen/ Sytox assay (Spectrofluorometry)	Extracellular and dead cell DNA	No	No	[112,124]
LDH assay (Spectrometry)	LDH release	No	No	[113]
MPO-DNA complexes (Capture ELISA)	MPO and DNA	Yes	No	[114,115]
NE-DNA complexes (Capture ELISA)	NE and DNA	Yes	No	[125]
Histone deamination (IF Microscopy, WB)	Citrullinated histones	Yes	No	[117,126]
Morphology	DNA (DAPI, Sytox)	Yes	No	[52,59,123]
(IF and Confocal Microscopy)	Granule protein (MPO, NE, CitH3)	Yes	No	
Micromorphology (Electron Microscopy)	Ultrastructure of nuclei / cytoplasm	Yes	No	[52,59]
Live cell imaging (Time Lapse Microscopy)	DNA (Sytox, Hoechst, etc), Cytoplasm (Cell tracking dye)	Yes	Yes	[59]
Combination of Microscopy and Flow Cytometry	Subcellular morphology	Yes	Yes	[127]

LDH: Lactate dehydrogenase, MPO: Myeloperoxidase, NE: Neutrophil elastase, WB: Western Blot, IF: Immunofluorescence, DAPI: 4', 6-diamidino-2-phenylindole, CitH3: Citrullinated histones etc. Table adapted from *Desai et. al 2016*[53]

In contrast, time-lapse video microscopy allowed observing NET formation[59]. Neutrophils are imaged using a combination of nuclear (Sytox, Hoechst, Pico), cytoplasmic (calcien, granular dyes e.g. NE) and cell death dyes (propidium iodide, annexin V) making it feasible to identify different components of NET formation process and cell death, in a manner dependent on each stimulus and time course[59]. Moreover, Zhao W. et. al. reported the

use of a combination of microscopy and flow cytometry for simultaneous detection and quantification of NET formation[127]. Interestingly, this technique also claimed to distinguish between NET formation with and without cell death[127]. Together, as few methods are suitable to clearly distinguish NET release from neutrophil death, these two phenomena often seem connected and are referred to as "NETosis". However, as neutrophils surviving NET release have been documented and when NET release upon certain stimuli can be inhibited with `conventional` cell death inhibitors it seems obvious that the term "NETosis" is no longer universally appropriate.

1.5.2 NET release without neutrophil death

Neutrophils can form NETs upon certain kind of bacterial infections *in vivo* without dying [60]. Pilsczeck et. al. reported that upon infection with *Staphylococcus aureus*, neutrophils formed NETs within 5-60 minutes without dying and were independent of ROS production. These early NETs were also observed *in vivo* using spinning disk microscopy within 10 min after subcutaneous injection of *S. aureus* [66]. Obviously, during this process, the neutrophil`s plasma membrane remains intact and the chromatin was released from the nucleus via intracellular vesicles that fused with the outer membrane to release NETs in the extracellular space [128]. NET release without neutrophil death was also observed within 30 minutes after stimulation of neutrophils with bacteria, fungi or LPS [66,67,128,129]. This rapid NET formation is mediated by the complement system, TLR2 or fibronectin [128,129]. Importantly, neutrophils releasing such NETs rapidly remained motile in-vivo, retaining the possibility to multitask during the early infection phase [128]. This rapid NET release indicates the dynamic functions of neutrophil to trap bacteria in NETs, while the anuclear neutrophils are still able to contribute to bacterial killing by phagocytosis[128,130].
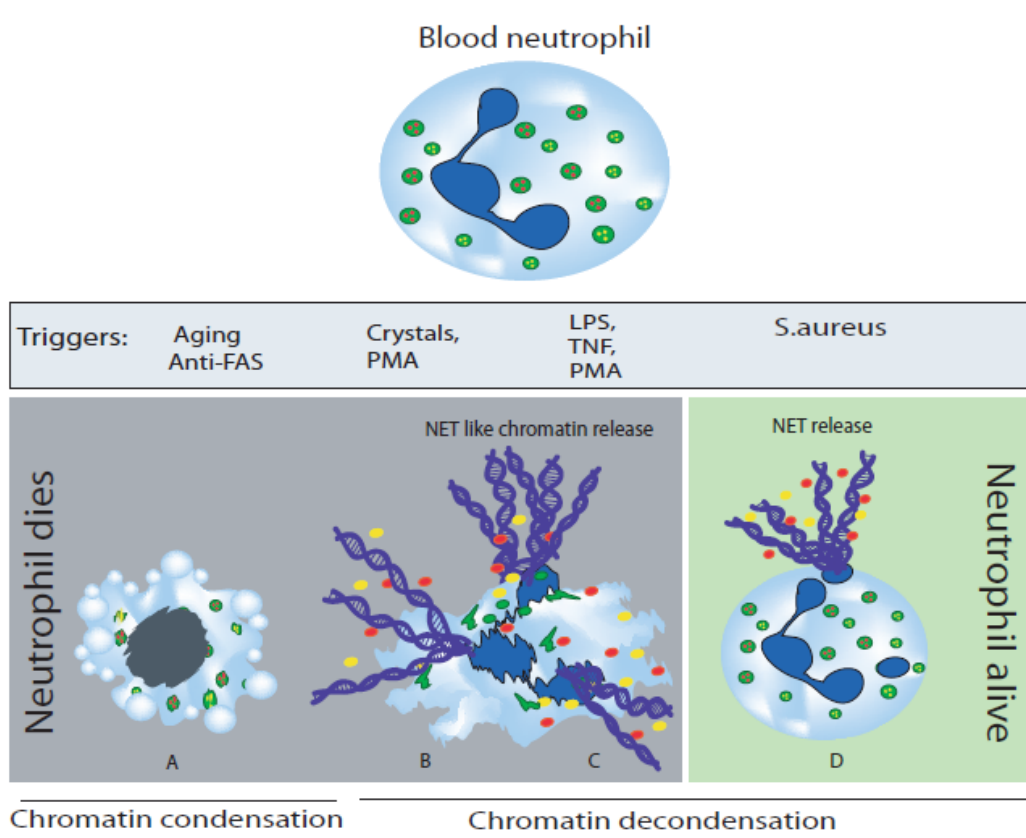
Figure 3. Neutrophil death and NET formation. Aging neutrophils die by apoptosis whereas stimuli like crystals, PMA, LPS, and TNF induce NET release associated with neutrophil death, referred to as necroptosis. Neutrophils are also known to release NETs without death, referred to as vital NET formation, upon certain bacterial stimuli, e.g. *S. aureus*. Inhibitors of necroptosis, e.g. RIPK1 and MLKL inhibitors as well as inhibitors of ROS, proteases and PAD can block NET release associated with neutrophil death. Figure adapted from *Desai et. al 2016[53]*.

Furthermore, *S. aureus*-induced rapid NETs are composed of histones, confirming that the NETs are originated from the nuclei, without involving mitochondrial DNA [66]. While other stimuli like LPS, complement factor C5a induce NETs release from mitochondrial DNA together with granular enzymes after GM-CSF priming in a ROS-dependent manner [131]. Interestingly, *S. aureus* rapidly induced NET release even before ROS were generated, whereas *Aspergillus*-induced NETs independent of ROS [66,129]. Moreover, statins (cholesterol-lowering drugs) have been reported to block the oxidative burst of PMNs, still enhancing NET formation against *S. aureus* [55]. Growing evidence demonstrated that NET formation with cell death involves oxidant generation, whereas rapid NET formation without cell death may or may not involve oxidant generation (figure 3). For example, stimuli like PMA or bacteria-induced ROS-dependent NET formation and cell death, while stimuli like ionomycin or certain bacterial/fungal products induced ROS-independent rapid NET formation without cell death[132].

Table 3: Definition of important NET-related terms

Term	Definition
NET	Neutrophil extracellular traps are chromatin expulsed from neutrophils decorated with nuclear and cytosolic components such as proteolytic enzymes
NETting	The process of NET formation by groups of neutrophils, e.g. in pus, tophus or thrombus formation
NETosing	The neutrophils/PMNs capable for forming NETs
NETosis	NET formation in association with death of the neutrophil, common in pus, tophi or thrombosis, but the term does not specify the mode of cell death
Suicidal NETosis	NET formation in association with the death of the neutrophil, but the term does not specify the mode of cell death. "Suicidal" implies that the trigger for death is intrinsic, which is usually not the case. Imprecise term that is to be avoided
Lytic NETosis	NET formation by pathogen-induced lysis of neutrophils e.g. *S. aureus*
Vital NETosis	NET formation without the death of the neutrophil. As "Osis" implies *death* and "Vital" implies *alive* the term is a contradiction in itself and should be avoided
Neutrophil necroptosis	Neutrophil death that can be blocked by inhibitors of the necroptosis pathway (RIPK3-MLKL)
Neutrophil apoptosis	Neutrophil death that can be blocked by inhibitors of caspase 3, 8, and 9

RIPK = receptor interacting protein kinase, MLKL = mixed lineage kinase domain-like. Adapted from Desai et. al 2016[53].

1.6 The necroinflammation concept

At the end of cellular necrosis, various DAMPs are released that in turn can initiate inflammatory tissue responses in neighboring healthy cells. Furthermore, the same inflammatory responses within tissue cells lead to necrotic cell death of the same, leading to release of more DAMPs. This auto-amplification look between cell necrosis and inflammatory responses is known as necroinflammation[93]. The auto-amplification loop of necroinflammation consists of two mechanisms that enforce each other, i.e. DAMP-mediated

activation of innate immunity and cytokine-induced regulated cell necrosis. Together, the auto-amplification loop of necrosis and inflammation drives the crescendo from local inflammatory tissue injury to acute organ dysfunction, organ failure or eventually up to a systemic inflammatory response syndrome and multiorgan failure[133].

Gouty arthritis is a strong inflammatory disease initiated by the accumulation of MSU crystals in synovial fluid. This leads to a strong inflammatory response and massive infiltration of immune cells like neutrophils and macrophages. These immune cells especially neutrophils upon the contact with MSU crystals may undergo necrotic cell death (NET-associated cell death) releasing DAMPs in extracellular space like DNA and histones. This may further trigger inflammation, setting up the loop of necroinflammation in the synovium and leading to further tissue damage.

NETosis was first described as form of neutrophil death that was different from classical apoptosis and necrosis[59]. In the last decade, cell biology domain re-classified the classical cell death categories of apoptosis and necrosis into a myriad of novel categories defined by distinct causative signaling pathways[134]. Whether NETosis is one of those or a distinct category has remained unclear. The immunology domain observed that leukocyte-death-upon-activation is a common phenomenon not only for effector T cells but also for inflammasome-activated macrophages and dendritic cells[135 126]. Furthermore, NET formation was described to occur also without immediate neutrophil death[60], which was quickly referred to as "vital NETosis"[60 127] (figure 3), although this term is an obvious contradiction in itself (Table 2). Such nomenclatures in the part mirror and potentially account for the general confusion about the evolving spectrum of evidence on NET formation. Therefore, the scope of this thesis is to decipher the molecular mechanisms involved in NET formation and neutrophil death, especially in crystallopathies.

2. Hypotheses/objectives

Based on above literature we hypothesized that-

1. Different crystals, irrespective of their nature, induce NET formation and neutrophil death.

   Various crystallopathies are associated with strong inflammatory responses.

2. Crystal-induced NET formation and neutrophil death involve regulated necrosis pathways.

3. Molecules involved in the regulated necrosis pathways will serve as potential therapeutic targets for the treatment of crystallopathies e.g. gout.

3. Material and Methods

3.1 Instruments and Chemicals

3.1.1 Instruments

<u>Balance:</u>

Analytic Balance, BP 110 S   Sartorius, Göttingen, Germany

Mettler PJ 3000   Mettler-Toledo, Greifensee, Switzerland

<u>Cell Incubators:</u>

Type B5060 EC-CO_2 Heraeus Sepatech, München, Germany

<u>Centrifuges:</u>

Heraeus, Minifuge T   VWR International, Darmstadt, Germany

Heraeus, Biofuge primo   Kendro Laboratory Products GmbH, Hanau, Germany

Heraeus, Sepatech Biofuge A   Heraeus Sepatech, München, Germany

<u>ELISA-Reader:</u>

Tecan, GENios Plus   Tecan, Crailsheim, Germany

<u>Fluorescence Microscopes:</u>

Leica DMi8   Leica Microsystems, Cambridge, UK

Olympus BX50   Olympus Microscopy, Hamburg, Germany

Zeiss observer microscope   Zeiss, Germany

Zeiss Libra 120 TEM   Zeiss, Germany

Spectrophotometer:

Beckman DU® 530   Beckman Coulter, Fullerton, CA, USA

TaqMan Sequence Detection
System:

ABI prism ™ 7700 sequence   PE Biosystems, Weiterstadt, Germany
detector

Other Equipments:

Nanodrop   PEQLAB Biotechnology GMBH, Erlangen, Germany

Cryostat RM2155   Leica Microsystems, Bensheim, Germany

Cryostat CM 3000   Leica Microsystems, Bensheim, Germany

Homogenizer ULTRA-TURRAX   IKA GmbH, Staufen, Germany

Microtome HM 340E   Microm, Heidelberg, Germany

pH meter WTW   WTW GmbH, Weilheim, Germany

Thermomixer 5436   Eppendorf, Hamburg, Germany

Vortex Genie 2™   Bender & Hobein AG, Zürich, Switzerland

Water bath HI 1210   Leica Microsystems, Bensheim, Germany

3.1.2 Chemicals and reagents

RNeasy Mini Kit   Qiagen GmbH, Hilden, Germany

RT-PCR primers   PE Biosystems, Weiterstadt, Germany

SYTOX green assay   Life Technologies, Eugene, OR, USA

Pico green dsDNA assay   Life Technologies, Eugene, OR, USA

ROS assay: DCFDA dye   Sigma lifesciences, Germany

LDH cytotoxicity assay   Roche, Germany

MTT viability assay	Sigma-Aldrich, Steinheim, Germany
TO-PRO®-3Iodide	Life Technologies, Eugene, OR, USA

Cell culture:

DMEM-medium	Biochrom KG, Berlin, Germany
RPMI-1640 medium	GIBCO/Invitrogen, Paisley, Scotland, UK
FSC	Biochrom KG, Berlin, Germany
Dulbecco's PBS (1×)	PAA Laboratories GmbH, Cölbe, Germany
Trypsine/EDTA (1×)	PAA Laboratories GmbH, Cölbe, Germany
Penicillin/Streptomycin (100×)	PAA Laboratories GmbH, Cölbe, Germany

Antibodies:

Ripk3	Abcam, Cambridge, UK
Ripk1	Abcam, Cambridge, UK
p-MLKL(human)	Merck Millipore, Germany
Histone	Cell signaling, Danvers, MA
Histone IgG	clone BWA3, Immunomedics, NJ, USA
Neutrophil elastase	Santa Cruz Biotechnology, Santa Cruz, CA
Myeloperoxidase	Cell signaling, Danvers, MA
Cit-H3	Cell signaling, Danvers, MA
DNA antibody	Roche, Mannheim, Germany
HRP linked Anti-Rabbit secondary Ab	Cell signaling, Danvers, MA
HRP linked Anti-Mouse secondary Ab	Cell signaling, Danvers, MA
HRP linked Anti-Goat secondary Ab	Dianova, Hamburg, Germany

β-Actin   Cell signaling, Danvers, MA

Antihuman CD15   BD Bioscience, Germany

Antihuman CD11B   BD Bioscience, Germany

Antihuman CD66b   Biolegends, Germany

Elisa Kits:

mouse IL-1ß   R &D Systems, Minneapolis, MN, USA

mouse TNF-α   Biolegend, San Diego, CA

Inhibitors

Necrostatin-1   Enzo Life Sciences, Lörrach, Germany

Necrostatin-1s   Biovision, Milpitas, CA

Necrosulfanamide   Millipore, Schwalbach, Germany

Ferrostatin-1   CalBiochem, Germany

Pan caspase inhibitor zVAD   Enzo Life Sciences, Lörrach, Germany

PAD inhibitor-Cl amidine   Merck Millipore, Germany

Crystals

Calcium oxalate   Alfa Aesar, Germany

Monosodium urate   Invivogen, Toulouse, France

Calcium phsphate   Chem Cruz

Calcium pyrophosphate (CPP)   Invivogen, Toulouse, France

Cystine   Sigma life sciences, Germany

Myoglobin   Sigma life sciences, Germany

Cholesterol   Invivogen, Toulouse, France

Crocidolite Asbestos   SPI-CHEM

Silica	Alfa Aesar
Alum	Invivogen, Toulouse, France
TiO$_2$ 20nm	Io-li-tec nanomaterials, Heilbronn, Germany
TiO$_2$ 80nm	Io-li-tec nanomaterials, Heilbronn, Germany

Chemicals:

PMA	Sigma–Aldrich, Steinheim, Germany
LPS	InvivoGen, San Diego, CA
TNFa	Immunotools, Germany
Histone	Roche, Germany
Acetone	Merck, Darmstadt, Germany
AEC Substrate Packing	Biogenex, San Ramon, USA
Bovines Serum Albumin	Roche Diagnostics, Mannheim, Germany
Skim milk powder	Merck, Darmstadt, Germany
DEPC	Fluka, Buchs, Switzerland
DMSO	Merck, Darmstadt, Germany
EDTA	Calbiochem, SanDiego, USA
30% Acrylamide	Carl Roth GmbH, Karlsruhe, Germany
TEMED	Santa Cruz Biotechnology, Santa Cruz, CA
Eosin	Sigma, Deisenhofen, Germany
Ethanol	Merck, Darmstadt, Germany
Formalin	Merck, Darmstadt, Germany
Hydroxyethyl cellulose	Sigma-Aldrich, Steinheim, Germany
HCl (5N)	Merck, Darmstadt, Germany
Isopropanol	Merck, Darmstadt, Germany
Calcium chloride	Merck, Darmstadt, Germany

Calcium dihydrogenphosphate	Merck, Darmstadt, Germany
Calcium hydroxide	Merck, Darmstadt, Germany
MACS-Buffer	Miltenyl Biotec, Bergisch Gladbach, Germany
Beta mercaptoethanol	Roth, Karlsruhe, Germany
Sodium acetate	Merck, Darmstadt, Germany
Sodium chloride	Merck, Darmstadt, Germany
Sodium citrate	Merck, Darmstadt, Germany
Sodium dihydrogenphosphate	Merck, Darmstadt, Germany
Potassium chloride	Merck, Darmstadt, Germany
Dextran	Sigma Aldrich, St.Louis, USA
Lymphoprep (density of 0,177g/mL)	Stemcell, Germany
RIPA buffer	Sigma, Deisenhofen, Germany
Chemiluminescence system	Amersham, Buckinghamshire, UK
Penicillin	Sigma, Deisenhofen, Germany
Roti-Aqua-Phenol	Carl Roth GmbH, Karlsruhe, Germany
Streptomycin	Sigma, Deisenhofen, Germany
Tissue Freezing Medium	Leica, Nussloch, Germany
Trypan Blue	Sigma, Deisenhofen, Germany
Oxygenated water	DAKO, Hamburg, Germany
Xylol	Merck, Darmstadt, Germany

Miscellaneous:

PVDF membrane	Millipore, Schwalbach, Germany
Microbeads	Miltenyl Biotech, Germany
Preseparation Filters	Miltenyl Biotec, Bergish Gladbach, Germany
Super Frost® Plus microscope slides	Menzel-Gläser, Braunschweig, Germany

Needles	BD Drogheda, Ireland
Pipette's tip 1-1000μL	Eppendorf, Hamburg, Germany
Syringes	Becton Dickinson GmbH, Heidelberg, Germany
Heparin tubes	S-monovette, Germany
Plastic histocasettes	NeoLab, Heidelberg, Germany
8 well chamber slides	Ibidi, Martinsreid, Germany
Lab Tek II chamber slides	Nunc international, USA
Tissue culture dishes Ø 100x20mm	TPP, Trasadingen, Switzerland
Tissue culture dishes Ø 150x20mm	TPP, Trasadingen, Switzerland
Tissue culture dishes Ø 35x10mm	Becton Dickinson, Franklin Lakes, NJ, USA
Tissue culture flasks 150 cm2	TPP, Trasadingen, Switzerland
Tubes 15 and 50 mL	TPP, Trasadingen, Switzerland
Tubes 1.5 and 2 mL	TPP, Trasadingen, Switzerland

All other reagents were of analytical grade and are commercially available from Invitrogen, SIGMA or ROTH.

3.2 Experimental procedures

3.2.1 Animals

C57BL/6 wild-type mice and *Ripk3*-deficient C57BL/6 mice were obtained from Charles River (Sulzfeld, Germany) and Genentech (Viswa Dixit) respectively. All mice were kept under normal housing conditions under a 12-h light and dark cycle. Water and standard chow (Ssniff, Soest, Germany) were available ad libitum for the complete duration of the study. Cages, bedding, nestles, food, and water were sterilized by autoclaving before use.

3.3 Blood collection

3.3.1 Human blood sample collection

All blood donors provided written informed consent forms approved by the local ethical committee for human neutrophil isolation. Blood samples from a healthy donor for most of the studies, as well as blood from CGD patients in some studies, were used. Whole blood was collected into heparin tubes from the facial vein and was processed for neutrophil isolation.

3.3.2 Mouse blood sample collection

Mouse blood samples were collected by retro-orbital bleeding technique, under isoflurane anesthesia, in microcentrifuge tubes containing heparin. Mice were carefully bled to harvest the maximum amount of peripheral blood.

3.4 Human and mouse neutrophil isolation

As mentioned above, whole blood from either mice or human subjects was collected into heparin tubes in a very careful manner to avoid the activation of neutrophils by physical means. The blood sample was mixed with 1,25% of high molecular weight dextran (molecular weight 450K-650K), and RBCs were allowed to settle at 4^0C. The upper clear yellowish leucocyte-rich layer was separated and lysed for the remaining RBCs using hypnotic lysis (ddH_2O) and tonicity was maintained by adding 0,15M KCl. Resultant leucocytes were enriched for neutrophils by gradient centrifugation with Biocoll solution (density of 0,177). As the neutrophils were very sensitive to the external stimuli, care was taken not to activate them by aggressive shaking and all the procedure were performed at 4^0C. No glass material was used as neutrophils sticks to the glass surface. Once the pure neutrophils were isolated, suspended in plain RPMI media and then incubated at 37^0C in CO_2 incubator for 30 minutes.

3.5 Induction of NETs

Isolated mouse or human neutrophils were suspended (0.5×10^6 or 5×10^6) in 200µl to 500µl plain RPMI. They were seeded into 8 well µ slides or 12-well plates (Ibidi, Martinsried, Germany) to settle for 30 min in a 5% carbon dioxide atmosphere at 37°C. These neutrophils were exposed to different doses of different cell death inhibitors Nec-1 (Enzo Life Sciences, Lörrach, Germany), Nec-1s (Biovision, Milpitas, CA), Ferrostatin (Calbiochem, Germany) , zVAD (Enzo Life Sciences, Lörrach, Germany), NSA (Millipore, Schwalbach, Germany),

PAD inhibitor-Cl-amidine (Merck Millipore,Germany) for 30 min pretreatment before adding stimulators of NETs.

To induce NETs various stimuli were used. Neutrophils were incubated for 2-6 hours after stimulations with stimuli like PMA (Sigma–Aldrich, Steinheim, Germany), LPS (InvivoGen, San Diego, CA), TNFα (Immunotools, Germany) or various crystals like CaOx (Alfa Aesar, Germany), MSU (Invivogen, Toulouse, France), CaP (Sigma life sciences, Germany), Cystine (Chem Cruz), CPPD (Invivogen, Toulouse, France), Cholesterol (Invivogen, Toulouse, France), alum (Invivogen, Toulouse, France), silica (Alfa Aesar, Germany), asbestos (SPI-CHEM), and TiO_2 (Io-li-tec nanomaterials, Heilbronn, Germany).The NET soups were harvested for different biochemical assays, whereas the neutrophils in culture plates were preceded for different imaging approaches.

3.6 Live cell SYTOX imaging

In order to study the neutrophil cell death after different treatments and stimulations with different stimuli, 0.1 μM Sytox green dye (Life Technologies, Eugene, OR, USA) was added post stimulation. The cells were incubated in dark for 10min at RT to allow the cells to take up the dye. Sytox green is a DNA staining dye, which is a cell membrane impermeable dye. Thus, the cell death, which involves plasma membrane and the release of extracellular DNA, can be detected. Neutrophil cell death was detected by performing live cell imaging using Zeiss observer microscope.

3.6.1 Quantification of Sytox+ dead cells

Multiple images per stimulation group were taken to perform the quantitative analysis of Sytox+ dead cells. In the case of mouse neutrophils, the sytox+ cells were counted manually using the imageJ software. Total %cell death was compared within the different groups. Due to the higher cell number for human neutrophils, the mean green area/field was calculated using ImageJ software to indicate the cell death.

3.7 Confocal imaging and immunostaining

For Confocal imaging, neutrophils were fixed using 4% formaldehyde for 10 min at RT after removing the supernatant. The cells were washed with 1X PBS for 3 times and were stored in PBS at -20 °C. The cells prepared as described above, were incubated with the

following primary antibodies: antihistone IgG (clone BWA3, Immunomedics, Morris Plains, NJ, USA) Neutrophil elastase (Santa Cruz Biotechnology, Santa Cruz, CA), citH3 (Cell signaling, Danvers, MA) and TO-PROR -3 Iodide (Life Technologies) for 1 h in PBS or 0.1% milk solution in room temperature. After washing, the sections were incubated with secondary antibodies guinea pig Alexa Fluor 488 (1:100, Invitrogen, Carlsbad, CA) or rabbit Cy3 (1:200, Jackson ImmunoResearch Laboratories, West Grove, PA) for 30 minutes at room temperature. Stainings were evaluated using confocal microscopy with LSM 510 microscope and LSM software (Carl Zeiss AG).

For immunohistological studies, tophus containing air pouch skin sections from each mouse were fixed in formalin (10 % in PBS or Saline) overnight and processed using tissue processors (Leica) and paraffin blocks were prepared. 2µm thick paraffin-embedded sections were cut. De-paraffinization was carried out using xylene (3 * 5 min) followed by re-hydration, which was carried out by incubating the sections in 100% absolute ethanol (3 * 3 min), 95% ethanol (2 * 3 min) and 70% ethanol (1 * 3 min) followed by washing with PBS (2 * 5 min). Blocking endogenous peroxidase was carried out by incubating sections in H_2O_2 and methanol mixture (20 ml of 30% H202 in 180ml of methanol) for 20 min in the dark followed by washing in PBS (2* 5min). For unmasking of antigen, sections were dipped in antigen unmasking solution (3 ml of antigen unmasking solution + 300 ml of distilled water) and cooked in the microwave for a total of 10 min (4*2.5 min, every 2.5 min water level was checked and made up to the initial levels with distilled water every time). After microwave cooking sections were cooled to room temperature for 20 min and washed with PBS. Blocking endogenous biotin was carried out by incubating sections with one drop of Avidin (Vector) for 15 min followed by incubation with Biotin (Vector) for further 15 min. After the incubation was over sections were washed with PBS (2* 5 min).

For several antibodies, the immunofluorescent studies were performed on five micrometer-thick cryo/frozen kidney or bladder sections without fixation with 4% formaldehyde.

Sections were incubated with different primary antibodies either for 1 hour at room temperature or overnight at 40C in a wet chamber followed by wash with PBS (2* 5 min). After washing sections were incubated with biotinylated secondary antibodies (1:300, dilution in PBS) for 30 min followed by a wash with PBS (2* 5 min). Substrate solution (ABC solution, Vector) was added and sections were incubated for 30 min at room temperature in a wet chamber followed by a wash with PBS (1* 5 min). Tris (1* 5 min) and sections were

stained for DAB followed by counterstaining with methyl green (Fluka). Then sections were washed with alcohol (96 %) to remove excess stain and xylene. Sections were dried and mounted with VectaMount (Vector).

The primary antibodies used in the study are mentioned above. For each immunostaining, negative controls staining was performed by incubation with a respective isotype antibody instead of primary antibody.

3.8 Transmission and scanning electron microscopy

Primary neutrophils with/without different stimuli were fixed in 2.0 % paraformaldehyde/ 2.0 % glutaraldehyde, in 0.1 M sodium phosphate buffer, pH 7.4 for 24 hours, followed by 3 washes x15 min in 0.1 M sodium phosphate buffer, pH 7.4 and distilled water. For transmission EM kidneys were post-fixed, in phosphate cacodylate-buffered 2 % $OsO4$ for 1h, dehydrated in graded ethanols with a final dehydration in propylene oxide and embedded in Embed-812 (Electron Microscopy Sciences, Hatfield, PA). Ultrathin sections (~90-nm thick) were stained with uranyl acetate and Venable's lead citrate. Specimens were viewed with a Zeiss Libra 120 Transmission electron microscope.

For scanning electron microscopy, kidney tissue was rinsed with PBS and postfixed with 1% aqueous osmium tetroxide for a total of 2.5 h. Subsequently, tissues were rinsed and dehydrated through a graded series of ethanol to absolute ethanol and critical point dried using liquid $CO2$. After mounting on stubs the specimens were sputter coated with a gold-palladium alloy for 1.5 min. Images were viewed with a Hitachi 2600 electron microscope.

3.9 Quantitative analysis of NETs and cell death

3.9.1 Pico green assay

The NETs include extracellular chromatin. The supernatant was harvested to quantify the DNA release from NET forming neutrophils post various NET inducing stimuli. After removing floating free nuclei (centrifugation at 1500 rpm for 5 min), DNA release in supernatant was determined by adding 50 μL of Pico green dsDNA assay kit reagent (Life Technologies; 1:250 in TE buffer) to 50 μLof cell culture supernatant, and fluorescence was read after 5 min with an excitation and emission wave lengths of 485 and 535 nm.

3.9.2 Reactive oxygen species assay

Primary neutrophils (0.5×10^6 /well) were seeded in 96 well plates. The cells were pre-incubated with DCFDA dye followed by the treatment with different cell death inhibitors and stimuli like PMA or MSU crystals for 2 hours. DCFDA is deacetylated by cellular esterases to a non-fluorescent compound, which is later oxidized by reactive oxygen species (ROS) into 2', 7' –dichlorofluorescein (DCF) after diffusion in the cells. The amount of the fluorescent compound was measured using the photospectrometer at excitation and emission wave lengths of 485 and 535 nm.

3.9.3 Lactate dehydrogenase cell death assay

Primary neutrophils (0.5×10^6 /well) were seeded in 96 well plates in plain RPMI medium. Post the treatment with different inhibitors and crystal stimulations for 2h, the supernatant was collected and transferred to a new 96 well plate. The cell-free supernatant was incubated with substrates of lactose dehydrogenase (LDH) cytotoxicity detection kit (Roche, Germany). LDH activity is higher in the case of cell death. During this assay, LDH activity is determined by a coupled enzymatic reaction between LDH and substrate dye. The absorbance of the dye was read at 492nm, which directly correlates, to the amount of LDH present in the supernatant.

3.9.4 Cell viability assay

To check the cell viability, cells were seeded (0.1×10^6 /well) in 96 well plates. Post the treatment with different inhibitors and crystal stimulations for 24h, the 15µl 3-(4,5-Dimethylthiazol-2-yl)-2,5-Diphenyltetrazolium Bromide (MTT) dye (Sigma-alderich, Germany) was added to the wells. The yellow coloured MTT dye interacts with mitochondrial dehydrogenases of viable cells and produces purple coloured crystals soluble in acidified isopropanol. The absorbance was read at 570nm using photospectrometer. The absorbance was directly proportional to the number of viable cells in the well.

3.10 Other *In-vitro* analysis

3.10.1 Cell culture

MTCs, human synovial fibroblasts (K4IM cells) and L929 cells were maintained in DMEM/F12 (GIBCO, Invitrogen, CA, USA) containing 10% fetal calf serum, 1% penicillin–streptomycin. Human kidney cells (HK-2) were maintained in RPMI (GIBCO, Invitrogen, CA, USA) containing 10% fetal calf serum and 1% penicillin–streptomycin. MTCs are a cell line immortalized with SV-40 virus41, and K4IM cells are a cell line immortalized with SV-

40 T large antigen42, 43. MTCs and K4IM cells were generously provided by EG Neilson and PJ Nelson, respectively. L929 cells and HK-2 cells were purchased from ATCC. Human renal progenitor cells were prepared from human kidney tissues using standard sieving technique through graded mesh screens (60, 80, 150 and 200 mesh)24. All cells were stimulated with different doses of crystals of CaOx (1–2 mm size; Alfa aesar, Germany), MSU (25–125 nm size; Invivogen, Germany), CPPD (25–125 nm size; Invivogen, Germany) and cystine (1–2 mm size; Sigma Aldrich, Germany) in different experiments. Cells were pretreated with necrostatin-1 (50 or 100 mM) or ZVAD-FMK (10 mM) or combination 30 min before crystals stimulations whenever required.

Primary tubular epithelial cells were isolated from the kidneys and were maintained in DMEM/F12 containing 10% fetal calf serum, 1% penicillin–streptomycin, 125 ng ml 1 prostaglandin E1 (Calbiochem, Germany), 25 ng ml 1 EGF, 1.8 mgml 1 l-thyroxine, 3.38 ng ml 1 hydrocortisone and 2.5 mg ml 1 of insulin–transferrin—sodium selenite supplement (all from Sigma Aldrich, Germany unless mentioned). Cells were grown to confluence before use in experiments. Primary renal human progenitor cells were plated in EGM-MV (Lonza Ltd., Basel, Switzerland) with 20% FBS (Hyclone, Logan, Utah). Generation of clones was achieved by limiting dilution in 96-well plates and in four-chamber glass slides (VWR International, West Chester, Pennsylvania). All the cells were cultured in an incubator at 37^0C, 5% CO_2. CellTiter 96 non-radioactive cell proliferation assay (MTT) kit (Promega, Germany) was used to evaluate cell survival after 24 h following the manufacturer's instructions. Results were expressed as a percentage of the vehicle control.

3.10.2 Cell freezing and thawing

At earlier passages, large amounts of cells were grown under standard culture conditions and were frozen for future use. Cells to be frozen were detached from the culture plates and were spun down under sterile conditions for 3 min at 1000 RPM. The cell pellet was maintained on ice and carefully re-suspended in cold freezing medium (90 % respective culture medium and 10 % DMSO) by pipetting the suspension repeatedly up and down. 1.5 ml aliquots were quickly dispensed into freezing vials (4^0C). The cells were slowly frozen at – 20^0C for 1 h and then at –80^0C overnight. The next day, all aliquots were transferred to liquid nitrogen.

In order to thaw cells, a frozen vial was removed from liquid nitrogen and put in a water bath at 37^0C. The cells were then dispensed in 5 ml of warm complete growth medium and spun down at 1000 RPM for 5-7 min. Then the old medium was removed and the cells were re-suspended in fresh medium and transferred to new culture plate. The medium was changed once more after 24 h.

3.10.3 Stimulation experiments

For cell stimulation experiments, the cells were seeded at a density of $5X10^5$ cells/well in six-well plates in DMEM and grown overnight to the confluence. Cells were treated with 5 µg/ml ultrapure LPS (InvivoGen, San Diego, CA) and incubated at 37^0C, 5% CO_2 for 0.5–18 h. Total cell protein was extracted for western blot analysis and supernatants were collected for IL-6 or TNF-α ELISA. Nuclear proteins were isolated by using high-salt extraction.

3.11 Protein isolation and western blotting

Proteins from primary neutrophils from cell culture were extracted using RIPA buffer (Sigma, Germany) containing protease inhibitors (Roche, Germany). In brief, after neutrophil stimulations to induce NETosis, the supernatant was harvested carefully without disturbing the NETs on the surface. The cells were then lysed in the RIPA buffer containing protease inhibitors. The lysates were then maintained at constant agitation for two hours at 4^0C. The samples were then centrifuged for 5 min at 5000 rpm at 4^0C. Then the supernatant (proteins) was separated in a new tube and the pellet was discarded. Protein estimation was done using Barford´s assay.

After determination of protein concentrations, 50µg of the protein was mixed with 5x SDS loading buffer (100 mM Tris-HCl, 4% SDS, 20% glycerol, and 0.2% bromophenol blue) for Western blot analysis. Samples were heated at 95°C for 5 min. Proteins were separated by SDS PAGE and then transferred to a polyvinylidene difluoride (PVDF) membrane. Nonspecific binding to the membrane was blocked for 1hr at room temperature with 5% milk in Tris-buffered saline buffer (20 mM Tris-HCl, 150 mM NaCl, and 0.1% Tween 20). The membranes were then incubated overnight at 4°C with primary antibodies. After washing, the membrane was incubated with respective secondary antibodies in Tris buffered saline buffer. The signals were visualized by an enhanced chemiluminescence system (Amersham, Buckinghamshire, UK).

3.12 Cytokine ELISA

All cytokine levels in supernatant collected from in-vitro cells stimulations were estimated using ELISA kits following the manufacturer's instructions. In brief, The NUNC ELISA plate wells were captured overnight at 4°C with the capture antibody in coating buffer. Next day the plates were washed 3 times with the washing buffer as given in protocol for 3 times and blocked with the blocking solution or assay diluent for 1 hour or as specified. Again the washings were repeated 3 times followed by addition of standards; samples and sample diluent (blank) into the wells of tap dried plate and incubated at RT for 2 hours. Washings followed this for 5 times or as specified. Then HRP/AP conjugated secondary antibody diluted in assay diluent was added. Incubate the plate as specified for the primary Ab. The wells were washed again for 5-7 times or as specified and incubated with the 100 μl of substrate A and B (1:1 mixture) for 25-30 min in the dark to develop colour. The reaction was stopped by addition of 100 μl 1 M H2SO4. The reading of the absorbance was taken at 450 nm and the reference wavelength was 620 nm using a spectrophotometer (TECAN-Genios Plus).

3.13 Flow cytometry for neutrophil population

Flow cytometric analysis of neutrophils after neutrophil isolation was performed on a FACS Calibur flow cytometer (BD) as described. Every isolate was incubated with binding buffer containing either anti-human CD15 (BD bioscience), CD11B (BD bioscience) and CD66b (Biolegend) for 45 min at 40C in the dark were used to detect neutrophils.

3.14 Statistical analysis

Data are presented as mean ±SEM. For multiple comparisons of groups one-way ANOVA was used followed by post-hoc Bonferroni`s test, using SigmaStat (Jandel Scientific, Erkarath, Germany). Paired Student`s t-test was used for the comparison of single groups. A value of $p < 0.05$ was considered to indicate statistical significance.

4. Results

4.1 Part I: Crystals induce neutrophil cell death and NET formation

Crystals are deposits of various sizes and shapes composed of atoms, ions or biomolecules. Crystal formation under physiological conditions can cause tissue injury and inflammation in diseases like gouty arthritis, pulmonary silicosis or asbestosis, cholesterol crystals driving atherogenesis and in oxalate, cystine or urate nephropathy. These crystals are known to induce direct cytotoxicity during injury. However, the mechanisms are not yet fully known. To understand the role of various crystals on cytotoxicity, we first screened a wide range of crystals like CaOx, MSU, CPPD, CaP, cholesterol, myoglobin, asbestos, silica, alum crystals and titanium dioxide nanoparticles. To understand the shape and size of these crystals, we performed transmission electron microscopy (figure 4).
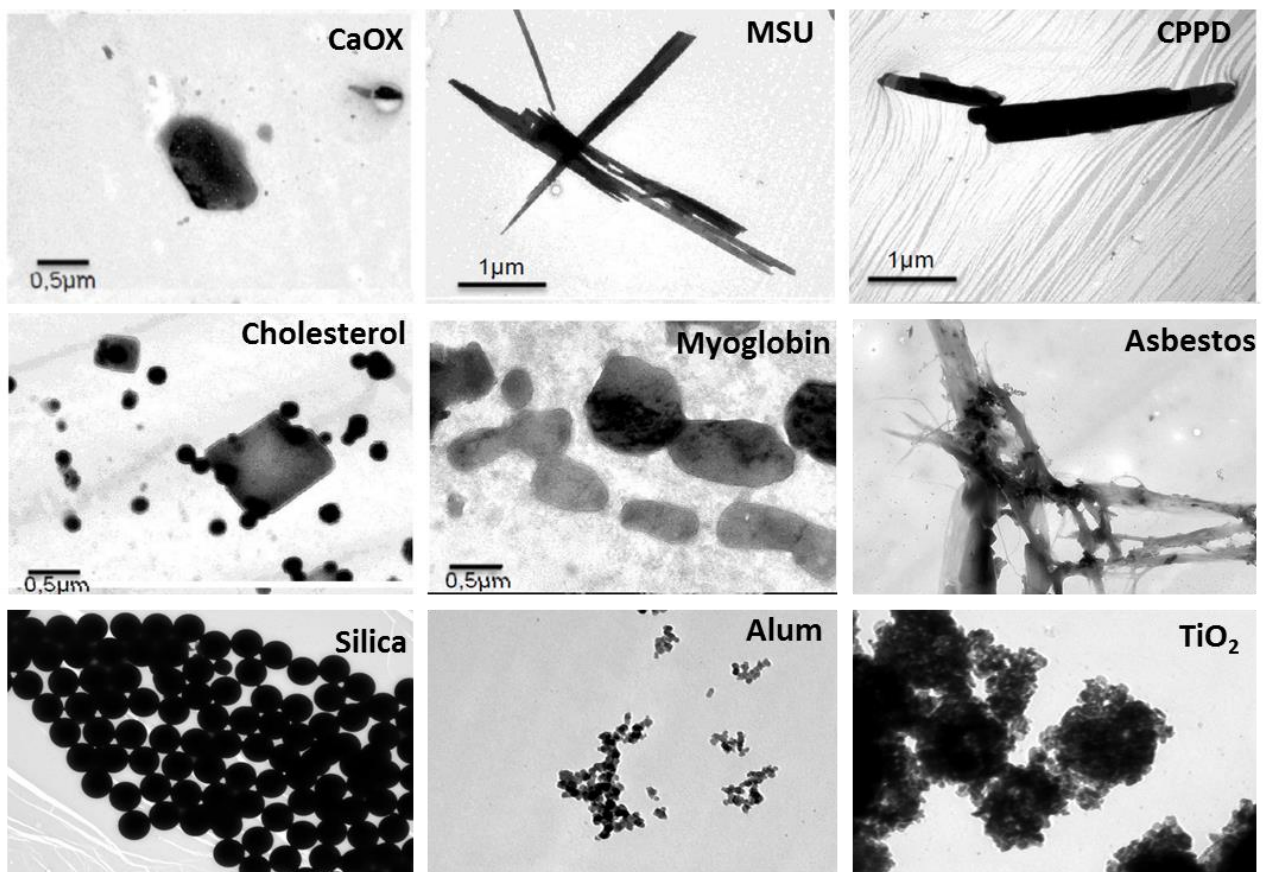
Figure 4: Transmission electron microscopy images of different crystals. Crystals were fixed with EM fixative and were subjected to perform TEM imaging. (Scale bar: 0.5 μm). CaOX: calcium oxalate, MSU: monosodium urate, CPPD: calcium pyrophosphate dihidrate, TiO_2: Titanium dioxide.
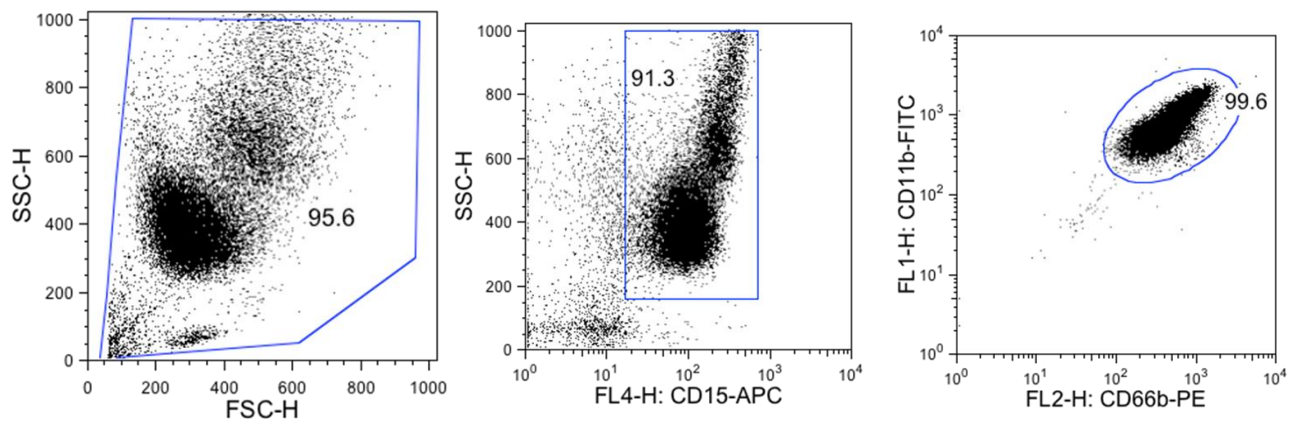
Figure 5: Flow cytometry of isolated human neutrophils. Human neutrophils were isolated using Ficoll. Density gradient and the obtained neutrophil pellet was stained for the surface markers, CD15, CD11b and CD66b. More than 95% purity was obtained for this isolation method.
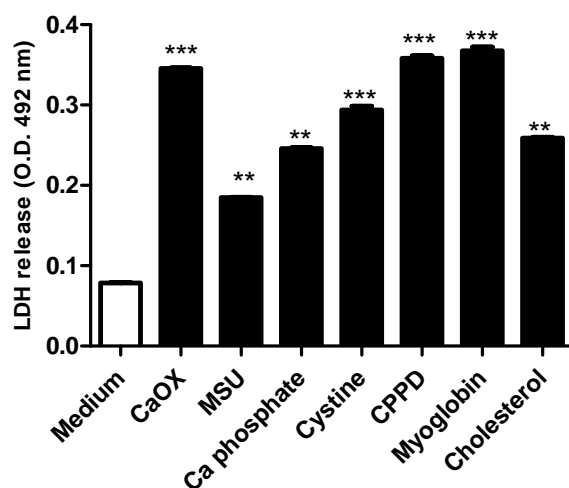
Figure 6: Various crystals induce necrotic cell death of neutrophils. Human primary neutrophils were exposed to different concentrations of CaOx, MSU, Calcium phosphate, CPPD, cysteine, Myoglobin and cholesterol crystals (500μg/ml). Cell death was assessed by LDH assay 2h later. Data are expressed as mean cell viability±s.e.m. of three independent experiments. Data were analyzed using Student's t-test. **P<0.01 and ***P<0.001 versus respective medium control. CaOX: calcium oxalate, MSU: monosodium urate, CPPD: calcium pyrophosphate dihidrate, TiO$_2$: Titanium dioxide.

It is known that crystals also exert direct cytotoxic effects leading to necrotic rather than apoptotic cell death. Since neutrophils are the first responder cells to reach the site of injury and infection, we were interested in understanding the interactions between crystals and neutrophils. Neutrophils were isolated from human peripheral blood. More than 95% pure

neutrophil population was obtained using Ficoll density gradient centrifugation (figure 5). Isolated neutrophils were then exposed to various crystals for 2 hours at 37°C. The supernatants were harvested and tested for LDH release. Almost all crystals led to necrotic cell death of neutrophils (figure 6).

To understand the morphology of neutrophil cell death upon crystal stimulation, we exposed primary neutrophils to various crystals for 2 hours and processed them for scanning electron microscopy and transmission electron microscopy. The SEM images (figure 7) showed that upon crystal stimulation, neutrophils undergo cell death that resembles NET formation and we observed NET-crystal aggregates upon stimulation of most of the crystals. Since NET formation can occur with or without cell death, we were interested in investigating the morphology of these crystal-induced NET like structures.
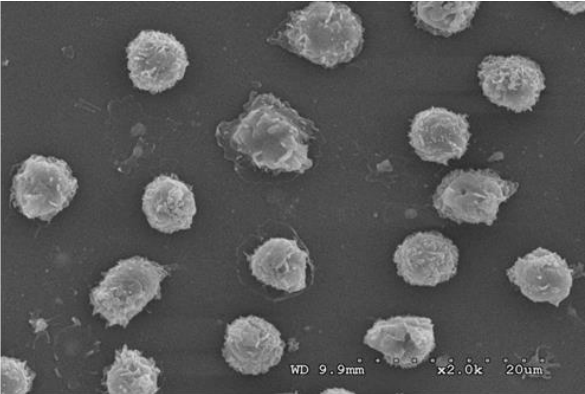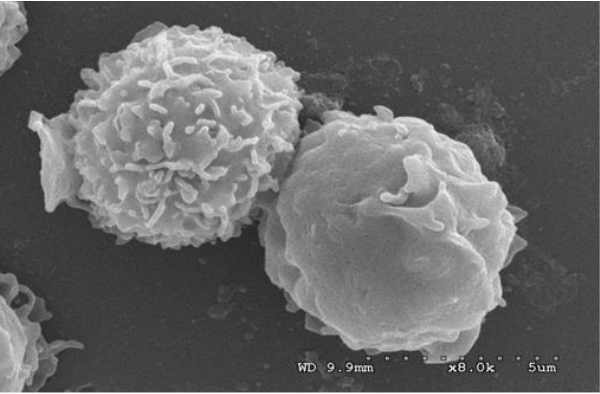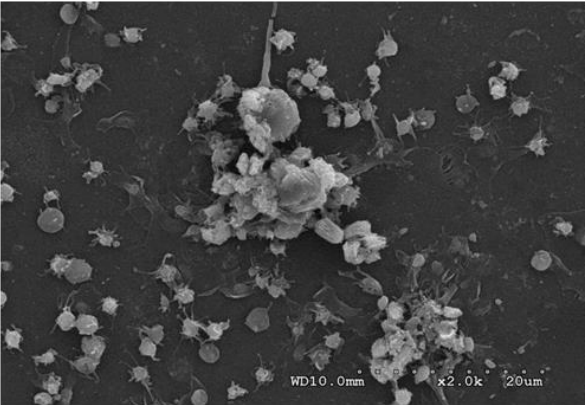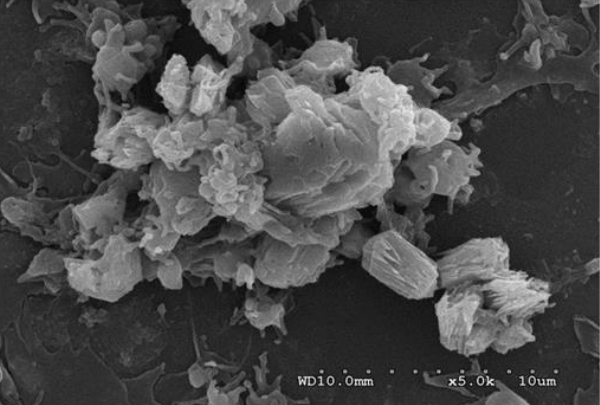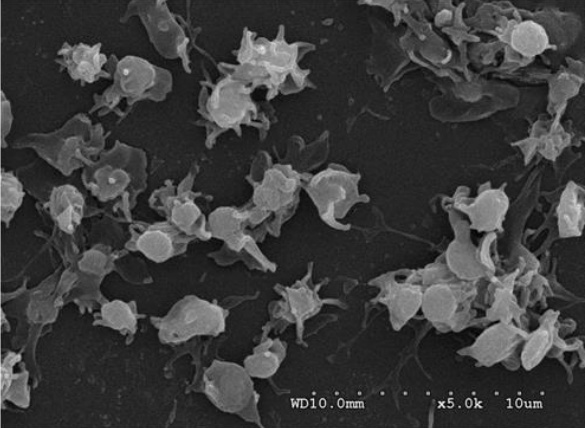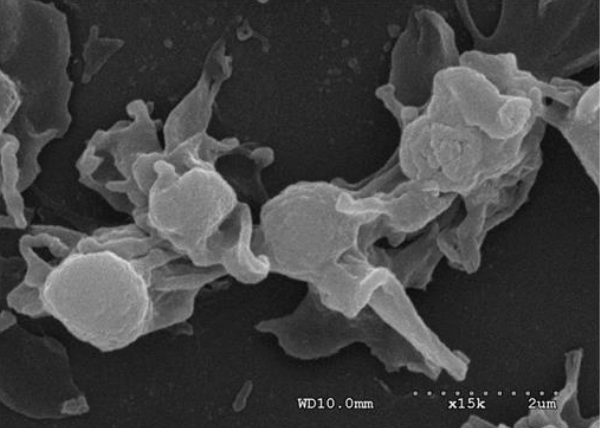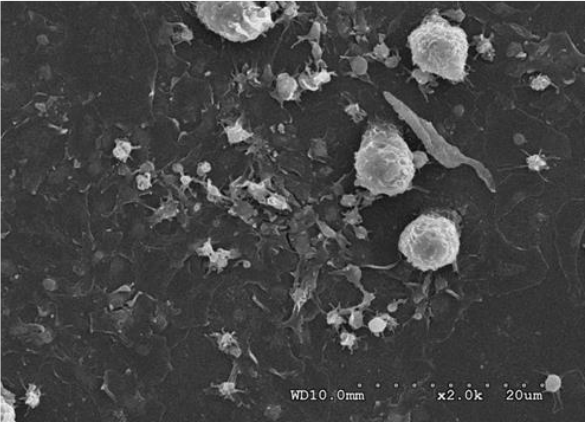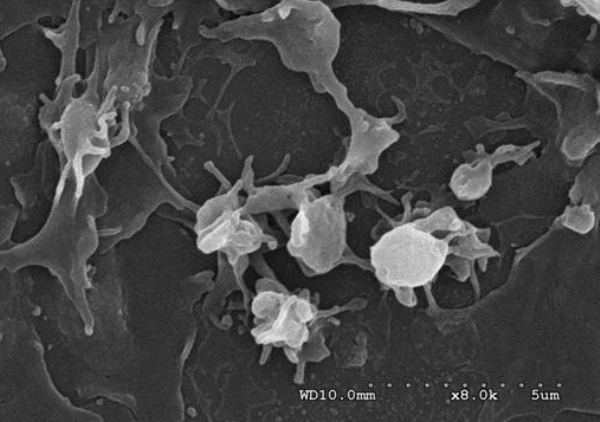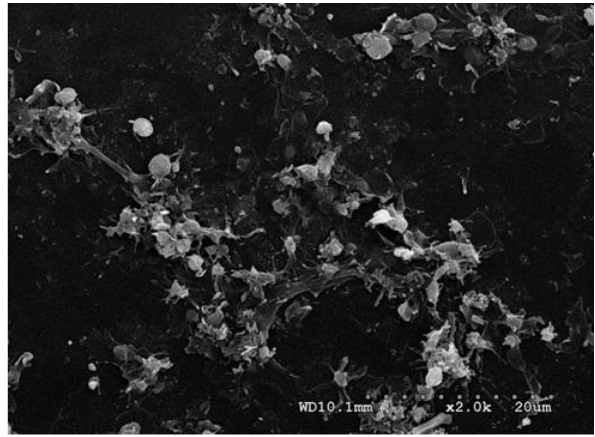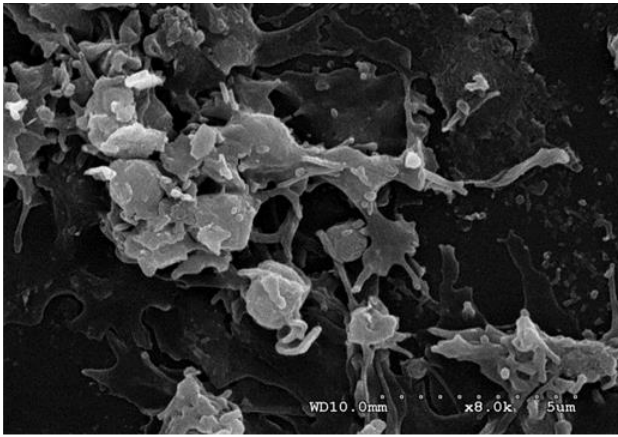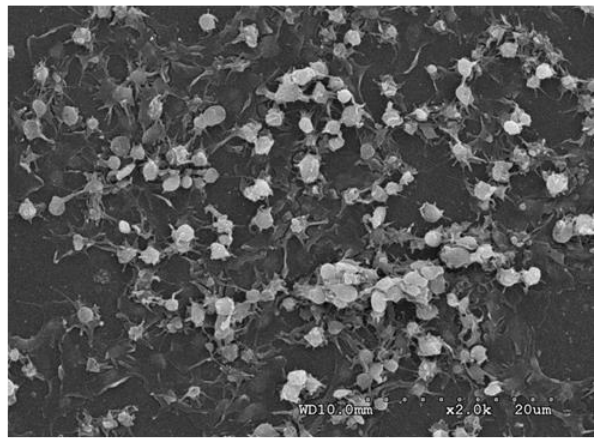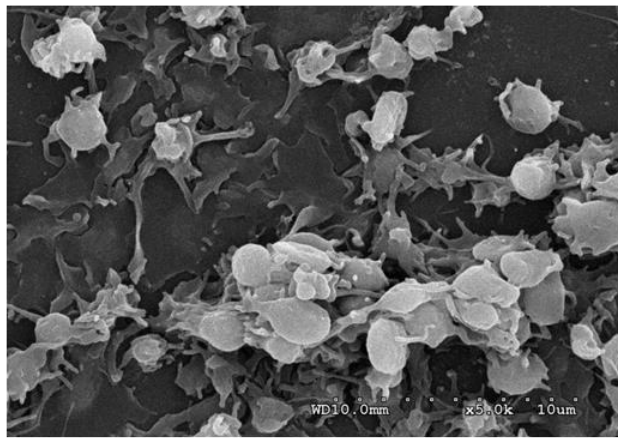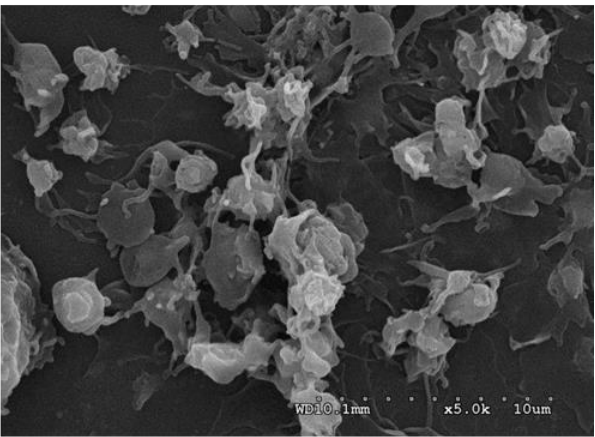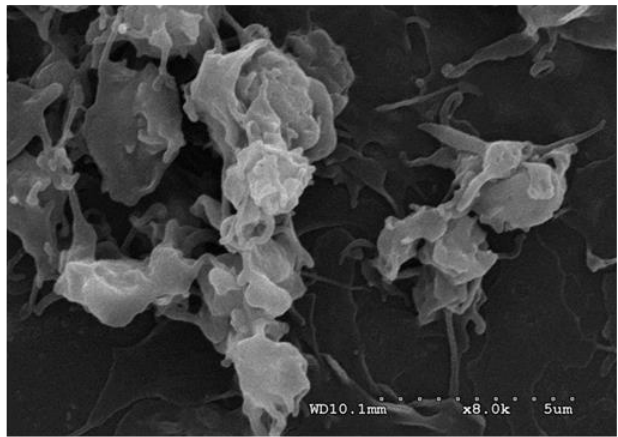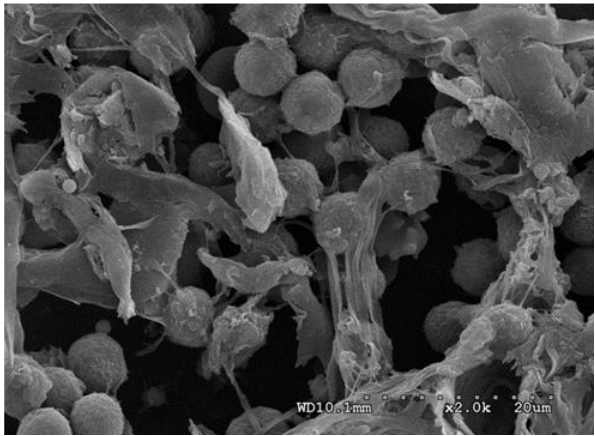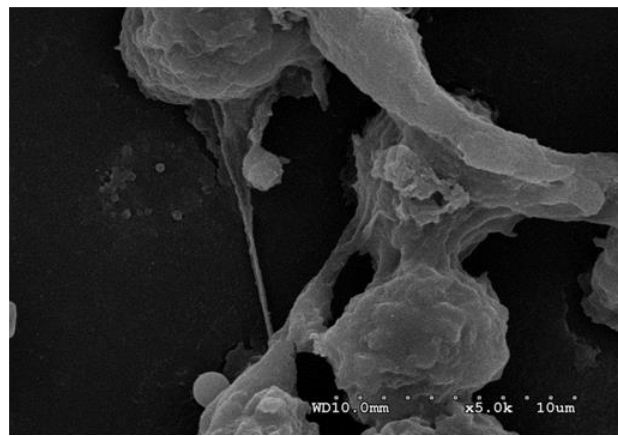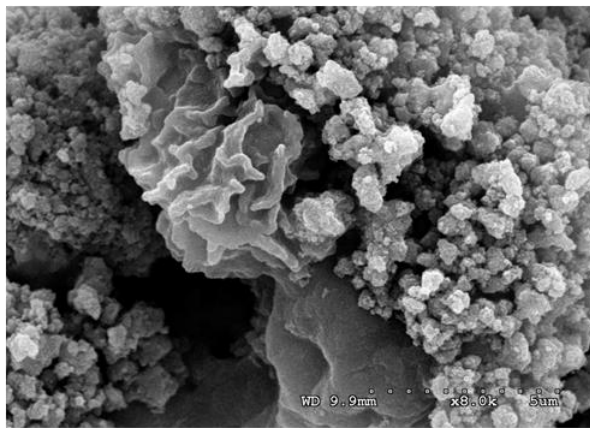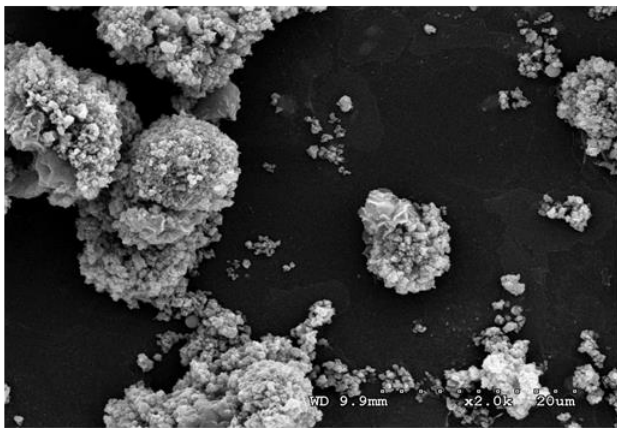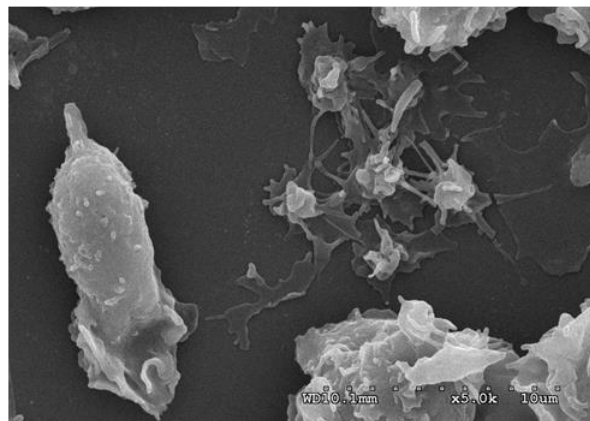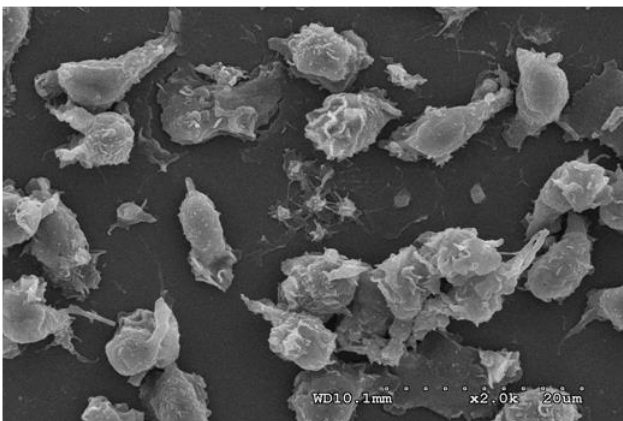
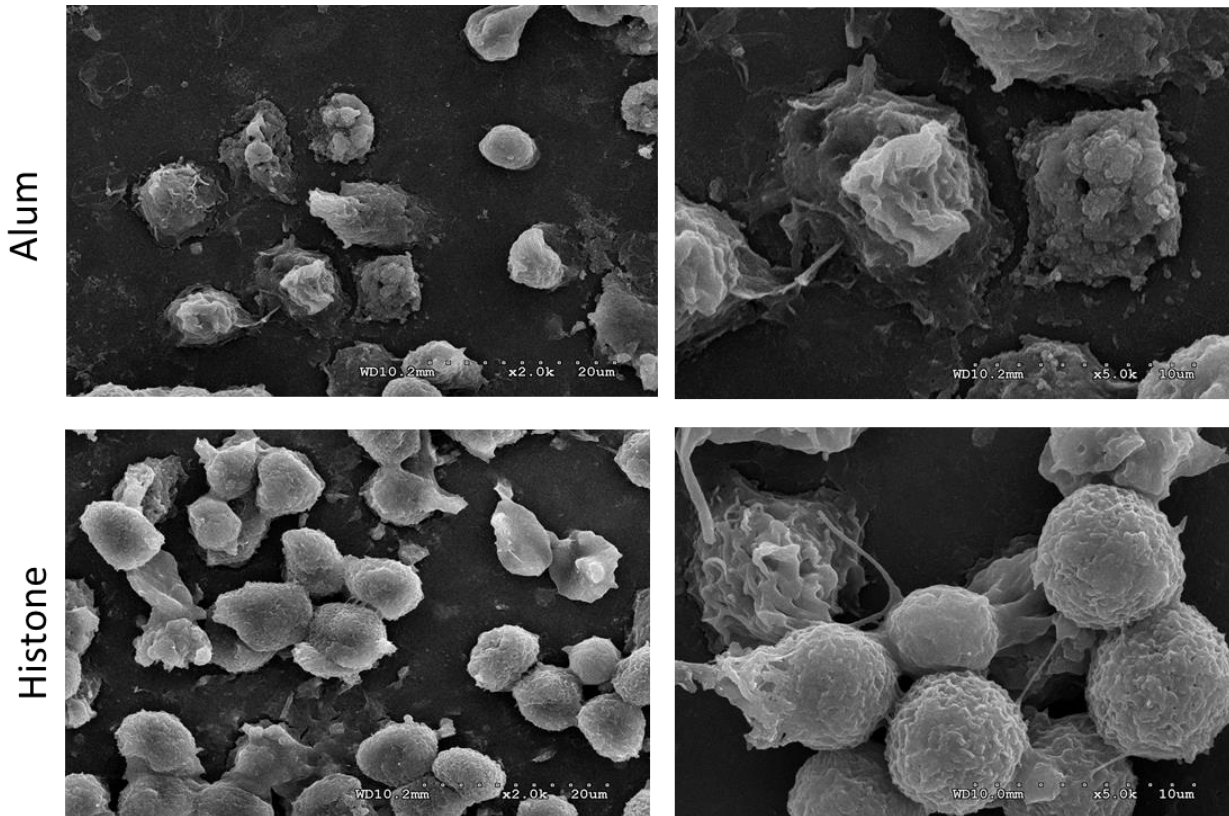Silica
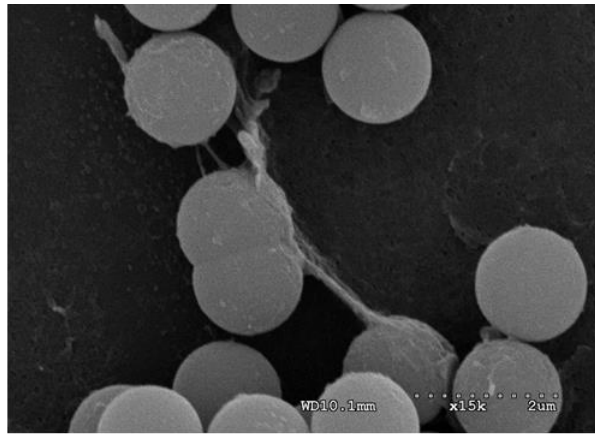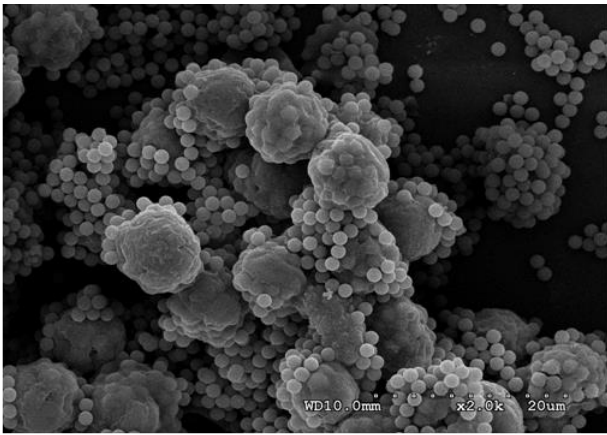
TiO2 20nm
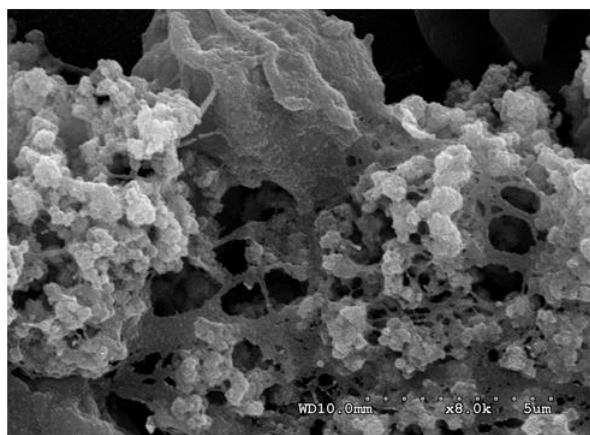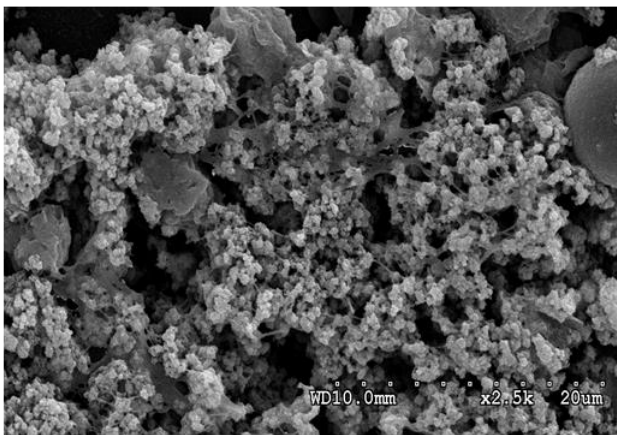
TiO2 80nm

Myoglobin

Figure 7: SEM images of neutrophils cell death and NET formation. Primary human neutrophils were fixed with EM fixative after 2h of various crystal stimulations. Images from each group are represented in both higher and lower magnifications. CaOX: calcium oxalate, MSU: monosodium urate, CPPD: calcium pyrophosphate dihidrate, TiO$_2$: Titanium dioxide.

For TEM, the primary neutrophils were stimulated with different crystals for 2 hours at 37°C in 1.5 ml eppendorf tubes and were fixed with EM fixative for 10 min at RT. The samples were processed further for TEM. We saw that upon stimulation with different crystals, most of the neutrophils appeared necrotic with plasma membrane ruptures. The nuclear material looked less condensed, leading to the assumption of chromatin being expelled during cell death. The TEM images (figure 8) showed that indeed the plasma membrane rupture was associated with neutrophil cell death upon crystal exposure, indicating NET related necrotic form of cell death. Furthermore, to study the crystal-NET aggregates, we performed immunofluorescence analysis of neutrophils stimulated with different crystals. Neutrophils were fixed with 4% paraformaldehyde post crystal stimulation. The cells were stained for NET markers: citH3, neutrophil elastase and DNA (figure 9). We observed that most of the crystals induced strong crystal-NET aggregates. These aggregates were not present, when neutrophils were treated with histones or myoglobin solutions. Thus, NET aggregates looked a very specific feature only associated with neutrophil-micro/nano particle interactions.
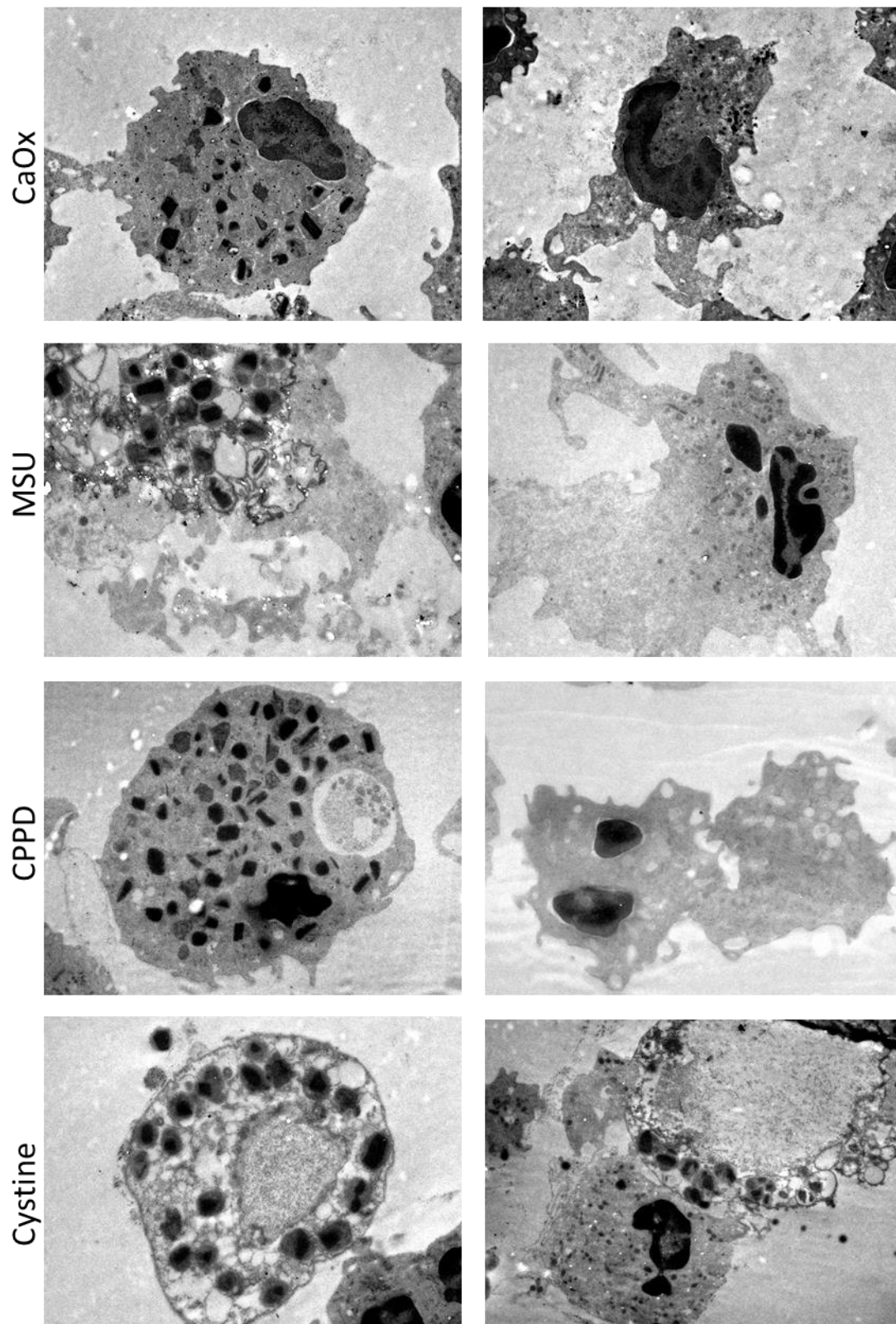
Figure 8: TEM images of neutrophil cell death upon crystal stimulation. Primary human neutrophils were fixed with EM fixative after 2h of various crystal stimulations. The neutrophil cell death appears to be associated with plasma membrane rupture and chromatin decondensation (Scale bar: 5µm) CaOX: calcium oxalate, MSU: monosodium urate, CPPD: calcium pyrophosphate dihidrate.
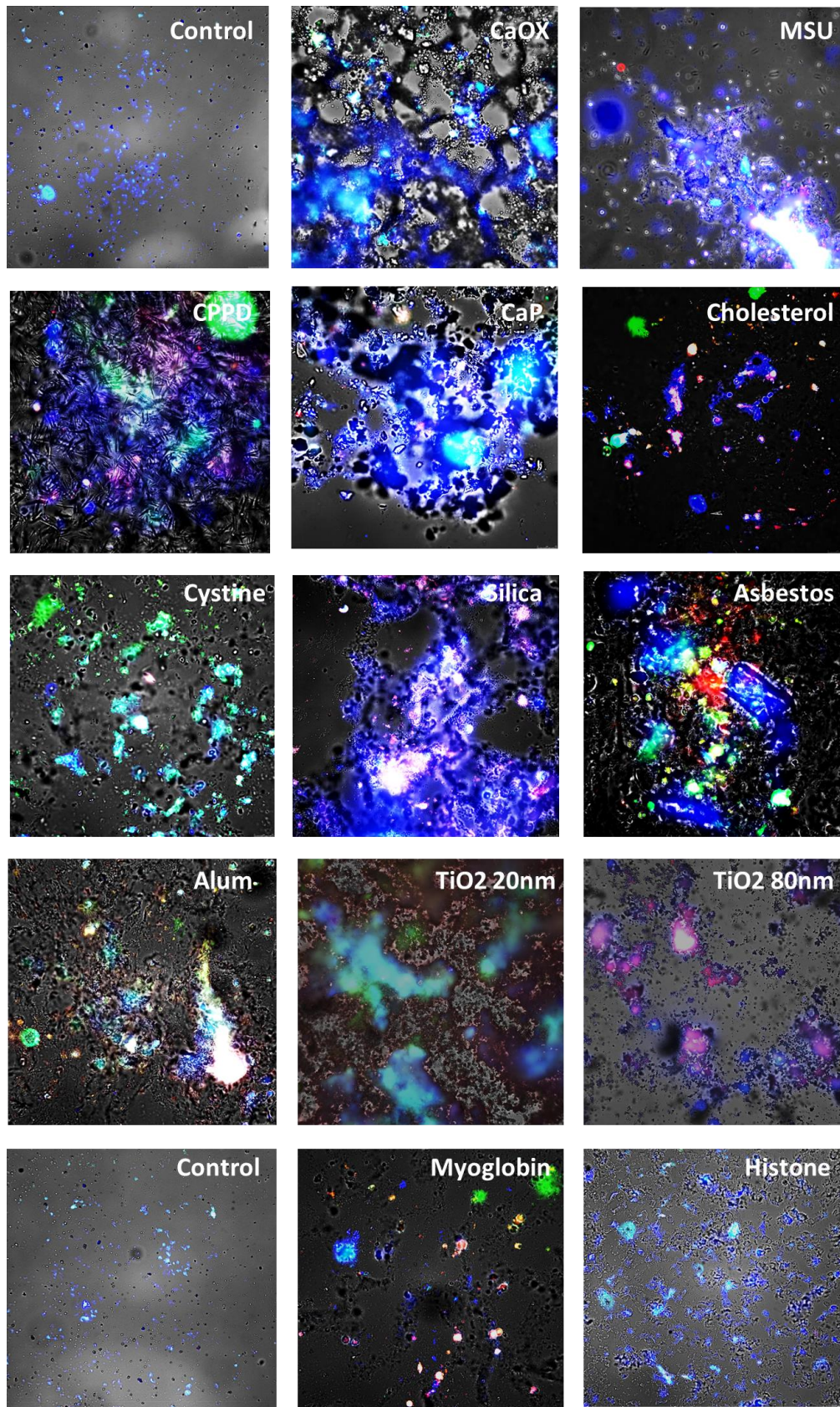
Figure 9: Immunofluorescence imaging of NET-crystal aggregates. Post 2h stimulation of human primary neutrophils with different crystals, cells were fixed and were stained for NET markers. (DNA: Blue, Neutrophil elastase: Green, citrunilated histone: Red). CaOX: calcium oxalate, MSU: monosodium urate, CaP: calcium phosphate, CPPD: calcium pyrophosphate dihidrate, TiO_2: Titanium dioxide.
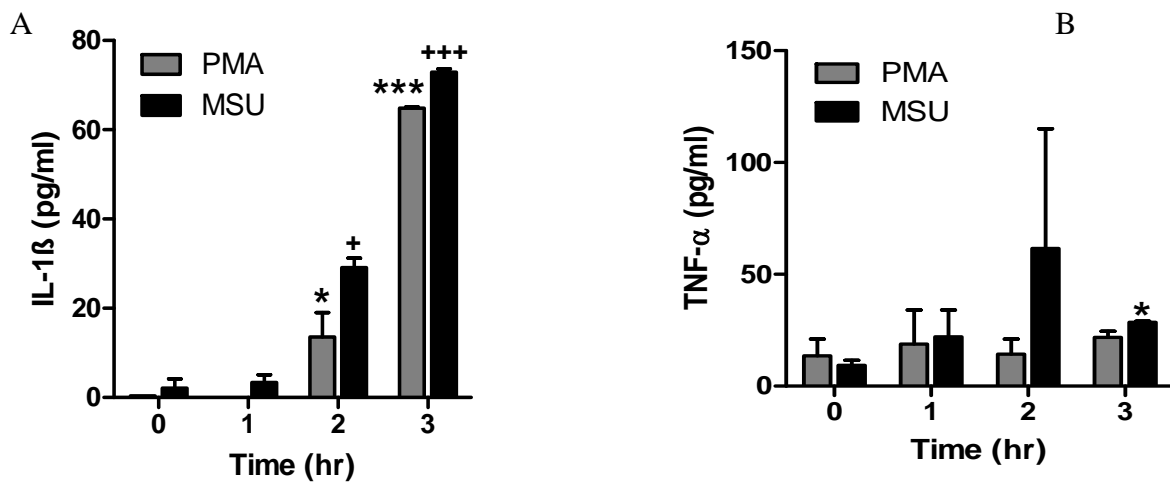
Figure 10: Human neutrophils were stimulated with either PMA or MSU for different time (0-3h). Release of IL-1β (A) and TNF-α (B) release in the supernatant was detected by ELISA. *p<0.05, +p<0.05, *** p<0.01, +++p<0.001 versus medium control. PMA: phorbol myristate acetate, MSU: monosodium urate.

4.2 Part II: Molecular mechanisms of MSU & PMA-induced NET formation & cell death

We specifically studied neutrophils since neutrophils are the first responder cells that reach at the site of crystal injury. We were particularly interested in dissecting the molecular mechanisms involved in MSU crystal-induced neutrophil NET formation and neutrophil cell death.

4.2.1 PMA and MSU induce release of IL-1β but not TNF-α from neutrophils

To analyze the chemokines and cytokines released during the PMA and MSU-induced NET formation as well as cell death, the supernatant of neutrophils was collected in a time-dependent manner (1-3 hours) after stimulations with PMA (25nM) and MSU crystals (20pg/cell). We observed that IL-1B was released in a time-dependent manner upon both PMA and MSU stimulations (figure 10A) for neutrophils isolated from healthy individuals. Whereas the cytokine TNFa was not released in a time-dependent manner during this process (figure 10 B).

4.2.2 Anakinra, etanercept, anti-TLR4, FAS deficiency do not block PMA & MSU induced NETs & cell death

To further check if the release of IL-1 or TNFa plays a role in the process of NET formation or cell death upon PMA and MSU crystal stimulations, the healthy control human neutrophils were pre-treated with the IL-1 receptor antagonist anakinra (dose) and TNFa

antagonist Etanercept followed by PMA or MSU crystal stimulations for 2 hours. The supernatant was collected and the DNA release into supernatant was checked using the Pico green assay to measure the cell death as well as NET release. Our data suggests that both the pre-treatment with neither anakinra nor etanercept had any effect on the DNA release upon PMA and MSU crystal stimulations (figure 11A). In fact, pre-treatment with TLR4 antibody did not affect the DNA release ruling out the role of TLR4 in this process (figure 11B). Moreover, the neutrophils isolated from Fas^{lpr} mice were able to form NETs and undergo cell death upon PMA and MSU which showed that the lack of Fas did not affect the neutrophil NETs and cell death (figure 11C).

4.2.3 Screening of different cell death inhibitors for PMA induced NETs and cell death

According to our hypothesis, we wanted to check if different cell death pathways are involved in the process of NETosis. We screened the chemical inhibitors of different cell death signaling pathways like pan-caspase inhibitor zVAD-FMK (10μM) for apoptosis, Stabilizer of RIPK1 necrostatin-1 and more specific necroptosis inhibitor necrostatin-1s for necroptosis or ferrostatin for the pathway of Ferroptosis (figure 12). The isolated human neutrophils from healthy controls were pre-treated with this cell death inhibitor for 30 min prior to stimulations with 25nM PMA, a standard NET and cell death inducer for 2h. The supernatant was harvested and the DNA release was measured using the Pico green assay. As shown in figure 13, neither zVAD-FMK nor ferrostatin-1 (Fer-1) had an effect, excluding caspase-mediated extrinsic apoptosis or pyroptosis, or ferroptosis respectively. In contrast, first-generation necrostatin Nec-1 and Nec-1s decreased overall cell death and NET formation as assessed by the release of DNA using Pico green dye. This indicated that RIP1-RIP3-MLKL mediated necroptosis cascade might be involved in the the process of neutrophil cell death.
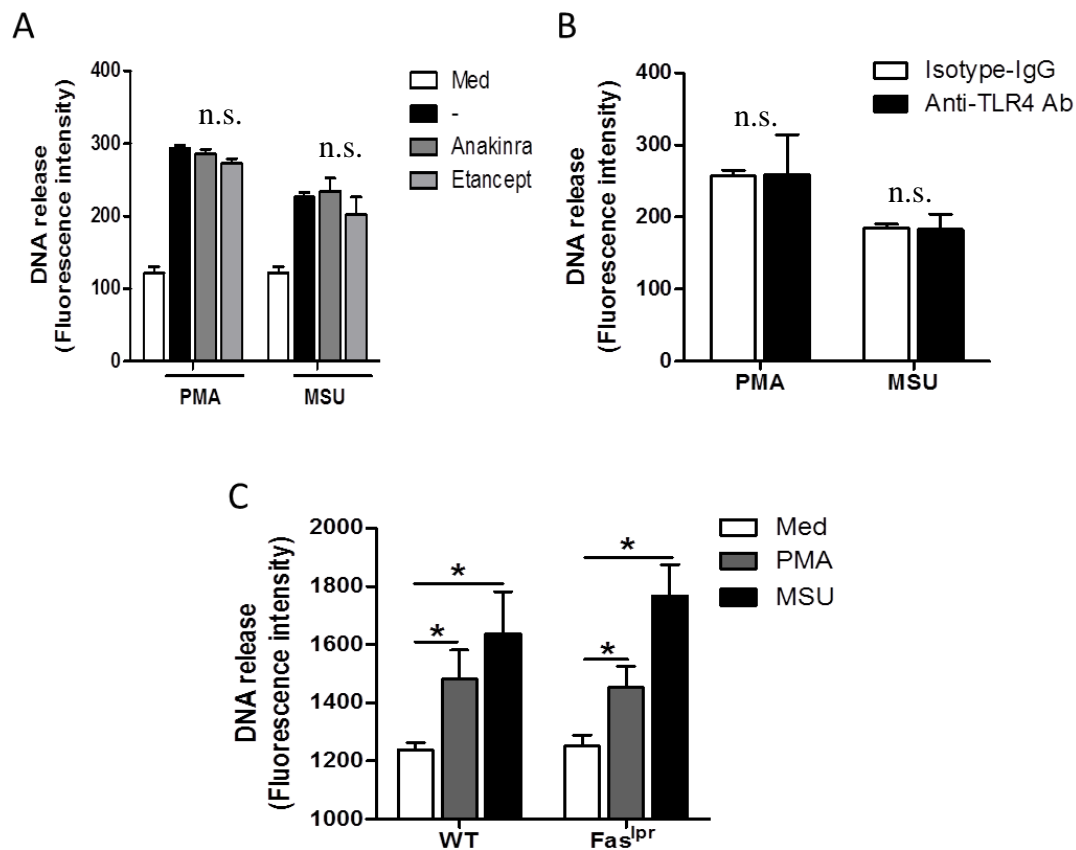
Figure 11: DNA release into the supernatant 2 hours after stimulation with either PMA or MSU crystals was quantified by PicoGreen. Human neutrophils were prestimulated with either Anakinra (IL-1R1 antagonist) (100ng/ml) or Etanercept (TNF-α antagonist) (100ng/ml) (D), Isotype IgG control antibody or anti-TLR4 neutralizing antibody (100ng/ml) (E) before adding either PMA or MSU crystals. F: Neutrophils were isolated from wild type and C57-BL6lpr mice, and were stimulated with either PMA or NSA. DNA release into the supernatant 2 hours after stimulation was quantified by PicoGreen. Data are means ± standard error of mean from three independent experiments. *p<0.05, N.S: not significant versus medium control. PMA: phorbol myristate acetate, MSU: monosodium urate.

4.2.4 Nec-1 and NSA inhibit overall PMA-induced NET formation and cell death

To address the involvement of the necroptosis cascade in PMA-induced NETs and neutrophil cell death, neutrophils isolated from healthy individuals were pre-treated with different doses of Nec-1 and Nec-1s. Nec-1 inhibits necroptosis via modulating RIPK1 and preventing downstream events of RIPK3 and MLKL phosphorylation and necrosome formation. Furthermore, we also pre-treated neutrophils with different doses of human species specific MLKL inhibitor necrosulfanamide (NSA).
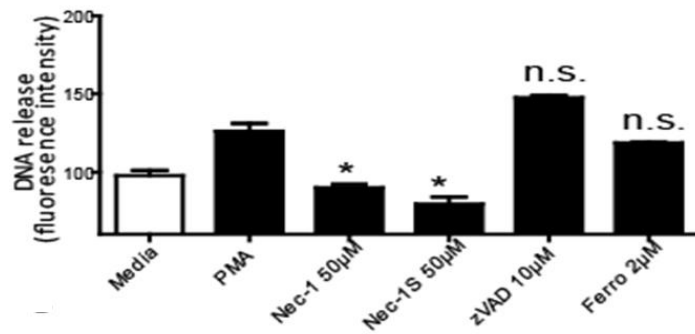
Figure 12: Human neutrophils were exposed to PMA in the presence of several cell death inhibitors Nec-1 (50 µM), Nec-1s (50 µM), zVAD-FMK (10 µM), and Ferrostatin-1 (Fer-1, 2 µM) as indicated. DNA release into the supernatant was quantified by PicoGreen detection after 2 h as a marker of NET-related chromatin release. *p<0.05 versus PMA treatment. PMA: phorbol myristate acetate, Nec-1: necrostatin-1, zVAD: pan-caspase inhibitor, Ferro: ferrostatin-1.

MLKL is a downstream protein of the necrosome complex. We observed that treatment with first-generation Nec)-1, Nec-1s, and the NSA decreased overall cell death and NET formation as assessed by nuclear SYTOX uptake, the release of DNA using Pico green dye, and chromatin release to induce NET structures (figures 13-16). Ultrastructurally, Nec-1 or NSA inhibited the rupture of nuclear and plasma membranes of neutrophils upon PMA stimulation (figure 17).
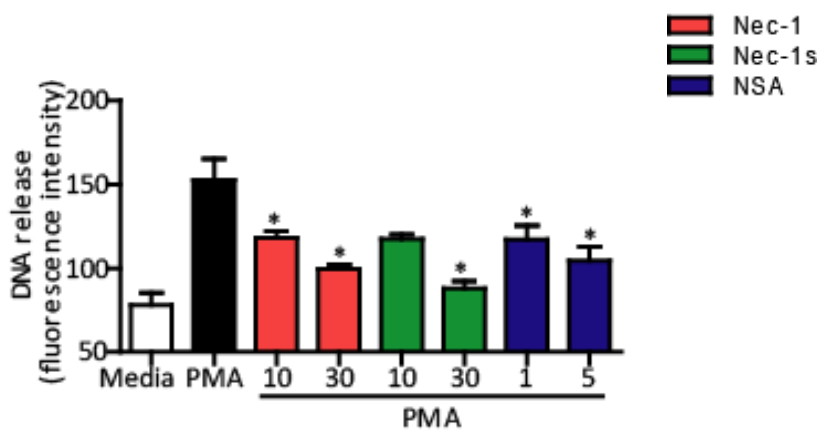
Figure 13: DNA release into the supernatant after exposure to PMA was quantified by PicoGreen detection after 2h as a marker of NET-related chromatin release. All data are expressed as means ± SE of the mean from three independent experiments. *p < 0.05 versus PMA. PMA: phorbol myristate acetate, nec-1: necrostatin-1, NSA: necrosulfanamide.

.

Figure 14: SYTOX green immunofluorescence 2h after 25nm PMA exposure to human neutrophils in after pretreatment with either necrostatin-1 (Nec-1) or necrosulfonamide (NSA) as indicated. SYTOX green detects permeability of plasma and nuclear membranes. Representative images are shown at an original magnification of 200x. PMA: phorbol myristate acetate, nec-1: necrostatin-1, NSA: necrosulfanamide.
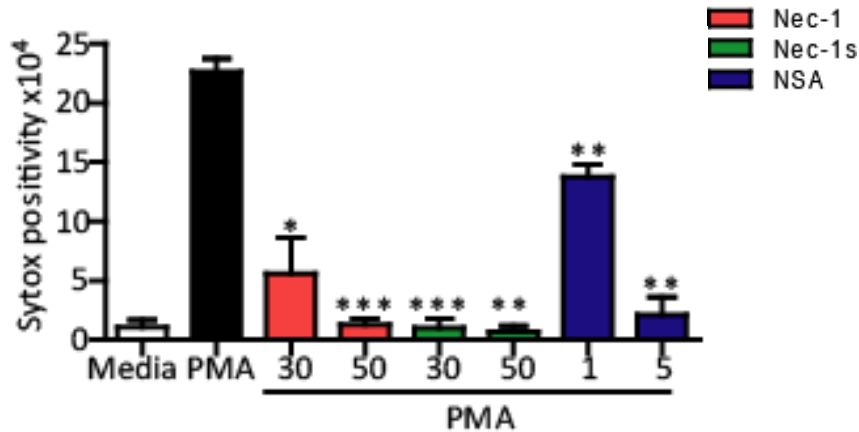
Figure 15: A quantitative analysis of Sytox+ve dead cells, NETs after 2h of PMA exposure is shown as means ± SE of the mean from three independent experiments. All data a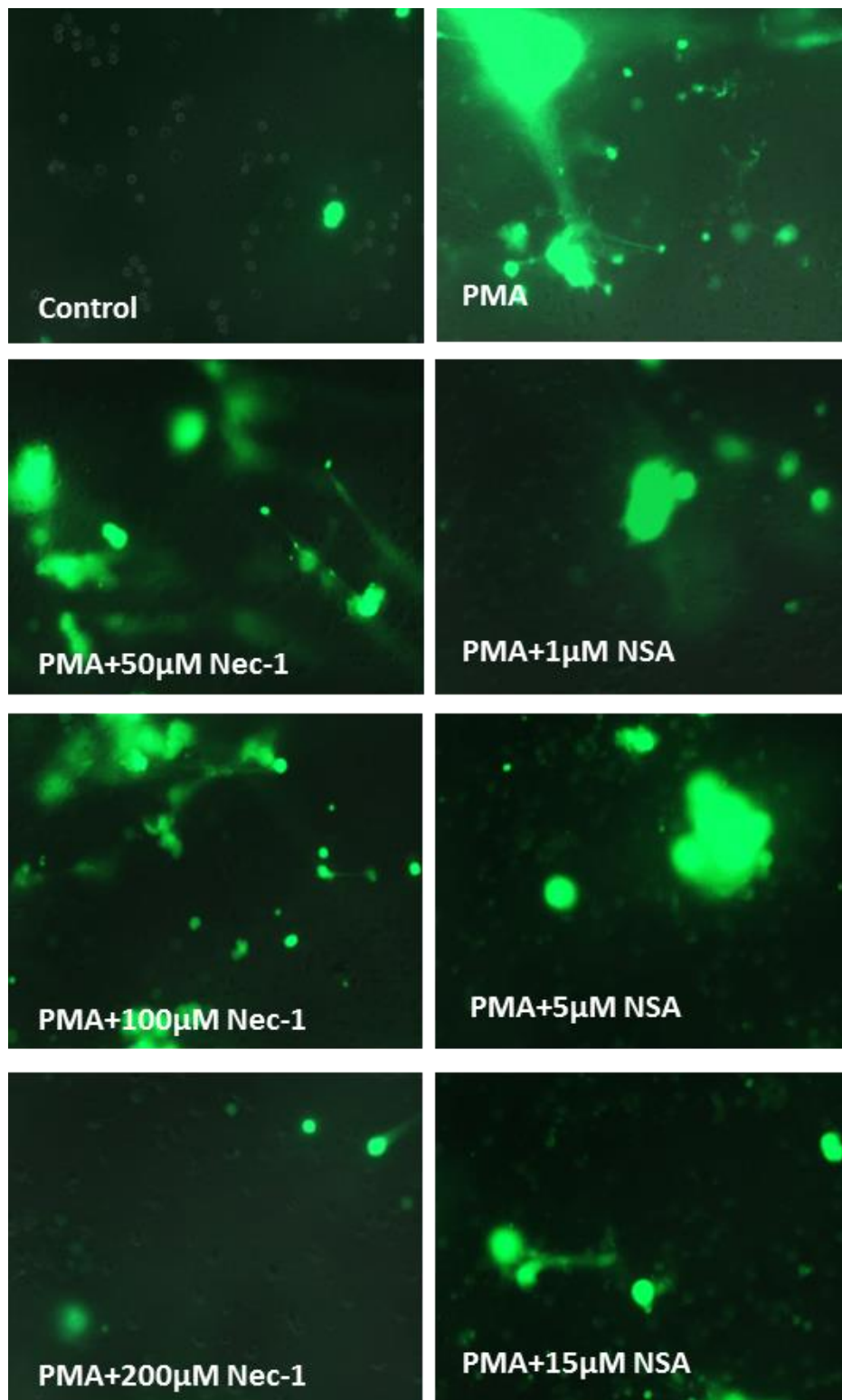re expressed as means ± SE of the mean from three independent experiments. *p < 0.05, **p < 0.01, ***p < 0.001 versus PMA. PMA: phorbol myristate acetate, nec-1: necrostatin-1, NSA: necrosulfanamide.

Figure 16: Confocal microscopy of human neutrophils post stimulating with 25nm PMA for 2h after pretreatment with either necrostatin-1 (Nec-1) or necrosulfonamide (NSA) as indicated stained with FITC-antihistones (green) and TOPRO (blue) to detect histones and DNA in extracellular traps. Representative images are shown at an original magnification of 400x. PMA: phorbol myristate acetate, nec-1: necrostatin-1, NSA: necrosulfanamide.
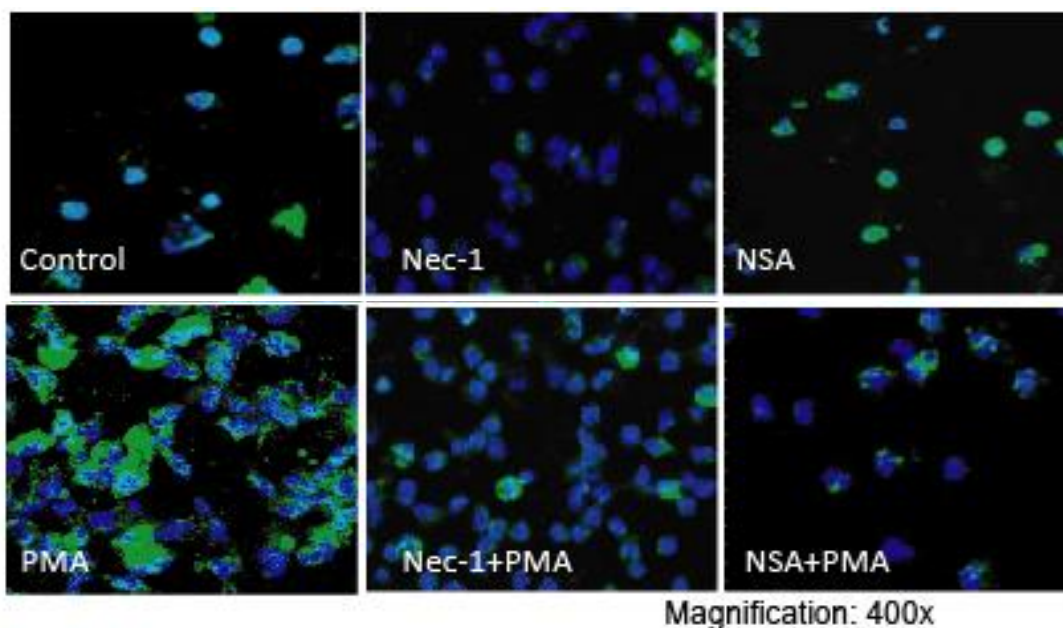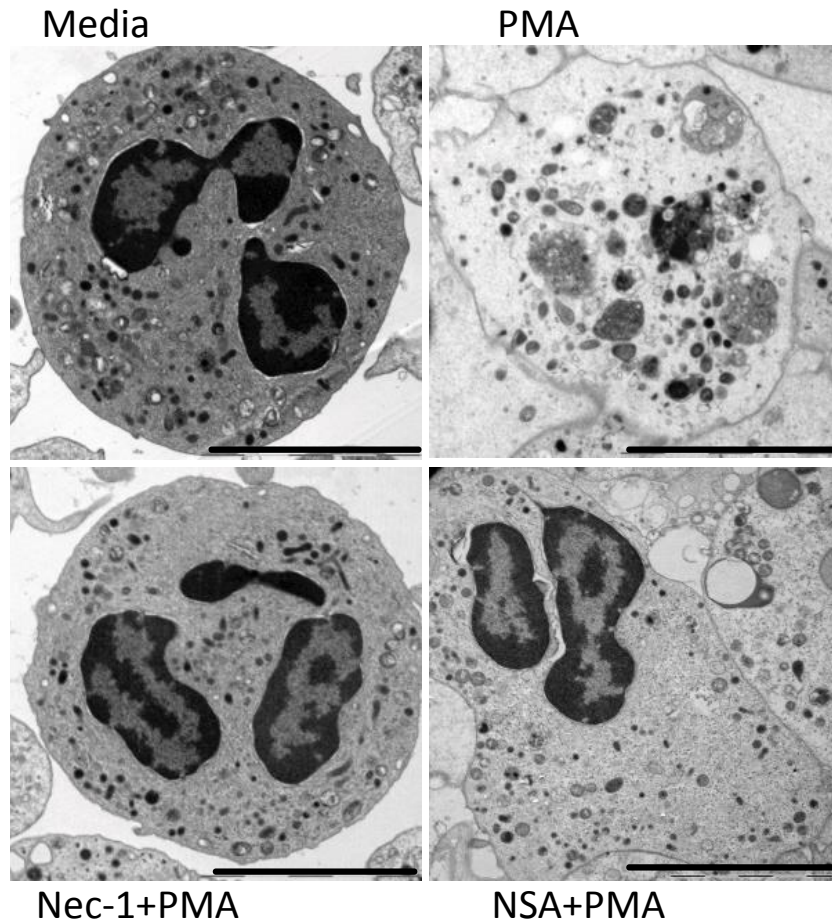
Figure 17: Transmission electron microscopy images of human neutrophils exposed to PMA in the presence or absence of necrostatin-1 (Nec-1) or NSA (scale bar: 5 μm). PMA: phorbol myristate acetate, nec-1: necrostatin-1, NSA: necrosulfanamide.

4.2.5 RIPK3 and p-MLKL is upregulated during PMA induced cell death and NETs

RIPK3 and MLKL proteins are central players of the necrosome complex that initiate and carry out necroptosis. During activation of this pathway, RIPK3 is upregulated and eventually phosphorylated. RIPK3 further phosphorylates the downstream MLKL protein. Phosphorylation of MLKL is a crucial event of the necroptosis cascade. Since RIPK3 is known to be involved in other signaling pathways, phosphorylation of MLKL is considered to be the best hallmark of necroptosis on-set. We found that both RIPK3 and phosphorylation of MLKL are upregulated in a time-dependent manner (0-3h) during PMA induced NET formation and neutrophil cell death (figure 18).

Overall, the data indicate that PMA, which is a very common stimulous for NET induction is activating the RIPK1-RIPK3-MLKL mediated necroptosis, cell death cascade. This is followed by plasma membrane rupture and release of the NETs in extracellular space.
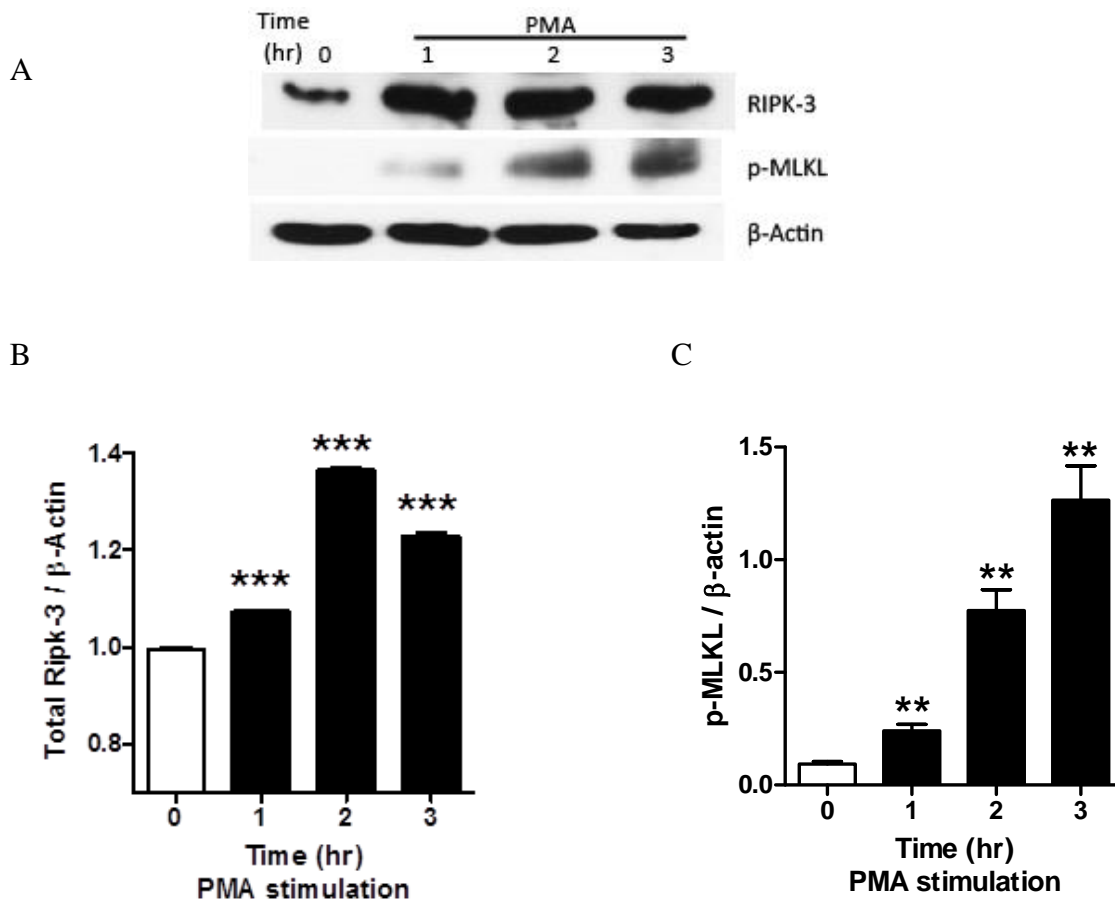
Figure 18: Western blot for RIPK3 and phosphorylated MLKL at different time points after PMA stimulation of human neutrophils. β-Actin serves as loading control (n=3). B), C) Quantitative analysis of Western blots at different time points for RIPK3 and P-MLKL after PMA stimulation of human neutrophils. ** $p < 0.01$, *** $p < 0.001$ versus baseline. PMA: phorbol myristate acetate, Ripk3: receptor interacting kinase 3, p-MLKL: phosphor mixed lineage kinase like.

4.2.6 Nec-1 and NSA inhibit both MSU-induced NET formation and cell death

PMA is a commonly used NET inducer *in-vitro*. However, it is not a physiologically relevant stimulous that is associated with infectious or inflammatory diseases, in-vivo. To understand the involvement of necroptosis in NET related neutrophil cell death, we focused on another stimulous MSU crystals, associated with the pathophysiology of gout. MSU crystals trigger NET formation, which first drives massive inflammation and subsequently fosters the resolution of inflammation, explaining both gouty arthritis and tophus related immune energy. We exposed human neutrophils isolated from healthy individuals to MSU

crystals for 2h in-vitro. MSU crystals are known to form NETs. We observed that pre-treatment with different doses of Nec-1 and NSA followed by MSU crystal stimulations decreased overall cell death and NET formation as assessed by nuclear SYTOX uptake, the release of DNA using Pico green dye, and chromatin release to induce NET structures (figures 19-21).
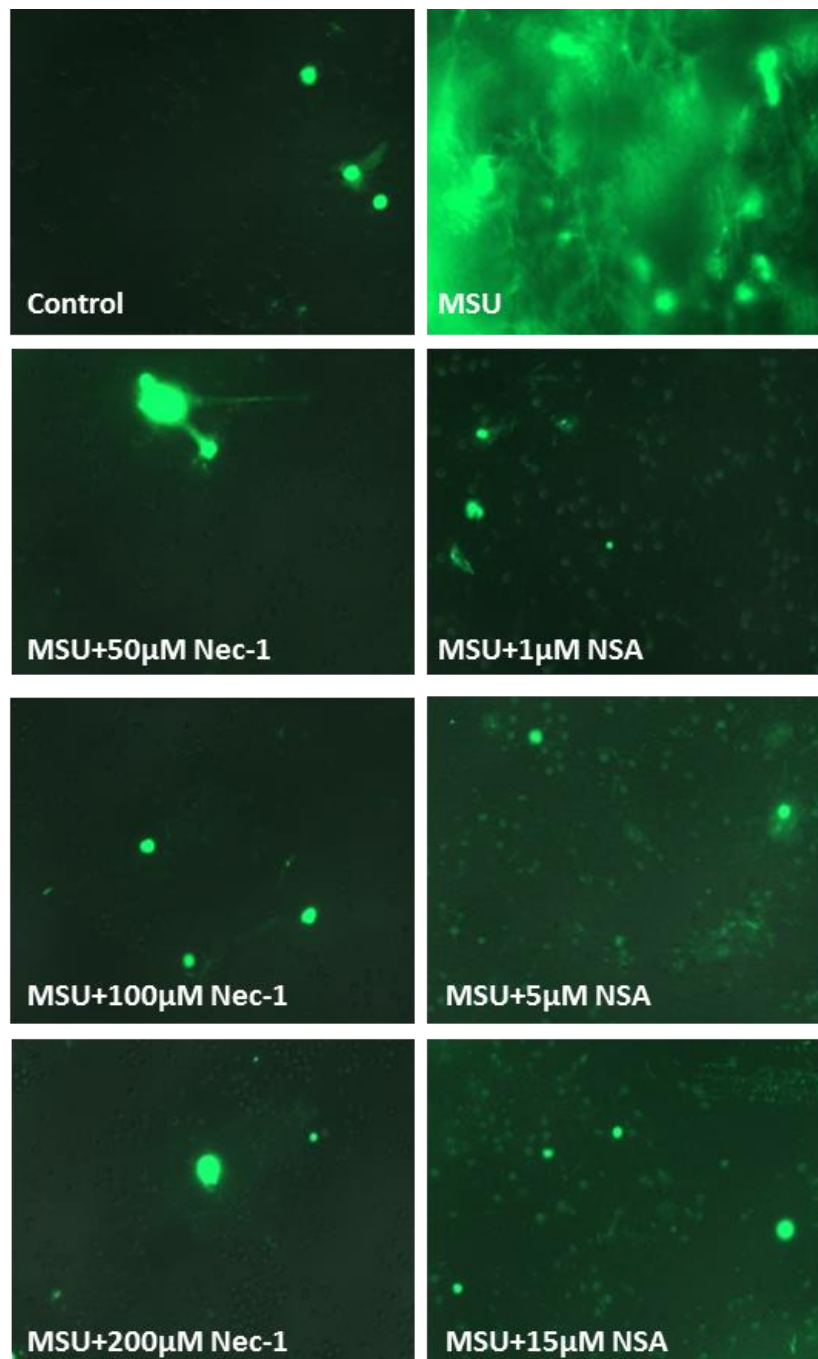
Figure 19: SYTOX green immunofluorescence 2h after 20pg/cell MSU exposure to human neutrophils in after pretreatment with either necrostatin-1 (Nec-1) or necrosulfonamide (NSA) as indicated. SYTOX green detects permeability of plasma and nuclear membranes. Representative images are shown at an original magnification of 200x.
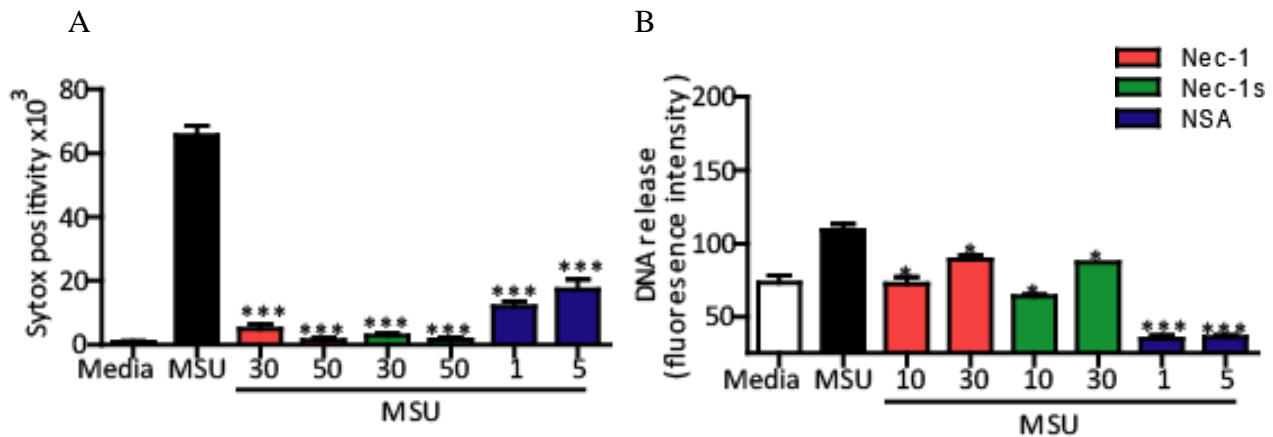
Figure 20: A) A quantitative analysis of Sytox+ve dead cells, NETs is shown as means ± SE of the mean from three independent experiments. B) DNA release into the supernatant after exposure to MSU crystals was quantified by PicoGreen detection after 2h as a marker of NET-related chromatin release. All data are expressed as means ± SE of the mean from three independent experiments. *p < 0.05,   ***p < 0.001 versus MSU. MSU: monosodium urate, nec-1: necrostatin-1, NSA: necrosulfanamide.
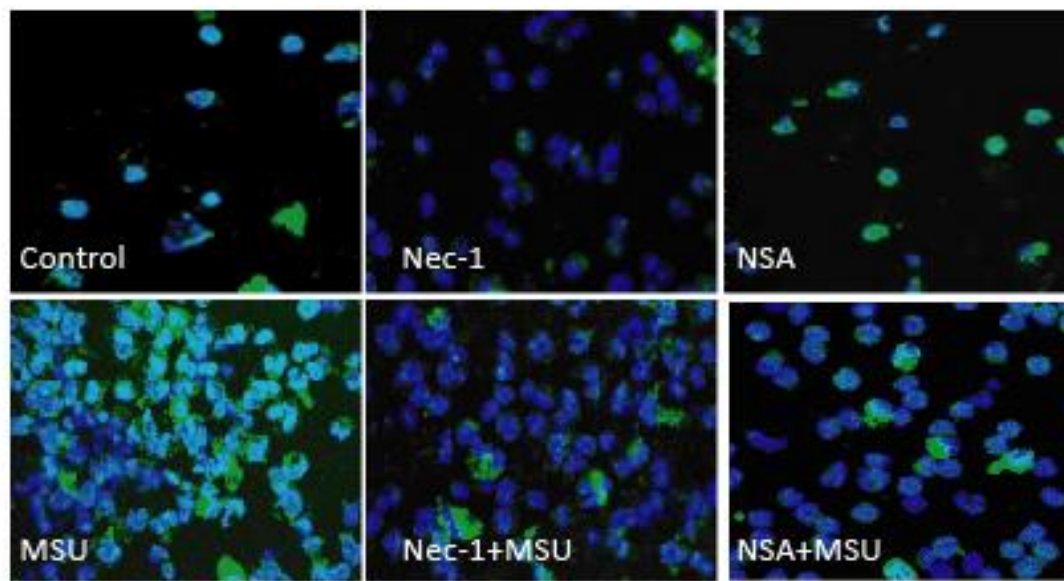
Figure 21: Confocal microscopy of human neutrophils post stimulating with 20pg/cell MSU crystals for 2h after pretreatment with either necrostatin-1 (Nec-1) or necrosulfonamide (NSA) as indicated stained with FITC-antihistones (green) and TOPRO (blue) to detect histones and DNA in extracellular traps. Representative images are shown at an original magnification of 400x. MSU: monosodium urate, nec-1: necrostatin-1, NSA: necrosulfanamide.

Moreover, Nec-1 or NSA inhibited the rupture of nuclear and plasma membranes of neutrophils upon PMA stimulation as observed in their ultrastructural appearances using TEM (figure 22).
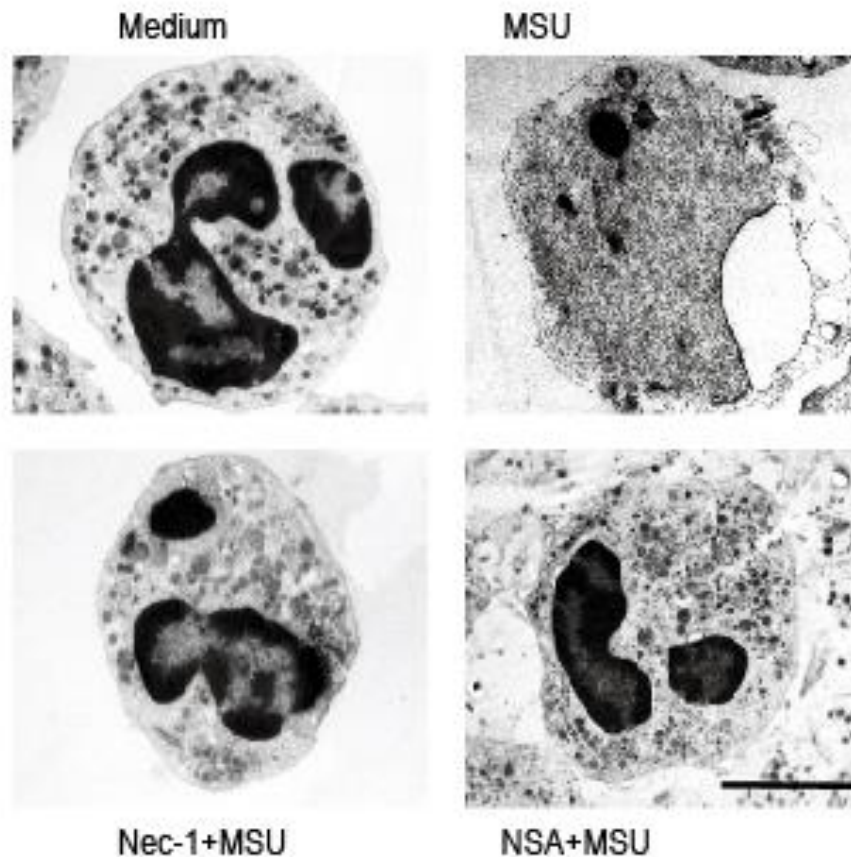
Figure 22: Transmission electron microscopy images of human neutrophils exposed to MSU in the presence or absence of necrostatin-1 (Nec-1) or NSA (scale bar: 5 μm). . MSU: monosodium urate, nec-1: necrostatin-1, NSA: necrosulfanamide.

4.2.7 p-MLKL is upregulated in MSU crystal-induced NET formation and cell death

In addition to the pharmacological inhibition of the RIP1-RIP3-MLKL mediated necroptosis pathway in MSU crystal-treated human neutrophils, we checked if the necroptosis cascade was activated during the MSU crystal-induced NET formation and neutrophil cell death. Human neutrophils isolated from the healthy controls were subjected to MSU crystals (20pg/cell) exposure for 0-2h. The cells were harvested and the expression of phosphor-MLKL was checked. As mentioned earlier, phosphorylation of MLKL protein is considered to be the most important and exclusive event of the onset of necroptosis cascade. We observed that indeed, the MLKL phosphorylation increased in a time-dependent manner upon MSU crystal stimulations, confirming the activation of necroptosis pathway during MSU crystal-induced neutrophil NET formation and cell death (figure 23).

Taken together, our data show the importance of necroptosis pathway during MSU crystal-induced neutrophil cell death. This to our knowledge is the first evidence of the involvement of necroptosis during the event of NETosis.

A

B
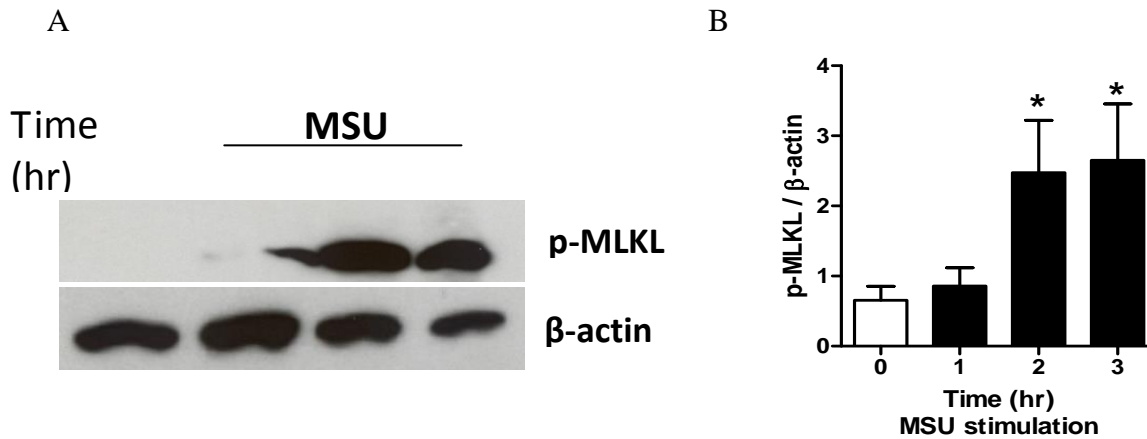
Figure 23: (A) Phospho-MLKL western blot after MSU stimulation of human neutrophils. (B) Phospho-MLKL quantification after MSU stimulation of human neutrophils. β-actin was used as loading control. (n=3). *$p<0.05$, ** $p<0.01$, *** $p<0.001$ versus baseline. . MSU: monosodium urate, p-MLKL: phosphor mixed lineage kinase like.

4.2.8 ROS production is upstream of p-MLKL in PMA and MSU-induced NETs and cell death

Generation of ROS is one of the key features of the NET formation event. We were further interested in checking if ROS are generated before or after the activation of necroptosis upon PMA or MSU crystal-induced NET formation and neutrophil cell death. We pre-treated the human neutrophils with Nec-1 or NSA before PMA or MSU crystal stimulations for 2h. After collecting the supernatant, we measured the quantity of ROS in the supernatant by using DCFDA dye (figure 24A and 24B). We observed no significant difference in ROS generation upon Nec-1 and NSA treatment suggesting that ROS might be produced upstream of the RIP1-RIP3-MLKL mediated cell death upon PMA and MSU stimulations. Moreover, we observed that MLKL phosphorylation was abrogated in neutrophils of patients with CGD upon PMA stimulation (figure 25). All in all, our experiments indicate the possibility of ROS being generated upstream of necroptosis.

A

B
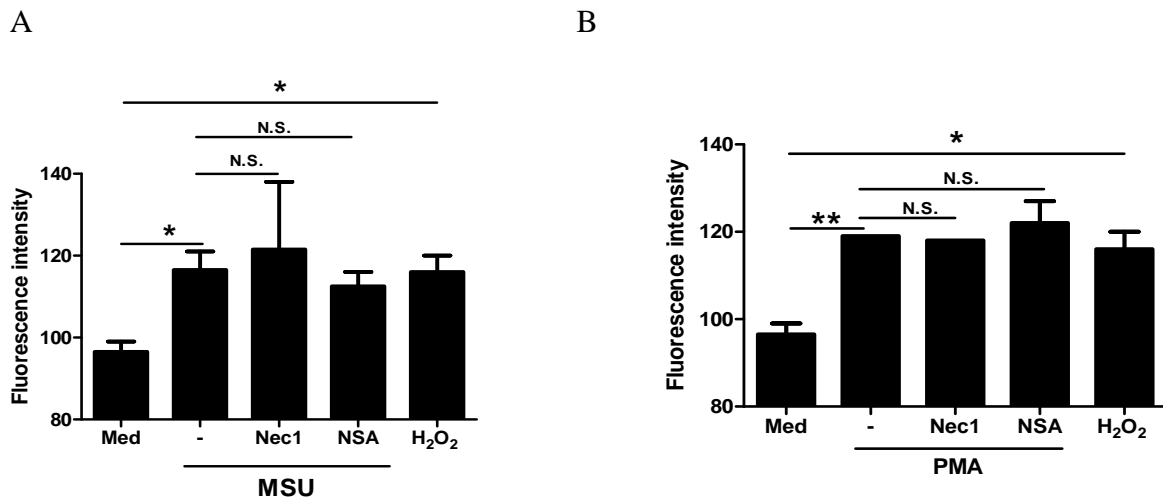
Figure 24: Human neutrophils were pre-stimulated with either Nec-1 or NSA before adding PMA (A) or MSU (B). ROS were quantified using DCFDA dye. H2O2 was used as a positive control. Data are means ± standard error of mean. *p<0.05, **p<0.01, *** p<0.01 versus medium control.

A

B
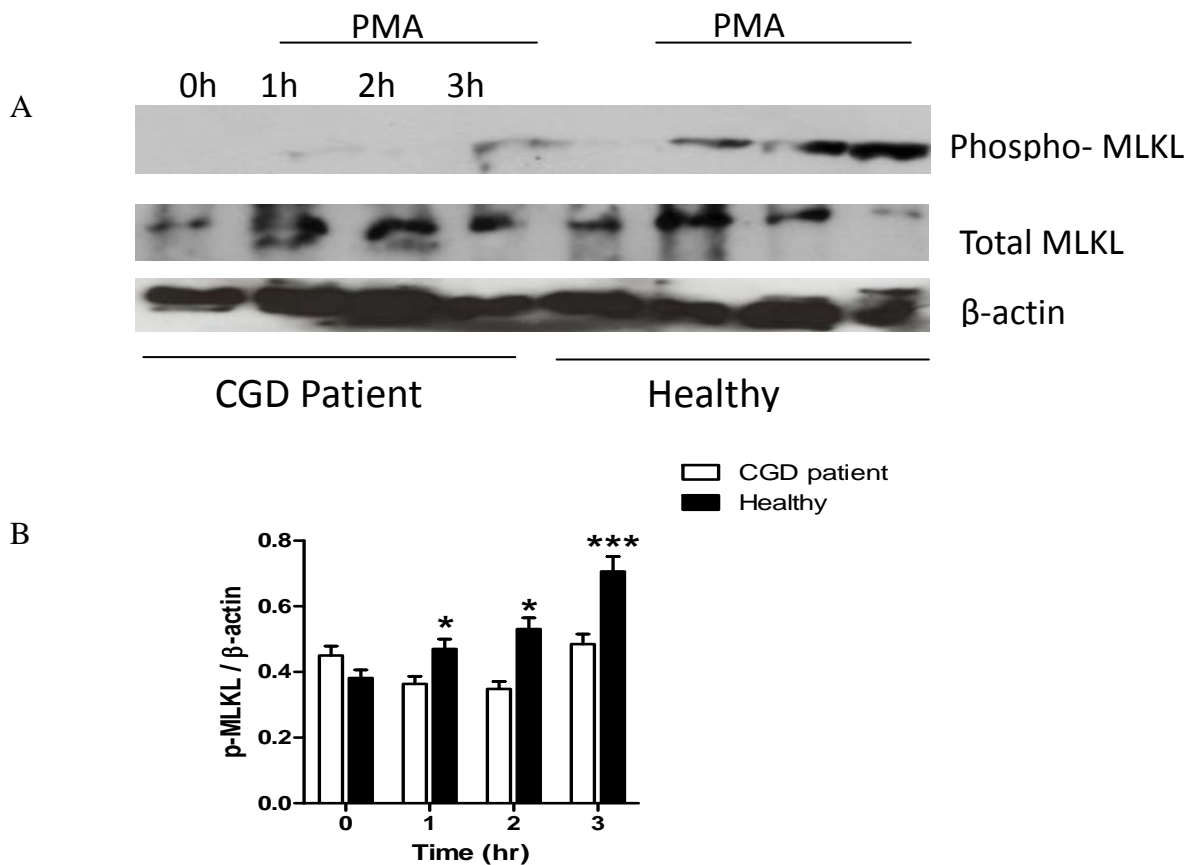
Figure 25: Representative western blot for phosphorylated MLKL, totals MLKL (A) and quantification (B) at different time points after PMA stimulation. The experiment was performed in neutrophils isolated from 2 healthy control or 2 chronic granulomatous disease (CGD) patients with NADPH-oxidase-deficiency (n=2 in each group). β-actin was used as loading control. *p<0.05, **p<0.01, *** p<0.01 versus medium control.

4.2.9 Ripk3-/- neutrophils do not undergo NET formation & cell death upon different stimuli

To understand the functional role of necroptosis during the NET formation and neutrophil cell death events, we switched to mouse neutrophils as our model system to take advantages from molecular and genetic tools developed over the last decade. We isolated neutrophils from peripheral blood collected from *Ripk3+/+* and *Ripk3−/−* mice and performed the *in-vitro* NETosis experiments like human neutrophils. *Ripk3−/−* mice are viable and physiologically normal. We exposed neutrophils from *Ripk3+/+* and *Ripk3−/−* mice to different stimuli like MSU crystals, LPS and PMA for 2h like human neutrophils to induce NET formation and cell death. Considering the fact that mice neutrophils might take longer time to undergo NET formation and cell death, we also performed MSU crystals, LPS and PMA stimulations for 6h time point. We found that for both the time points, the *Ripk3−/−* neutrophils lacked the Sytox uptake upon the MSU, LPS and PMA stimulations. Overall neutrophil cell death decreased significantly compared to control *Ripk3+/+* mice (figure 26, figure 27). The total number of NETs formed in *Ripk3−/−* mic*e* was significantly decreased (figure 28, figure 29). Furthermore, through confocal imaging we observed that while the *Ripk3+/+* neutrophils formed spectacular NETs made up of DNA (blue) and histones (green) decorated with neutrophil elastase (red), the *Ripk3+/+* neutrophils failed to make these NETs (figure 30).

Together, the in-vitro studies with mice neutrophils showed that RIPK3 is a central protein involved in PMA or MSU-induced NET formation. This observation is in line with our results with the treatment with pharmacological antagonists in human neutrophils.

Figure 26: Neutrophils were isolated from the blood of WT and Ripk3- deficient mice and exposed to MSU crystal, LPS, and PMA for 6h. Sytox green was used to identify dying cells in culture. Representative images are shown at an original magnification of 200x.

Sytox green
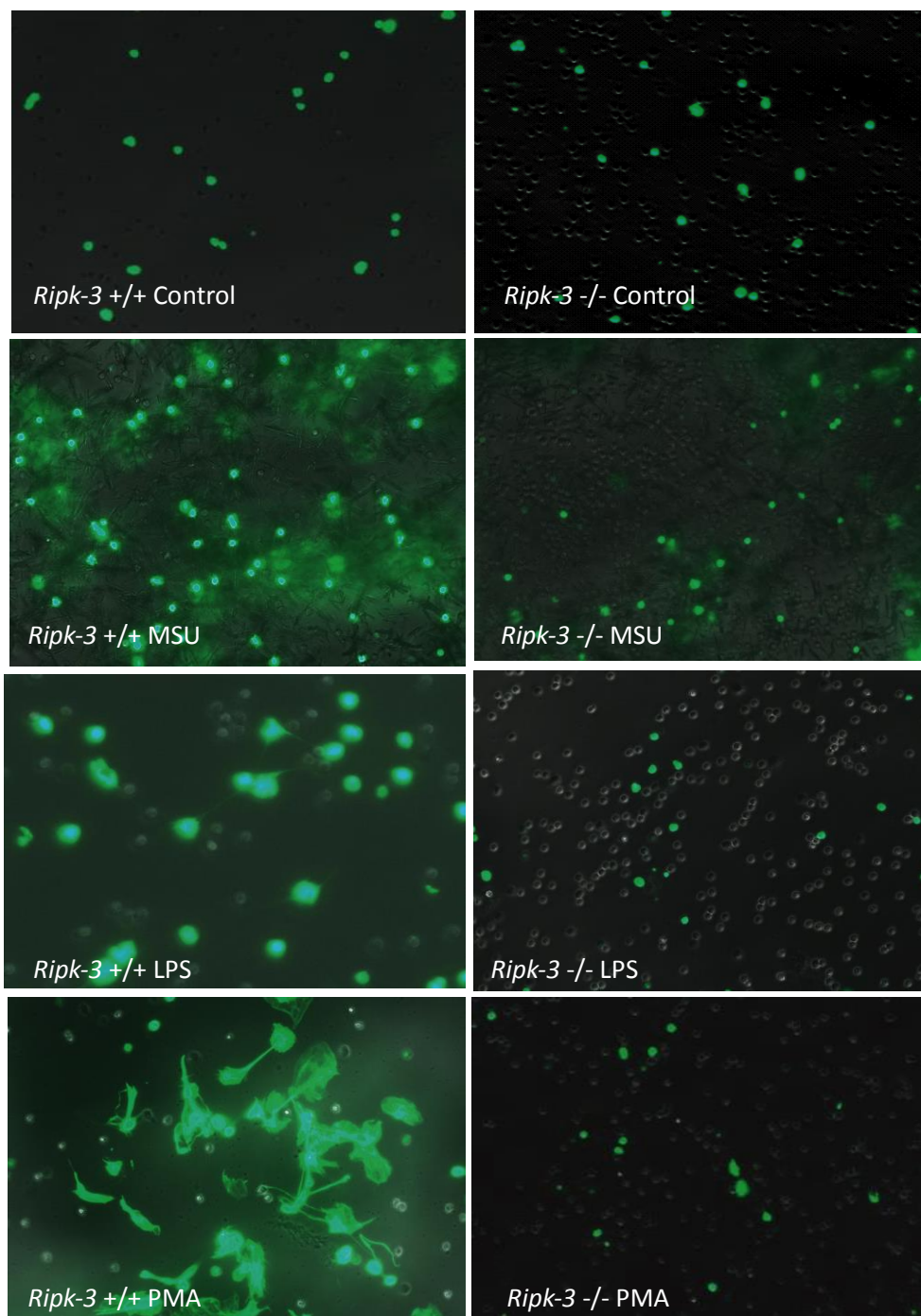
Magnification 200X

Figure 27: Neutrophils were isolated from the blood of WT and Ripk3- deficient mice and exposed to MSU crystal, LPS, and PMA for 2h. Sytox green was used to identify dying cells in culture. Representative images are shown at an original magnification of 200x
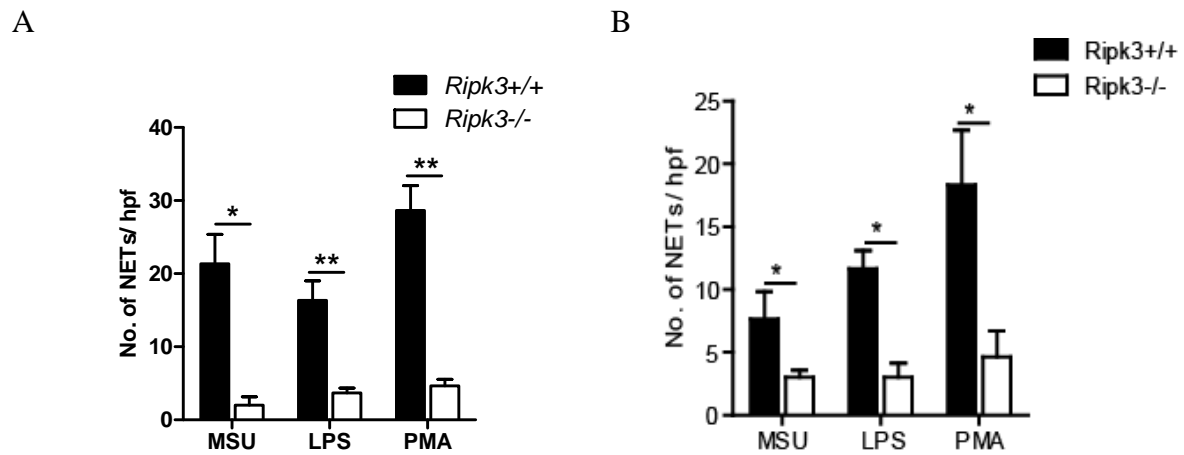
Figure 28: A quantitative analysis of number of NETs MSU crystals (20pg/cell) LPS (100nM) and PMA (25nM) stimulations for A)6h and B) for 2h is shown as means ± SE of the mean from three independent experiments. *p<0.05, **p<0.01 versus medium control, t-test. N.S: not significant.
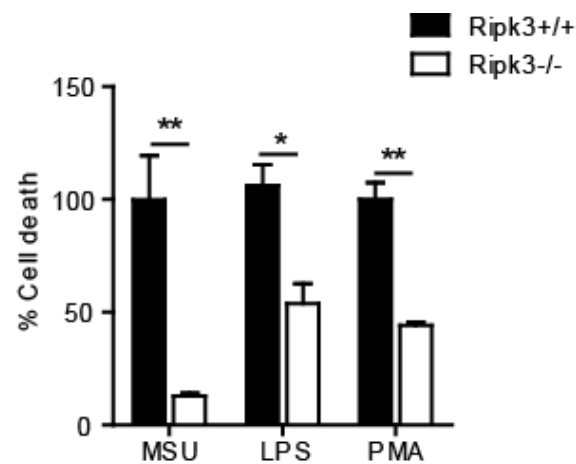
Figure 29: A quantitative analysis of Sytox+ dead cells upon MSU crystals (20pg/cell) LPS(100nM) and PMA(25nM) stimulations for 2h is shown as means ± SE of the mean from three independent experiments. *p<0.05, **p<0.01 versus medium control, t-test. N.S: not significant
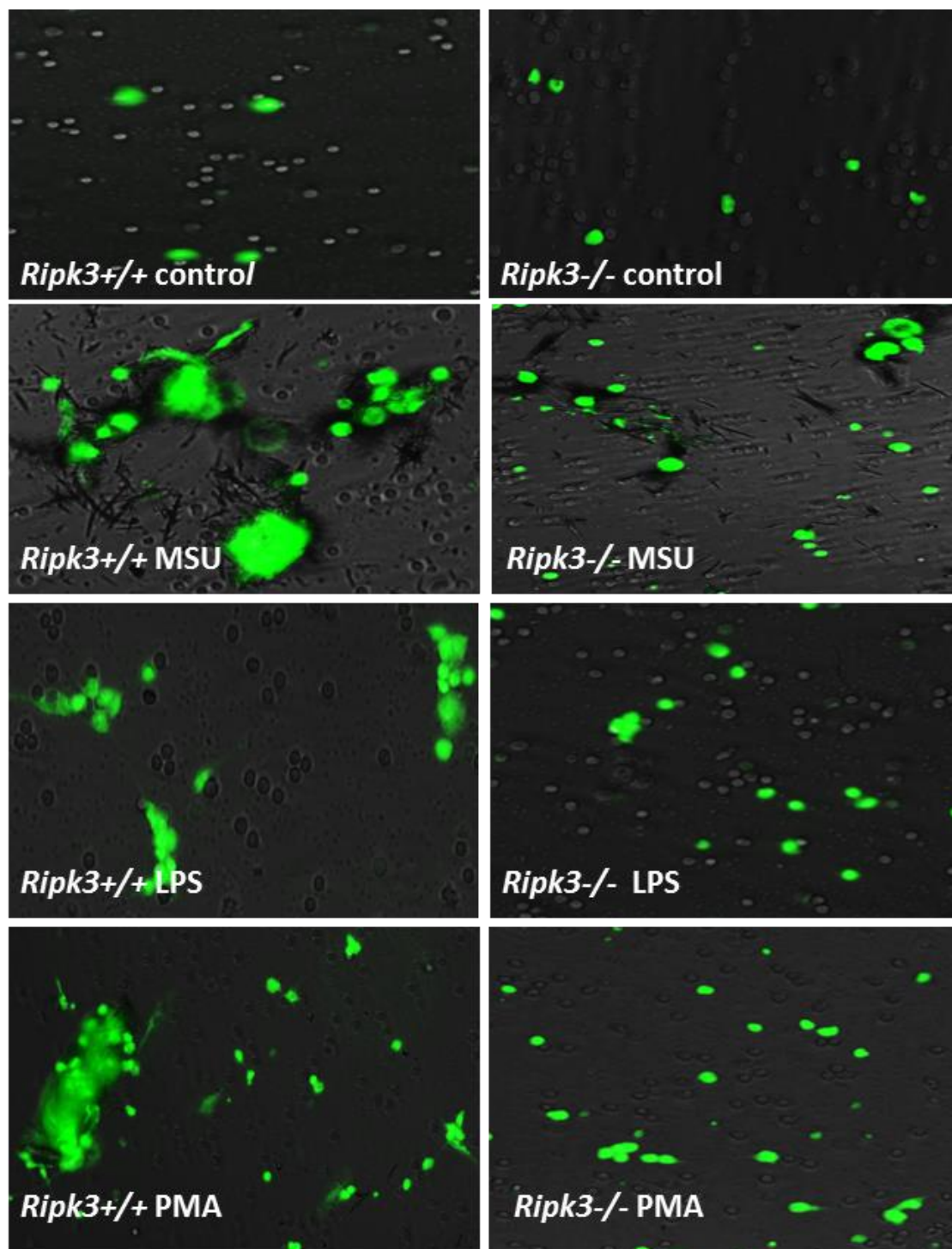
DNA   Histone   Neutrophil elastase   Magnification: 400x
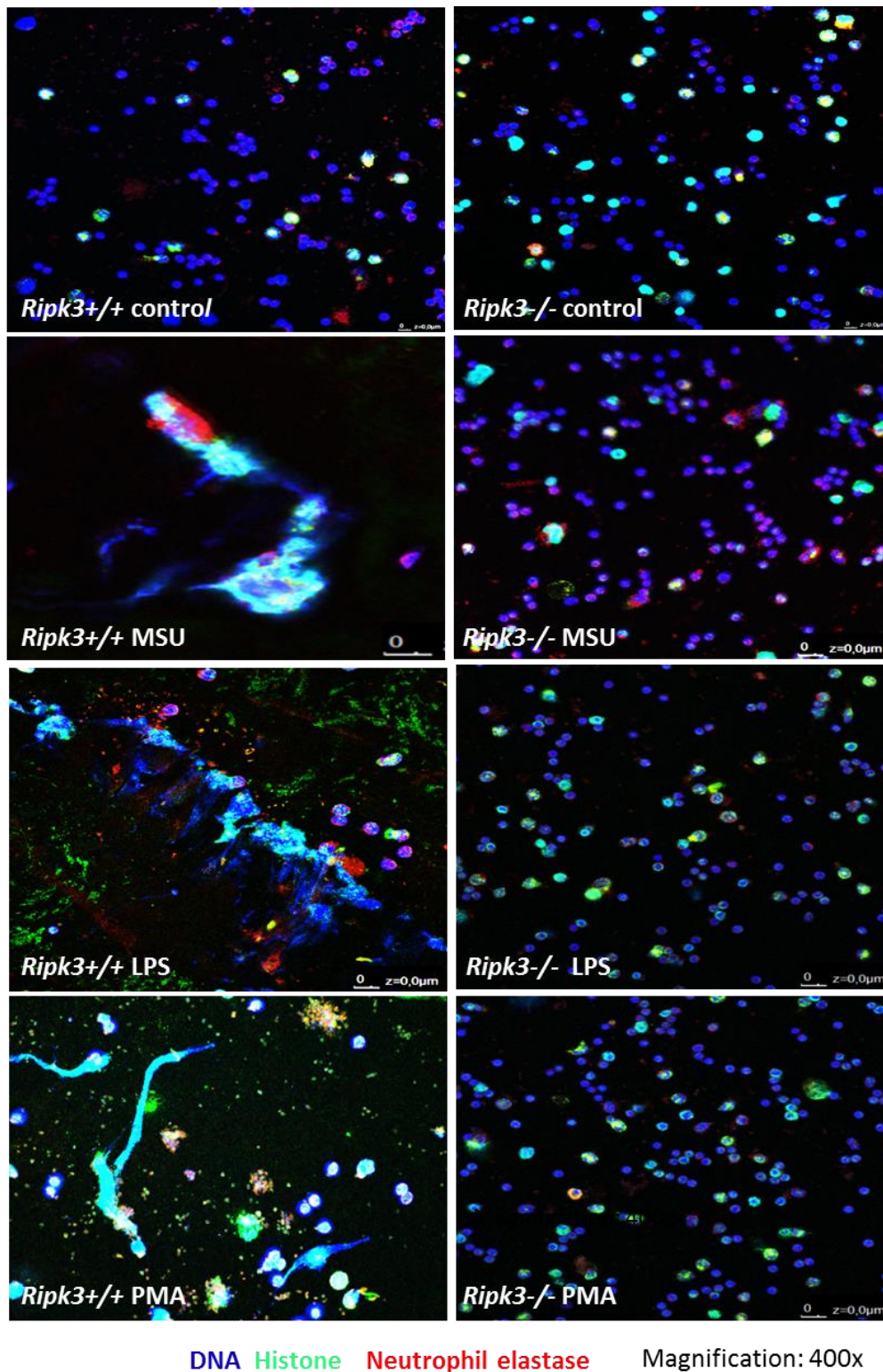
Figure 30: Neutrophils were isolated from the blood of wild type and Ripk3-deficient mice and exposed to MSU, LPS, and PMA for 6hrs. A: Confocal microscopy for these cells stained with FITC-anti-histones (green) and TOPRO (blue) to identify NETs. Representative images are shown at an original magnification of 400x

4.3 Part III: Crystal-induced necroptosis in non-immune cells

4.3.1 Crystal cytotoxicity involves necroptosis of non-immune cells

The involvement of necroptosis cascade upon MSU crystal stimulations in neutrophils led us to our next interest of understanding the crystal induced non-immune cell death. What is the mode of crystal-induced non-immune cell death? To address this question we first studied the cytotoxic effects of calcium oxalate (CaOx), monosodium urate (MSU), calcium pyrophosphate dehydrate (CPPD) and cystine crystals on kidney epithelial cells *in vitro*. Transmission electron microscopy images and rhodamine-sytox stains to identify living and dead cells, respectively, showed that kidney tubular epithelial cells die by primary necrosis after crystal exposure (figure 31).
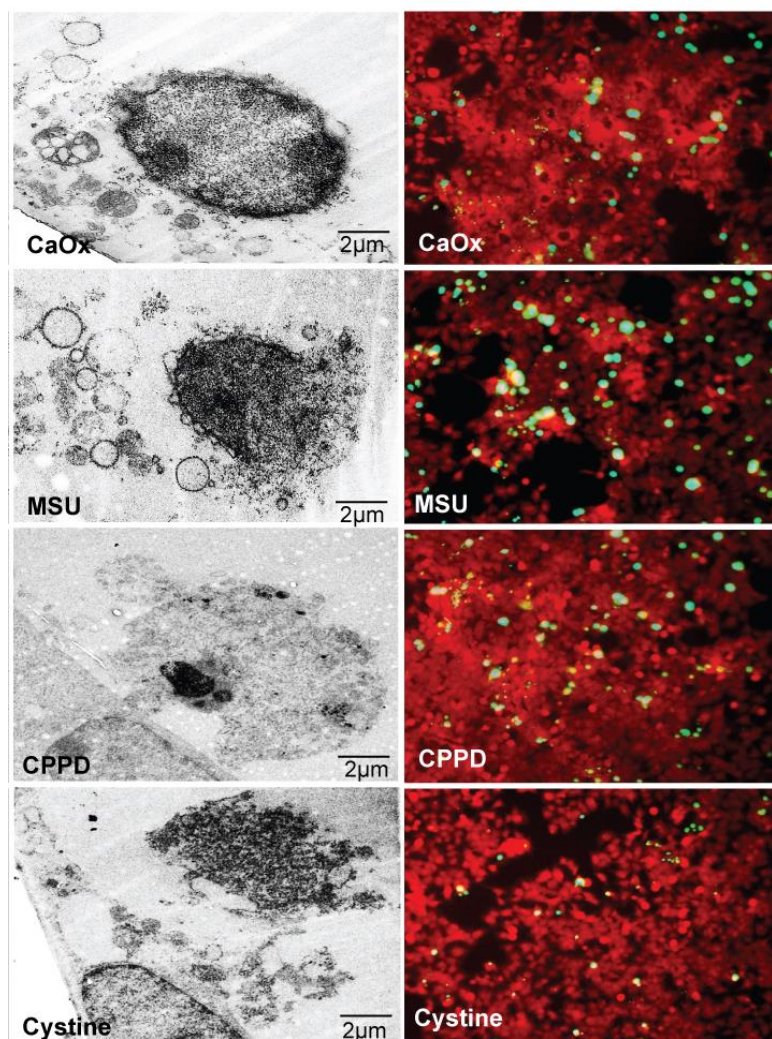
Figure 31: TEM images show that these crystals induce necrosis of tubular epithelial cells as indicated by ruptured plasma membranes (middle,   2,000), scale bar, 2 mm. The images on the right show the same

rhodamine-labelled monolayers (red) 24 h later. When Sytox green is added to the medium cells with permeable plasma membranes turn green indicating cell death (x 200), scale bar, 40 mm.

A

B
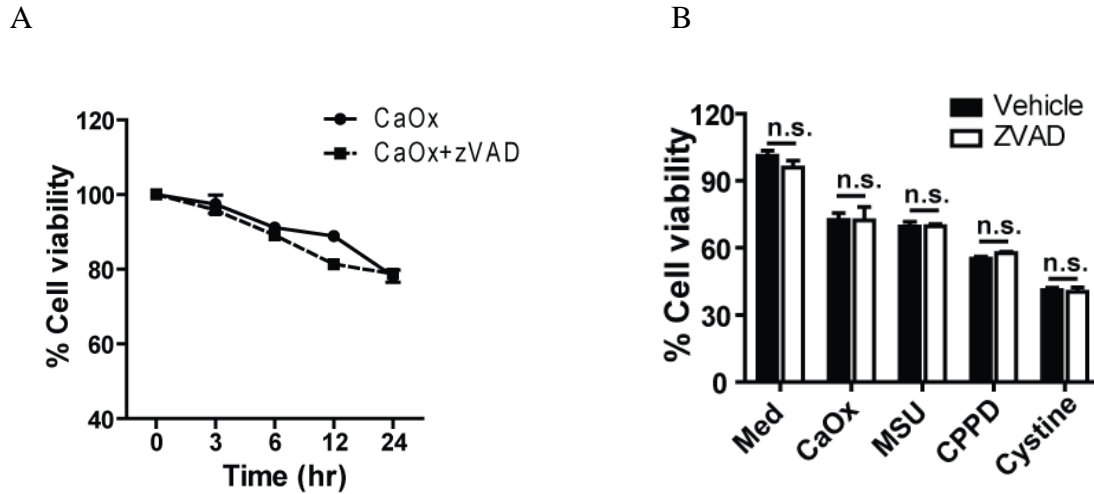
Figure 32: (A): Mouse tubular epithelial cell viability on crystal exposure by 3-(4,5- dimethylthiazol-2-yl)-2,5-diphenyltetrazolium bromide assay with and without the pan-caspase inhibitor ZVAD–FMK–FMK. All data are s.e.m.±means of at least three independent experiments. CaOx, MSU, CPPD, NS, not significant. *P< 0.05 versus medium control, ***P< 0.001 versus respective control. (B). Mouse tubular epithelial cells were pretreated with zVAD-FMK (10μM) and exposed to calcium oxalate (CaOx) crystals (1000μg/ml). Cell viability was determined by MTT assay.

We found that different crystal induced cytotoxicity was not affected by pan-caspase inhibition (figure 32A and 32B). Having excluded the contribution of caspase-dependent forms of cell death, we focussed on necroptosis, a known regulated form of necrosis of non-immune cells. The RIPK1 stabilisator necrostatin-1 partially (MSU, CPPD and cystine) or entirely (CaOx) prevented crystal-induced tubular epithelial cell death also in the absence of ZVAD–FMK (figure 33 and figure 34) suggesting a role for RIPK1 independent of caspases. When crystals were replaced by recombinant TNF-α as a stimulus, necrostatin-1 had the same effect. However, the TNF-α blocker etanercept had no protective effect on crystal-induced necroptosis (figure 35). This showed that TNF-α does not mediate the crystal induced necroptosis in tubular epithelial cells.

We further validated our finding in different cell types. We found that necrostatin-1 also suppressed crystal cytotoxicity in L929 cells, primary human synovial fibroblasts, primary renal progenitor cells and HK-2 cells in a dose dependent manner (figures 36-39).
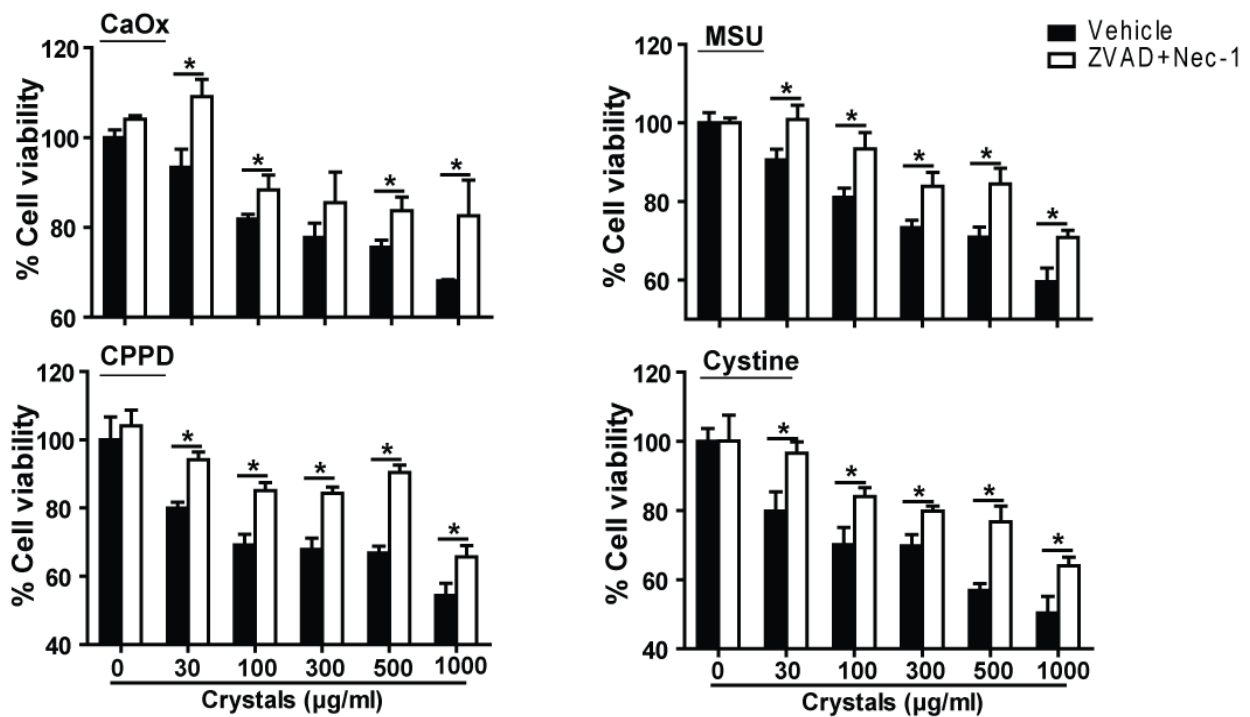
Figure 33: Mouse tubular epithelial cells were exposed to different concentrations of CaOx, MSU, CPPD or cystine crystals as indicated in the presence or absence of necrostatin (Nec)-1 (100 mM) together with the pan-caspase inhibitor ZVAD–FMK–FMK posed to recombinant TNF-α (300ng/ml) as well as crystals of calcium oxalate (CaOx) (1000µg/ml), monosodium urate (MSU) (500µg/ml), calcium pyrophosphate dehydrate (CPPD) (500µg/ml) and cystine (500µg/ml). Cell viability was determined by MTT assay 24h later. Data are expressed as mean c(10 mM). Cell viability was assessed by MTT assay 24 h later. Data are expressed as mean cell viability±s.e.m. of three independent experiments. Baseline viability is set as 100%. Data were analysed using Student's t-test. *Po0.05, **Po0.01 and ***Po0.001 versus respective medium control. NS, not significant. MTT, 3-(4,5-dimethylthiazol-2-yl)-2,5-diphenyltetrazoliumbromide)
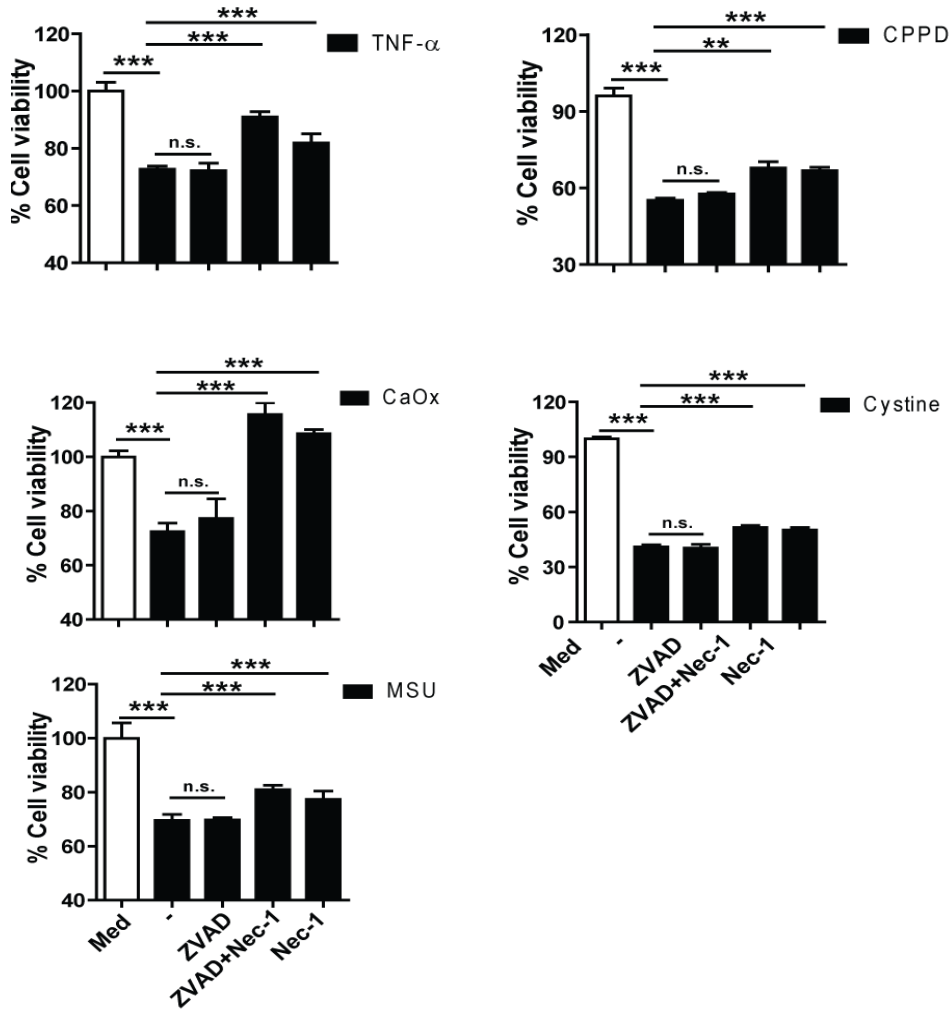
Figure 34: Mouse tubular epithelial cells were pretreated with ZVAD-FMK (10μM), necrostatin (Nec)-1 (100μM) or combination and ex ell viability ± SEM of three independent experiments. Baseline viability is set as 100%. ** p<0.01, *** p<0.001 versus medium control. N.S. not significant.
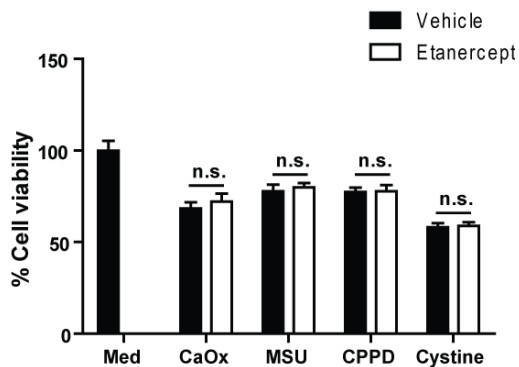
Figure 35: Crystal induced necroptosis does not involve TNF-α. Tubular epithelial cells were pretreated with etanercept (100mg/ml) and exposed to crystals of calcium oxalate (CaOx) (1000μg/ml), monosodium urate (MSU) (500μg/ml), calcium pyrophosphate dehydrate (CPPD) (500μg/ml), and cystine (500μg/ml). Cell viability was determined by MTT assay 24h later. Data are expressed as mean cell viability ± SEM of three independent experiments. Baseline viability is set as 100%. Data was analyzed using student's t test. N.S. = not significant.
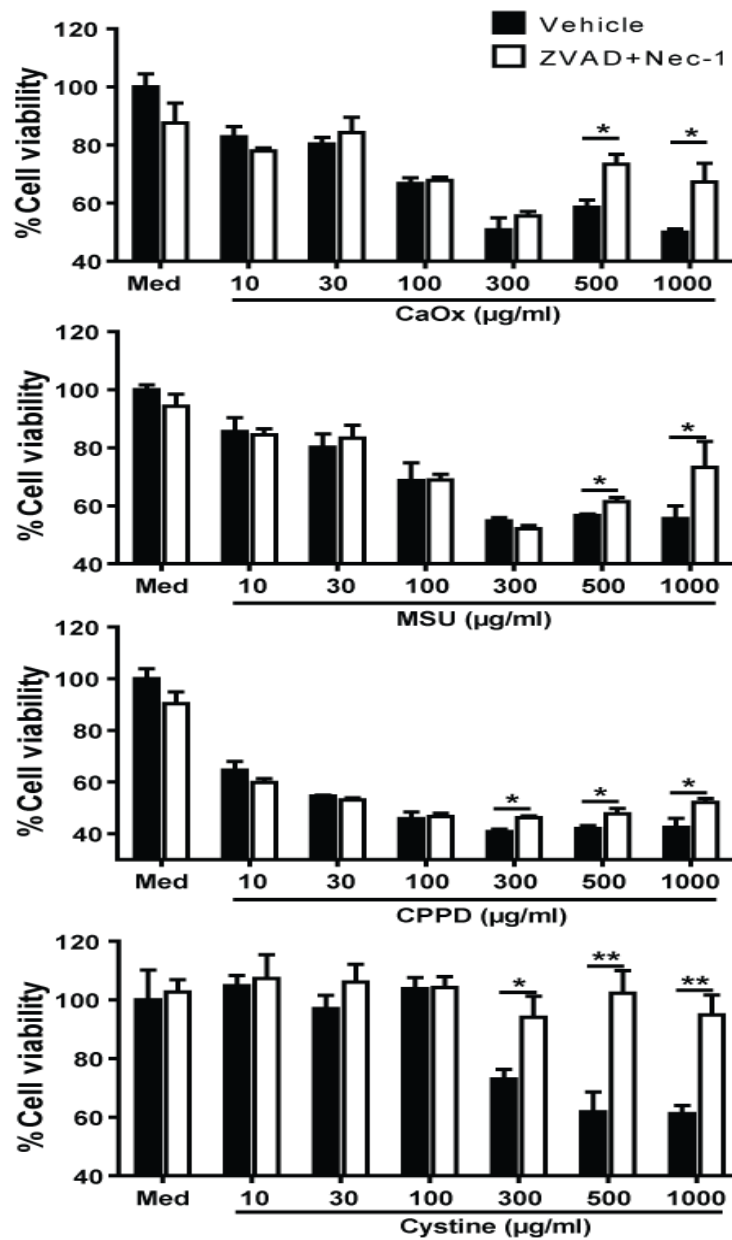
Figure 36: Crystals induce necroptosis in human synovial fibroblasts. Human synovial fibroblasts cells were exposed to crystals of calcium oxalate (CaOx), monosodium urate (MSU), calcium pyrophosphate dehydrate (CPPD) and cystine at different concentrations as indicated in the presence or absence of ZVAD-FMK-FMK (10μM) and necrostatin (Nec)-1 (100μM). Cell viability was determined by MTT assay 24h later. Data are expressed as mean cell viability ± SEM of three independent experiments. Baseline viability is set as 100%. Data was analyzed using student's t test. * $p < 0.05$, ** $p < 0.01$, *** $p < 0.001$ either versus vehicle control.
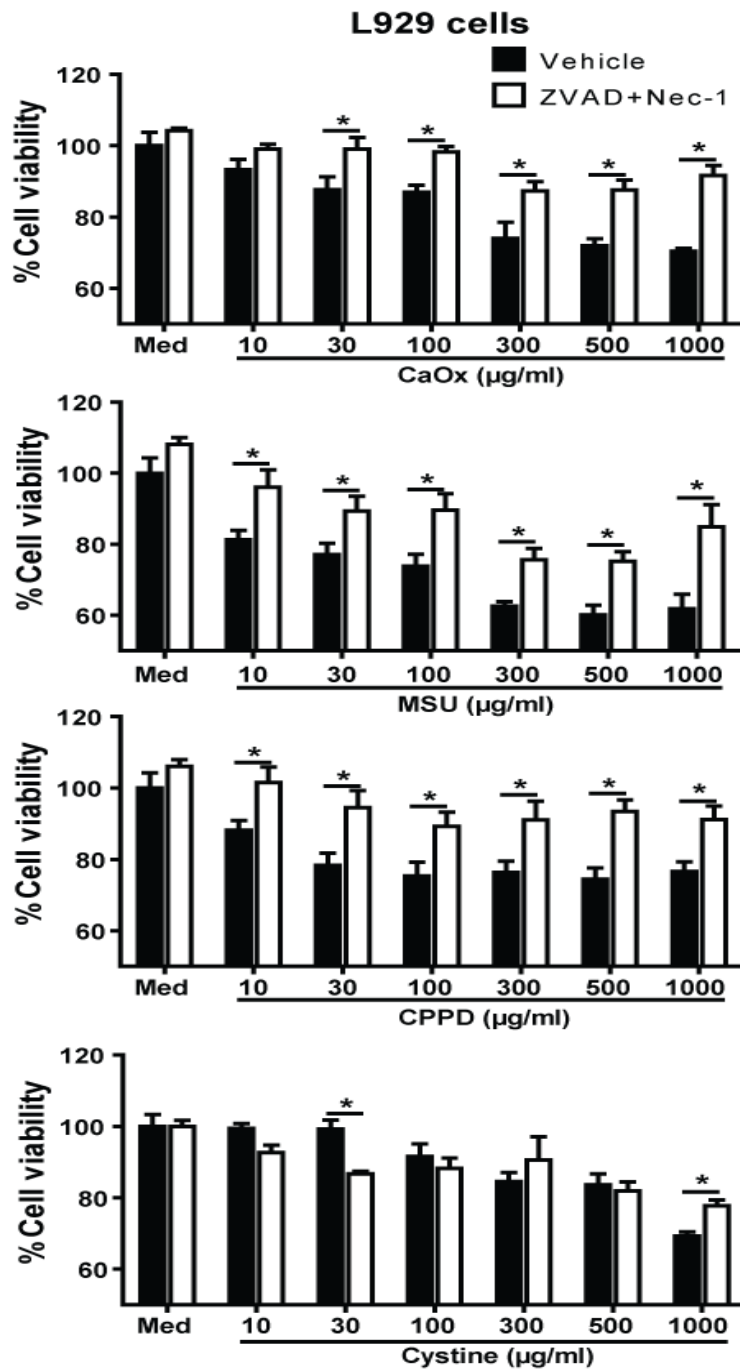
Figure 37: Crystals induce necroptosis in L929. L929 cells were exposed to crystals of calcium oxalate (CaOx), monosodium urate (MSU), calcium pyrophosphate dehydrate (CPPD) and cystine at different concentrations as indicated in the presence or absence of ZVAD-FMK-FMK (10μM) and necrostatin (Nec)-1 (100μM). Cell viability was determined by MTT assay 24h later. Data are expressed as mean cell viability ± SEM of three independent experiments. Baseline viability is set as 100%. Data was analyzed using student's t-test. * p<0.05, ** p<0.01, *** p<0.001 either versus vehicle control.
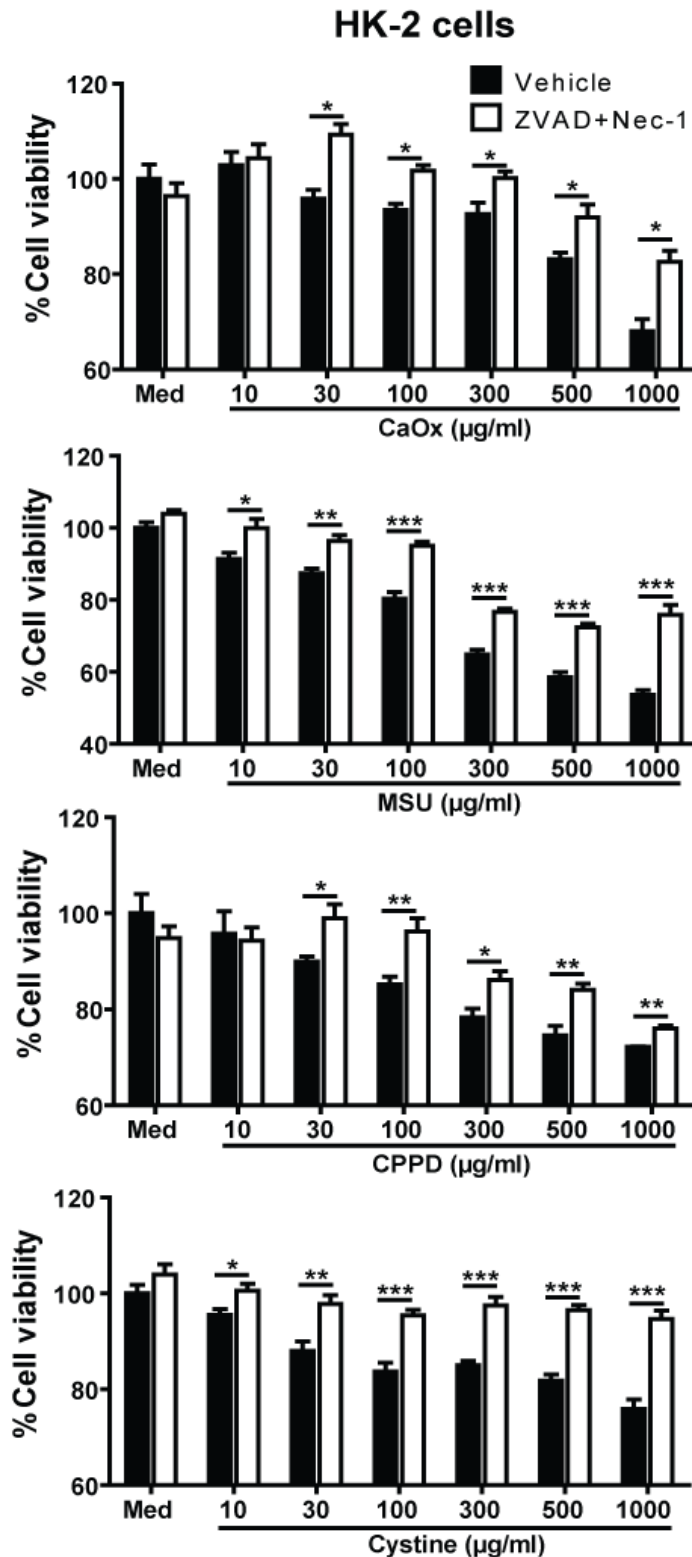
Figure 38: Crystals induce necroptosis in HK-2 cells. HK-2 cells were exposed to crystals of calcium oxalate (CaOx), monosodium urate (MSU), calcium pyrophosphate dehydrate (CPPD) and cystine at different concentrations as indicated in the presence or absence of ZVAD-FMK-FMK (10μM) and necrostatin (Nec)-1 (100μM). Cell viability was determined by MTT assay 24h later. Data are expressed as mean cell viability ± SEM of three independent experiments. Baseline viability is set as 100%. Data was analyzed using student's t test. * p<0.05, ** p<0.01, *** p<0.001 either versus vehicle control.
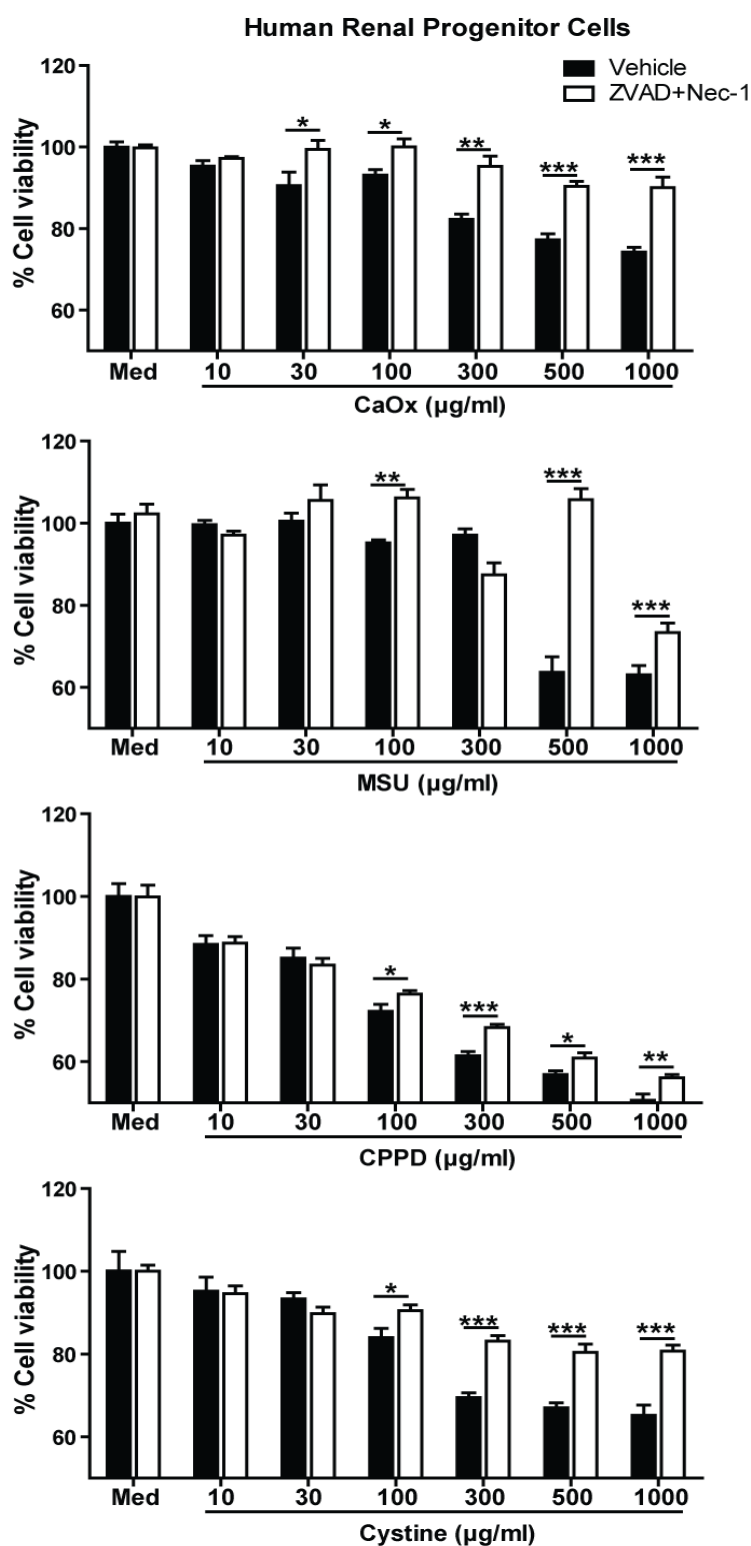
Figure 39: Crystal-induced necroptosis in human renal progenitor cells. Primary human renal progenitor cells were exposed to calcium oxalate (CaOx), monosodium urate (MSU), calcium pyrophosphate dehydrate (CPPD) and cystine at different concentrations as indicated in the presence or absence of ZVAD-FMKFMK (10μM) and necrostatin (Nec)-1 (100μM). Cell viability was determined by MTT assay 24h later. Data are expressed as percentage cell viability ± SEM of three independent experiments. Baseline viability is set as 100%. Data was analyzed using student's t-test. * p<0.05, ** p<0.01, *** p<0.001 all versus vehicle control.

5. Discussion

Various crystallopathies share certain common pathomechanisms, i.e. mechanical obstruction due to crystal deposits, cytotoxicity of cells that interact with crystals, and crystal induced inflammatory responses and activation of immune system. Various examples of crystallopathies include kidney stones that are formed as a result of hyperoxaluria or hypercalcuria leading to nephrocalcinosis. In the urinary tract, crystallization usually starts in the renal tubules where supersaturation is a consequence of stepwise concentrating the glomerular filtrate and of the active secretion of calcium, uric acid, oxalate, phosphate or drug metabolites (Table 1)[136,137] and this eventually hinder normal kidney functions. Furthermore, crystal masses may also cause vascular obstruction but through mechanisms other than stone formation. For example, atherosclerosis is a consequence of an accumulation of cholesterol crystals in the tunica intima of the arteria wall, the atheroma [138]. In gouty arthritis, non-aggregating crystal masses of MSU form creamy tophi in subcutaneous layer of skin. Particles like silica and asbestos are known to induce silicosis and asbestosis, diseases associated with lung inflammation.

Crystals induce direct inflammation, cytotoxicity and inflammation-driven necrosis, an auto-amplifying process referred to as "necroinflammation".Upon interactions with crystals, cells experience significant cell stress, actin depolymerization, ROS production, and enhanced autophagy and cell death [139] In various crystallopathies, associated crystals act as DAMPs that activate the innate immune system.. A wide range of sterile particulates like crystals formed as a result of aberrant metabolism (calcium oxalate, monosodium urate, calcium pyrophosphate dehydrate, cystine, adenine, cholesterol etc.), external toxins (asbestos, silica), ischemia-reperfusion injury, and chemotherapy or irradiation to target depletion of specific cell population can elicit inflammation[140 141].

Neutrophils are the first immune responder cells which are largely recruited at the site of injury caused by various crystals. Our data suggest that beyond their capacity to trigger inflammation, crystals of calcium oxalate, MSU, calcium phosphate. CPPD, cystine, cholesterol, silica, asbestos and different sizes of titanium dioxide nanoparticles induce direct cytotoxic effects in neutrophils. We observed that upon exposure to a large variety of crystals, primary human neutrophils undergo cell death *in vitro*. From various imaging approaches using TEM, SEM and confocal microscopy methods, we observed that the neutrophils often make crystal-NET aggregates. Thus, upon different crystal stimulation, neutrophils often form NETs which are associated with neutrophil cell death named NETosis.

Cell death categories are no longer defined by morphological features but by the executing biochemical pathway, vice versa, the involved route of cell death is proven by preventing death via specific inhibition of the causative pathway[134]. Alike apoptosis, necrosis can be a programmed form of cell death, referred to regulated cell necrosis[96]. Based on the molecular mechanisms involved, these regulated necrosis pathways are named as RIPK-mediated necroptosis, iron-mediated ferroptosis, PARP-mediated parthanatos, mitochondrial permeability transition-related regulated necrosis, caspase-1/11-mediated pyroptosis etc[134]. However, it remained unclear if NETosis is at all a unique cell death category also because none of the other cell death categories is cell type-specific. In contrast, NETosis is mode of cell death distinguished just based on morphological appearance. Moreover, as none of the aforementioned signaling elements is specific for neutrophils, the underlying route of "NETosis" remained elusive. In addition, NET release has been reported in cells other than neutrophils, referred to as "ETosis"[58]. We were interested in dissecting the exact mode of cell death beyond the morphological appearance of 'NET structures' upon crystal stimulations. Is NETosis a unique mode of cell death? Are these NET-like structures consequence of mere another known regulated necrosis pathways that involve plasma membrane rupture?

Since we were interested in the pathophysiological mechanisms of gout, we focused on MSU crystals induced neutrophil cell death. We observed that only chemical inhibitors of the necroptosis pathway such as RIPK1 stabilizers necrostatin (Nec)-1 and Nec-1s or the MLKL inhibitor NSA inhibited NET release and neutrophil necrosis upon 2 hours of PMA or MSU crystals stimulation of human neutrophils[142]. These stimuli also increased the expression of RIPK3 and pMLKL, two core proteins of necroptosis signaling, in a time-dependent manner, suggesting the involvement of the necroptosis signaling pathway in PMA- and MSU crystal-induced NET release[142] (figure 40).

These findings were corroborated by similar observations in Ripk3-deficient murine neutrophils. Furthermore, Nec-1 or NSA did not affect MSU crystals- or PMA-induced ROS production in neutrophils and neutrophils of patients with chronic granulomatous disease (non-functional NADPH oxidase) did not express pMLKL after PMA stimulation[142] , suggesting that pMLKL is a downstream event to ROS. Obviously, PMA and MSU crystals trigger NET-like chromatin release in the context of neutrophil necroptosis. Recently, Schauer et. al. demonstrated that MSU crystals can induce aggregates of NETs, and the tophi, pathognomonic structures of chronic gout, share characteristics of aggregated NETs[37].
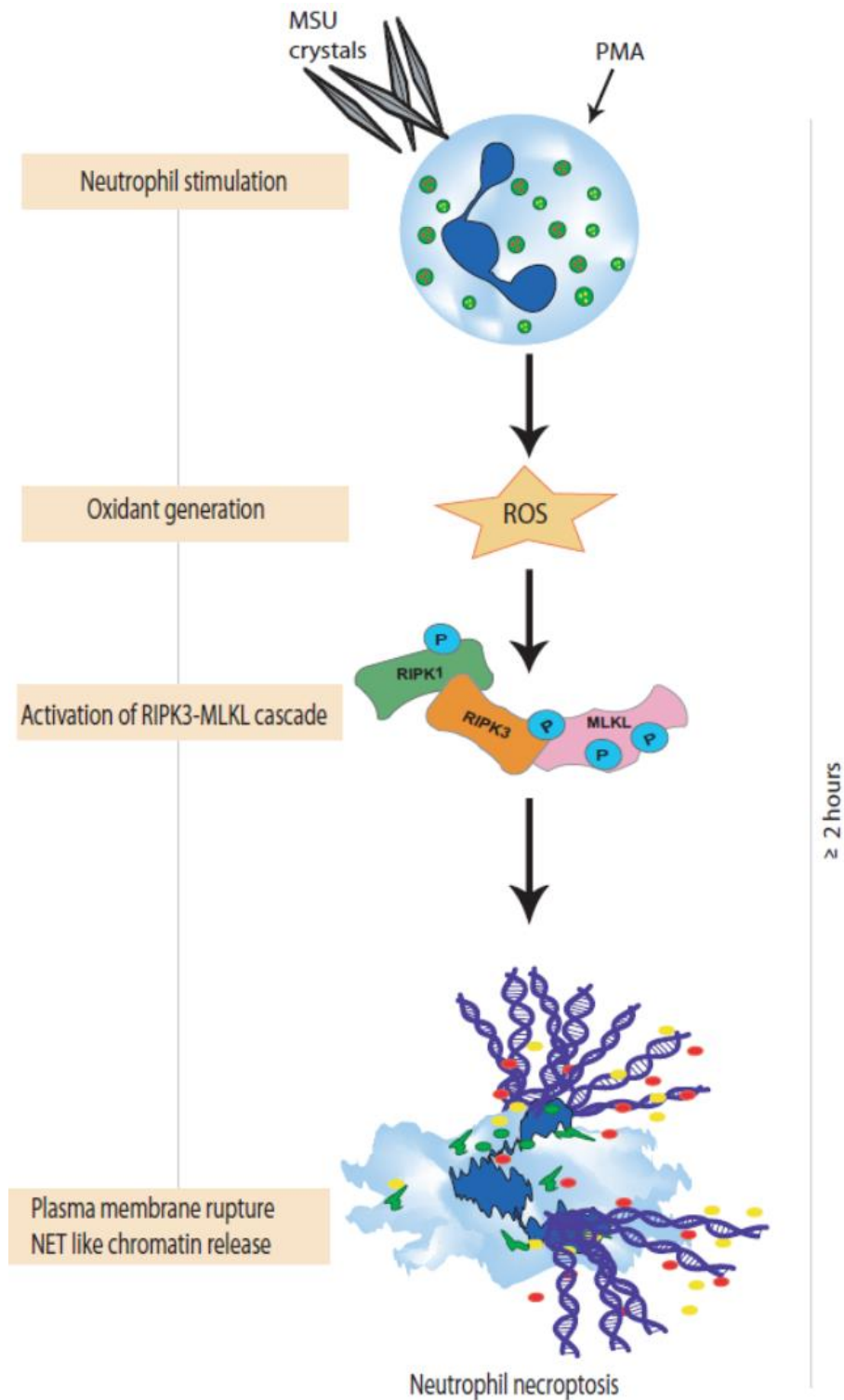
Figure 40: Chromatin release as a consequence of neutrophil necroptosis. Stimuli like MS) crystals and PMA induce activation of a receptor interacting protein kinase (RIPK)3- and mixed lineage kinase domain-like (MLKL)-dependent signaling pathway downstream of ROS. This leads to plasma membrane rupture and NET-like chromatin release together with granular enzymes as a consequence at around 2 hours of stimulation.

We observed that the deficiency of Ripk3, as well as inhibitors of the necroptosis pathway, inhibited MSU crystal-induced NET formation and gout-like tophus formation *in vivo*[142], confirming the involvement of neutrophil necroptosis along NET release (figure 40).

Unlike RIPK3/MLKL-mediated neutrophil necroptosis[143], the rapid NET formation without cell death does not involve perforation of the plasma membrane[66]. Accordingly, the independency of RIPK3/MLKL pathway for this rapid NET formation (45 min after neutrophil stimulation) was also recently demonstrated by Amini et. al. using stimuli like *E. coli*, GM-CSF-primed LPS or complement factor C5a [144]. On first view, these observations seem contradictory to the involvement of necroptosis in PMA- and MSU crystal-induced NET release during neutrophil necrosis[143]. But obviously the nature of NET formation can differ in terms of timing, type of stimuli or context of disease. The term 'NETosis' is inappropriate not only to describe a vital process but also when NET release comes as a passive process secondary to plasma membrane rupture of neutrophils undergoing necroptosis or even other forms of regulated cell death. On the other hand NET formation from neutrophils that remain vital is a primary event and a particular feature of host defense unique to neutrophils. In addition, it becomes important to carefully design future studies related to NETs and carefully distinguish the process of NET formation from that of neutrophil cell death.

In an independent study, we investigated crystal induced cell death mechanisms in different non-immune cell types[37]. Crystals in the micrometer range of calcium oxalate, calcium pyrophosphate, cystine or monosodium urate induce direct cell necrosis in a variety of different epithelial and mesenchymal cell types [145]. Crystal-induced cell death involve RIPK-3 and MLKL hence, crystals kill cells via a regulated form of necrosis classified as necroptosis (Figure 41) [146]. This finding could be validated *in vivo* as *Ripk3-* or *Mlkl*-deficient mice are protected from calcium oxalate crystal-induced tubular necrosis as acute kidney injury[147]. RIPK1 is an upstream inhibitor of necroptosis and small molecule modulators of RIPK1, the necrostatins, enhance this inhibitory effect and can suppress crystal-induced necroptosis[145,148].
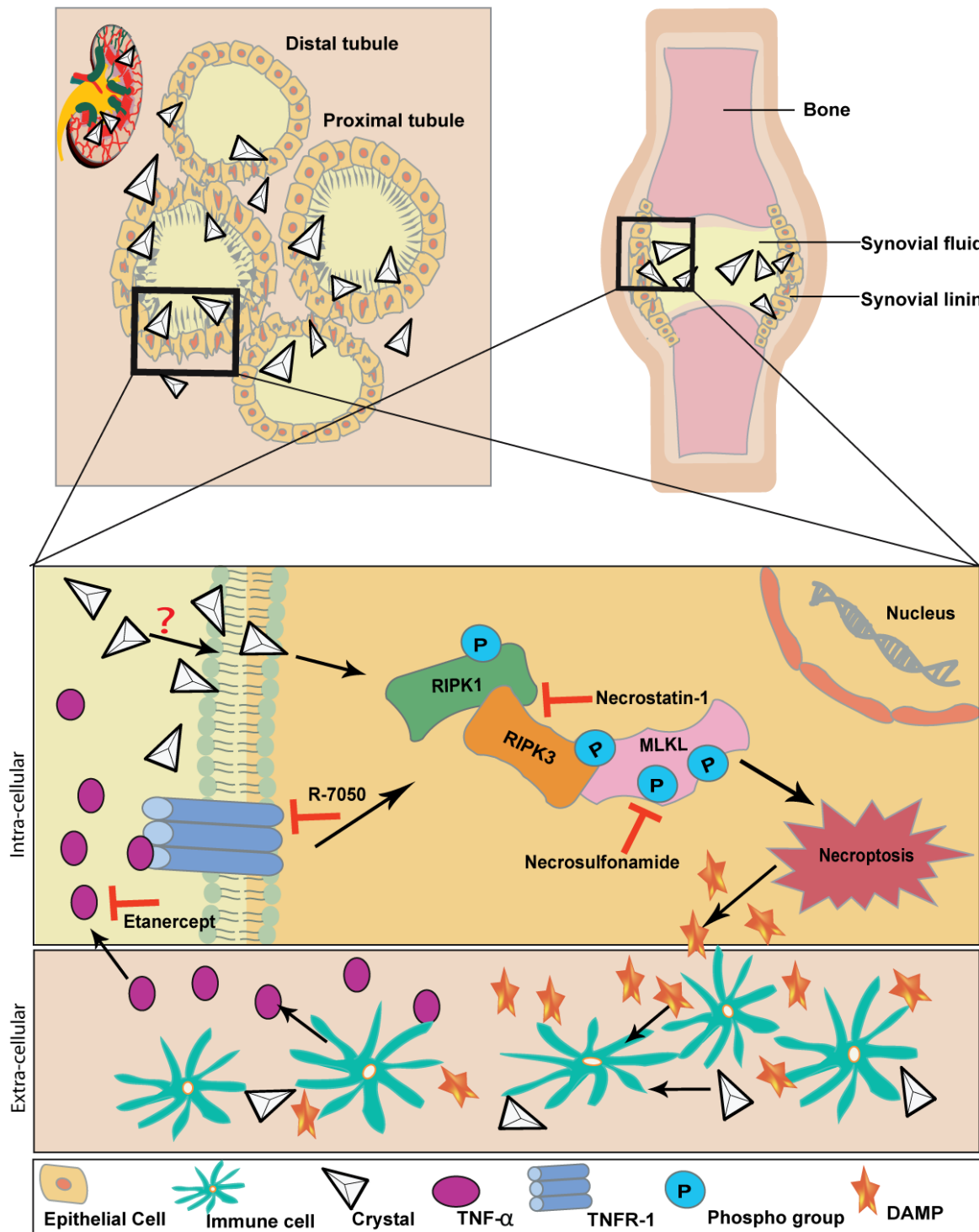
Figure 41: Schematic illustration of crystal-induced necroptosis and inflammation (necroinflammation).
During crystallophathies, crystals are formed and deposited inside the organ, for example, kidney stone disease
or joint, for example, gouty arthritis. On crystallization, crystals are phagocytized by parenchymal cells where
they activate the RIPK1, RIPK3 and MLKL pathway of necroptosis, a prototype form of regulated necrosis, by
inducing a series of phosphorylation events.

How exactly crystals trigger RIPK1 activation in both immune and non-immune cells remains uncertain. It was shown that MSU crystals can switch on the Syk signalling in dendritic cells via binding to lipid rafts[149]. Crystals activate the NLRP3 inflammasome via lysosomal leakage of cathepsins into the cytosol[150]. Cathepsin B was reported to inhibit necroptosis by cleaving RIPK1[151]. This could also be a possibility of upstream events that lead to crystal-induced necroptosis. Our data also suggest that crystal-induced cytotoxicity might not involve TNFα since TNFα blocker etanercept did not block necroptosis in-vitro. However, it is certain that secondary TNF-driven necroptosis further contributes to cytotoxicity in *in-vivo* conditions (figure 41). Consequently, the therapeutic blockade of this pathway, for example, with the soluble TNFR2-IgG fusion protein or the RIPK1 stabilisator necrostatin-1 prevented crystal-induced tissue necrosis and organ dysfunction[152]. These data indicate that crystal-induced necroptosis can be one of the initial responses upon onset of various crystallopathies.

Apart from cytotoxic effects, crystals can directly activate immune system and promote inflammation. Martinon & Tschopp showed that MSU and CPPD crystals activate macrophages for caspase-1-dependent release of mature IL-1β by activating the NLRP3 inflammasome[6]. Subsequently, this finding was confirmed in large range of crystals and microparticles[153]. These include crystals or particulates of cholesterol [154], calcium oxalate [155], calcium phosphate [156], calcium pyrophosphate [157], cystine [158], silica [159,160], asbestos [160], cigarette smoke-related microparticles [161], and nanoparticles, e.g. formed by titanium dioxide [162,163], carbon [164], polysterene [165]. Whether crystal cytotoxicity is a consequence of NLRP3 activation or an inflammasome-independent event with distinct signalling pathways are the important questions. Crystal-induced NLRP3 activation could imply NLRP3-caspase-1/11-mediated pyroptosis as a mode of crystal-induced regulated cell death, as it has been described to occur in infected macrophages[166 107 167]. However, we excluded this option since caspase blockade did not affect crystal cytotoxicity of neutrophils as well as other non-immune cells. Moreover, caspase blockade also excluded apoptosis as another form of regulated cell death.

Together with direct interaction with immune system, crystals also trigger inflammation by killing cells because necrotic cells release numerous proinflammatory elements such as cytokines like IL1-ß, IL-6, TNFα, proinflammatory alarmins, proteases, and DAMPs that have the capacity to activate Toll-like receptors (e.g. HMGB1, histones, mitochondrial DNA, demethylated DNA/RNA, etc.) or inflammasomes (e.g. ATP, histones,

uric acid, dsDNA, etc.) [168,169] (Figure 42). Activation of these receptors ultimately leads to the release of proinflammatory cytokines, kinins, and lipid mediators that install a local inflammatory response, i.e. vasodilation endothelial dysfunction with increased vascular permeability (swelling) and leukocyte infiltration. Crystal induced neutrophil necroptosis lead to release of chromatin made up of histones and DNA. Histones are known to have direct cytotoxic affects and can further act as DAMPs. Also local complement activation can be involved[170,171]. Thus, crystal induced necroptosis of immune cells (neutrophils) and non-immune cells leads to an inflammatory response and pro-inflammatory cytokines like TNFα can also further activate the RIPK1, RIPK3 and MLKL pathway of necroptosis via TNFR1 in neighbouring cells. This auto-amplification loop between cell death and inflammation is known as necroinflammation (figure 42).

Necroinflammation eventually leads to aggravation of tissue injury, and if remain uncontrolled then to organ failure[51]. Thus, blocking necroptosis during the early stage of tissue injury may help to prevent subsequent auto-amplification loop of inflammation, immune-mediated pathology and organ failure. Thus, Necroinflammation contribute to the typical clinical presentations of acute crystallopathies such as gouty arthritis [3].

However, there are some limitations to the conclusions drawn from the present study.

1. Most of the conclusions of the study are based on *in vitro* observation. Activity of neutrophils in physiological condition is highly influenced by surrounding environment and presence of various factors.

2. Neutrophils are highly sensitive cells and can be activated by mere errors in physical handling. This leads to different observations in different settings (different laboratories).

3. One of the limitations of the study is methods that are used to study neutrophil NETs and cell death. We have combined approaches from cell death fields to use chemical inhibitors of cell death mechanisms and approaches of imaging to study the morphology of NETs. However, various imaging approach cannot distinguish between NETs and cell death. Whether chromatin release is a secondary event to neutrophil necroptosis after plasma membrane rupture or it involves another specific biochemical pathway cannot be fully be answered with present approach.
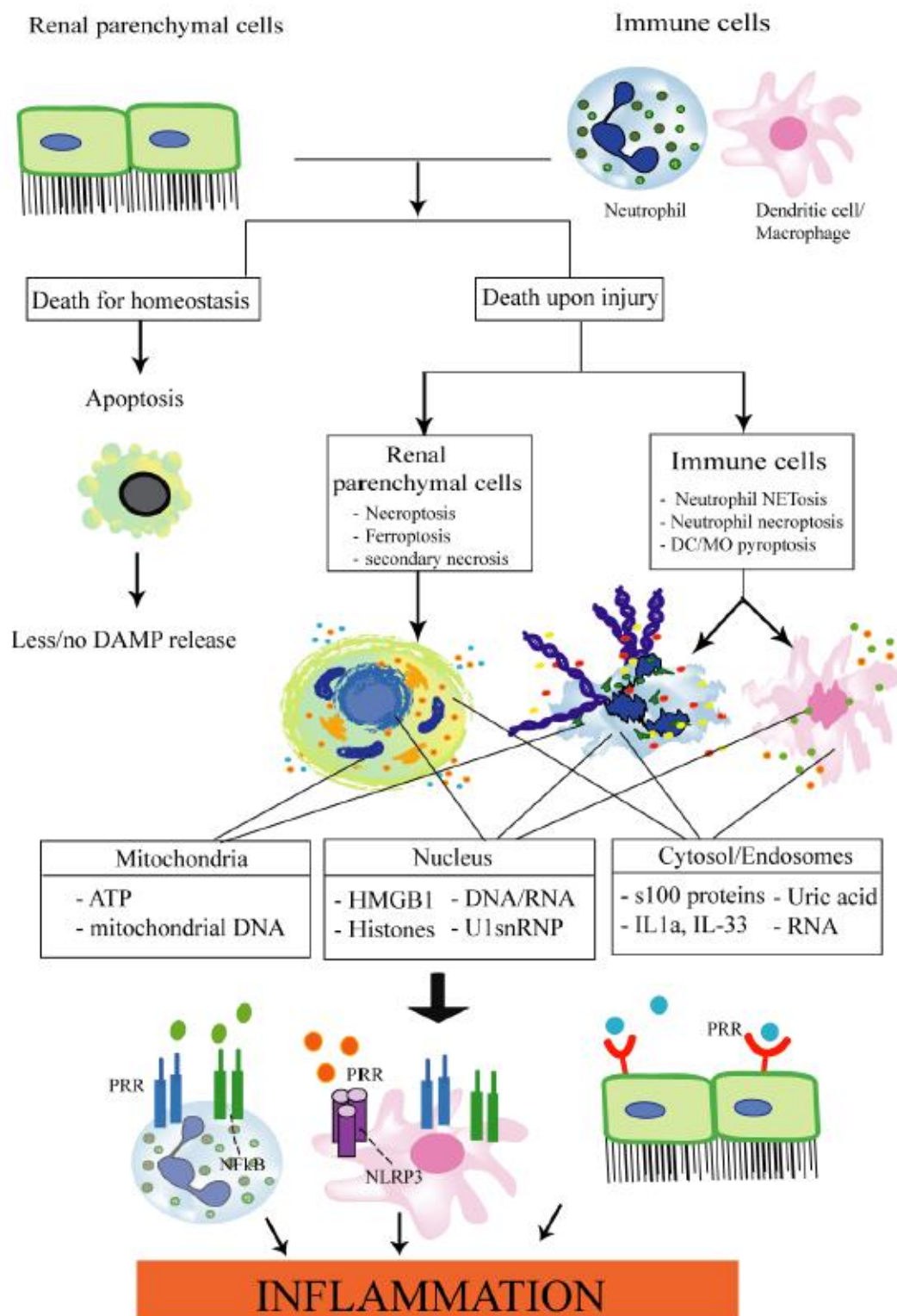
Figure 42: Schematic representation of necroinflammation. The regulated necrosis in immune and non-immune cells like necroptosis or NETs lead to the release of various DAMPs like mitochondrial protein, chromatin or cytosolic proteins. These DAMPs can induce strong inflammatory responses by activating inflammatory signaling pathways like inflammosomes or NET formation. Furthermore, these inflammatory responses lead to induction of more DAMPs, inducing the vicious cycle of necroinflammation.

4. The source of neutrophils may affect the NET formation process in case of mouse neutrophils. Different stimuli may also lead to NET formation without involving cell death. Amini et. al showed 'vital NETs' in mouse neutrophils derived from Ripk3-deficient mice upon stimulations with *E. coli*, GM-CSF-primed LPS or complement factor C5a but not with crystals [144]. This look contradictory to our observation. However, the source of neutrophils was different in both the studies. Amini et. al showed rapid NETs in bone-marrow derived mouse neutrophils whereas our study used peripheral blood neutrophils. More detail studies are thus needed to understand NET formation procedures and their interaction with neutrophil cell death.

5. To study and image NETs in *in vivo* models is extremely difficult. Imaging NETs and cell death *in vivo* may help understand neutrophil necroptosis in a better manner.

6. Whether the variety of the involved forms of regulated cell death depend on the crystal type, crystal size or the affected cell type remains to be further characterized in detail.

In conclusion, crystals are potent inducers of necroptosis in immune and non-immune cells, and NET-like chromatin release is a consequence or a secondary event following necroptotic neutrophil death. These findings imply TNFR1, RIPK1, RIPK3 and MLKL being potential therapeutic targets to limit tissue injury in crystallopathies i.e. gouty arthritis.

6. References

1.   Mulay, S.R. & Anders, H.J. Crystallopathies. *N Engl J Med* **374**, 2465-2476 (2016).

2.   Harris, B.J. & Dalhaimer, P. Particle shape effects in vitro and in vivo. *Front Biosci (Schol Ed)* **4**, 1344-1353 (2012).

3.   Neogi, T. Clinical practice. Gout. *N Engl J Med* **364**, 443-452 (2011).

4.   Martillo, M.A., Nazzal, L. & Crittenden, D.B. The crystallization of monosodium urate. *Curr Rheumatol Rep* **16**, 400 (2014).

5.   Dalbeth, N.*, et al.* Cellular characterization of the gouty tophus: a quantitative analysis. *Arthritis Rheum* **62**, 1549-1556 (2010).

6.   Martinon, F., Petrilli, V., Mayor, A., Tardivel, A. & Tschopp, J. Gout-associated uric acid crystals activate the NALP3 inflammasome. *Nature* **440**, 237-241 (2006).

7.   Giamarellos-Bourboulis, E.J.*, et al.* Crystals of monosodium urate monohydrate enhance lipopolysaccharide-induced release of interleukin 1 beta by mononuclear cells through a caspase 1-mediated process. *Ann Rheum Dis* **68**, 273-278 (2009).

8.   Liu-Bryan, R., Pritzker, K., Firestein, G.S. & Terkeltaub, R. TLR2 signaling in chondrocytes drives calcium pyrophosphate dihydrate and monosodium urate crystal-induced nitric oxide generation. *J Immunol* **174**, 5016-5023 (2005).

9.   Liu-Bryan, R., Scott, P., Sydlaske, A., Rose, D.M. & Terkeltaub, R. Innate immunity conferred by Toll-like receptors 2 and 4 and myeloid differentiation factor 88 expression is pivotal to monosodium urate monohydrate crystal-induced inflammation. *Arthritis Rheum* **52**, 2936-2946 (2005).

10.   Nathan, C. Points of control in inflammation. *Nature* **420**, 846-852 (2002).

11.   Colotta, F., Dower, S.K., Sims, J.E. & Mantovani, A. The type II 'decoy' receptor: a novel regulatory pathway for interleukin 1. *Immunol Today* **15**, 562-566 (1994).

12.   Iwami, K.I.*, et al.* Cutting edge: naturally occurring soluble form of mouse Toll-like receptor 4 inhibits lipopolysaccharide signaling. *J Immunol* **165**, 6682-6686 (2000).

13.   Chen, Y.H.*, et al.* Spontaneous resolution of acute gouty arthritis is associated with rapid induction of the anti-inflammatory factors TGFbeta1, IL-10 and soluble TNF receptors and the intracellular cytokine negative regulators CIS and SOCS3. *Ann Rheum Dis* **70**, 1655-1663 (2011).

14.   Yoshimura, A., Nishinakamura, H., Matsumura, Y. & Hanada, T. Negative regulation of cytokine signaling and immune responses by SOCS proteins. *Arthritis Res Ther* **7**, 100-110 (2005).

15.   Liote, F.*, et al.* Inhibition and prevention of monosodium urate monohydrate crystal-induced acute inflammation in vivo by transforming growth factor beta1. *Arthritis Rheum* **39**, 1192-1198 (1996).

16.   Savill, J.S.*, et al.* Macrophage phagocytosis of aging neutrophils in inflammation. Programmed cell death in the neutrophil leads to its recognition by macrophages. *J Clin Invest* **83**, 865-875 (1989).

17.   Fadok, V.A.*, et al.* Macrophages that have ingested apoptotic cells in vitro inhibit proinflammatory cytokine production through autocrine/paracrine mechanisms involving TGF-beta, PGE2, and PAF. *J Clin Invest* **101**, 890-898 (1998).

18.   Steiger, S. & Harper, J.L. Neutrophil cannibalism triggers transforming growth factor beta1 production and self regulation of neutrophil inflammatory function in monosodium urate monohydrate crystal-induced inflammation in mice. *Arthritis Rheum* **65**, 815-823 (2013).

19.   Fava, R., Olsen, N., Keski-Oja, J., Moses, H. & Pincus, T. Active and latent forms of transforming growth factor beta activity in synovial effusions. *J Exp Med* **169**, 291-296 (1989).

20.   Scanu, A.*, et al.* Cytokine levels in human synovial fluid during the different stages of acute gout: role of transforming growth factor beta1 in the resolution phase. *Ann Rheum Dis* **71**, 621-624 (2012).

21.   Dubois, C.M.*, et al.* Transforming growth factor beta is a potent inhibitor of interleukin 1 (IL-1) receptor expression: proposed mechanism of inhibition of IL-1 action. *J Exp Med* **172**, 737-744 (1990).

22.   Redini, F., Mauviel, A., Pronost, S., Loyau, G. & Pujol, J.P. Transforming growth factor beta exerts opposite effects from interleukin-1 beta on cultured rabbit articular chondrocytes through reduction of interleukin-1 receptor expression. *Arthritis Rheum* **36**, 44-50 (1993).

23.   Furst, D.E. Anakinra: review of recombinant human interleukin-I receptor antagonist in the treatment of rheumatoid arthritis. *Clin Ther* **26**, 1960-1975 (2004).

24.   Schiff, M.H. Role of interleukin 1 and interleukin 1 receptor antagonist in the mediation of rheumatoid arthritis. *Ann Rheum Dis* **59 Suppl 1**, i103-108 (2000).

25.   Seckinger, P.*, et al.* Natural and recombinant human IL-1 receptor antagonists block the effects of IL-1 on bone resorption and prostaglandin production. *J Immunol* **145**, 4181-4184 (1990).

26. McColl, S.R., Paquin, R., Menard, C. & Beaulieu, A.D. Human neutrophils produce high levels of the interleukin 1 receptor antagonist in response to granulocyte/macrophage colony-stimulating factor and tumor necrosis factor alpha. *J Exp Med* **176**, 593-598 (1992).

27. Ulich, T.R.*, et al.* The intratracheal administration of endotoxin and cytokines. III. The interleukin-1 (IL-1) receptor antagonist inhibits endotoxin- and IL-1-induced acute inflammation. *Am J Pathol* **138**, 521-524 (1991).

28. Turner, M.*, et al.* Induction of the interleukin 1 receptor antagonist protein by transforming growth factor-beta. *Eur J Immunol* **21**, 1635-1639 (1991).

29. Wahl, S.M., Costa, G.L., Corcoran, M., Wahl, L.M. & Berger, A.E. Transforming growth factor-beta mediates IL-1-dependent induction of IL-1 receptor antagonist. *J Immunol* **150**, 3553-3560 (1993).

30. Roberge, C.J.*, et al.* Crystal-induced neutrophil activation. V. Differential production of biologically active IL-1 and IL-1 receptor antagonist. *J Immunol* **152**, 5485-5494 (1994).

31. So, A., De Smedt, T., Revaz, S. & Tschopp, J. A pilot study of IL-1 inhibition by anakinra in acute gout. *Arthritis Res Ther* **9**, R28 (2007).

32. Terkeltaub, R.*, et al.* The interleukin 1 inhibitor rilonacept in treatment of chronic gouty arthritis: results of a placebo-controlled, monosequence crossover, non-randomised, single-blind pilot study. *Ann Rheum Dis* **68**, 1613-1617 (2009).

33. Gratton, S.B., Scalapino, K.J. & Fye, K.H. Case of anakinra as a steroid-sparing agent for gout inflammation. *Arthritis Rheum* **61**, 1268-1270 (2009).

34. Murakami, Y., Akahoshi, T., Kawai, S., Inoue, M. & Kitasato, H. Antiinflammatory effect of retrovirally transfected interleukin-10 on monosodium urate monohydrate crystal-induced acute inflammation in murine air pouches. *Arthritis Rheum* **46**, 2504-2513 (2002).

35. Rose-John, S. IL-6 trans-signaling via the soluble IL-6 receptor: importance for the pro-inflammatory activities of IL-6. *Int J Biol Sci* **8**, 1237-1247 (2012).

36. Choe, J.Y., Lee, G.H. & Kim, S.K. Radiographic bone damage in chronic gout is negatively associated with the inflammatory cytokines soluble interleukin 6 receptor and osteoprotegerin. *J Rheumatol* **38**, 485-491 (2011).

37. Schauer, C.*, et al.* Aggregated neutrophil extracellular traps limit inflammation by degrading cytokines and chemokines. *Nat Med* **20**, 511-517 (2014).

38.   Kolaczkowska, E. & Kubes, P. Neutrophil recruitment and function in health and inflammation. *Nat Rev Immunol* **13**, 159-175 (2013).

39.   Pillay, J.*, et al.* In vivo labeling with 2H2O reveals a human neutrophil lifespan of 5.4 days. *Blood* **116**, 625-627 (2010).

40.   Quinn, M.T., DeLeo, F.R. & Bokoch, G.M. Neutrophil methods and protocols. Preface. *Methods Mol Biol* **412**, vii-viii (2007).

41.   Mary, J.Y. Normal human granulopoiesis revisited. II. Bone marrow data. *Biomed Pharmacother* **39**, 66-77 (1985).

42.   Fliedner, T.M., Cronkite, E.P., Killmann, S.A. & Bond, V.P. Granulocytopoiesis. Ii. Emergence and Pattern of Labeling of Neutrophilic Granulocytes in Humans. *Blood* **24**, 683-700 (1964).

43.   Martin, C.*, et al.* Chemokines acting via CXCR2 and CXCR4 control the release of neutrophils from the bone marrow and their return following senescence. *Immunity* **19**, 583-593 (2003).

44.   Mukaida, N., Harada, A. & Matsushima, K. Interleukin-8 (IL-8) and monocyte chemotactic and activating factor (MCAF/MCP-1), chemokines essentially involved in inflammatory and immune reactions. *Cytokine Growth Factor Rev* **9**, 9-23 (1998).

45.   Gambardella, L. & Vermeren, S. Molecular players in neutrophil chemotaxis--focus on PI3K and small GTPases. *J Leukoc Biol* **94**, 603-612 (2013).

46.   Allen, L.A. & Aderem, A. Molecular definition of distinct cytoskeletal structures involved in complement- and Fc receptor-mediated phagocytosis in macrophages. *J Exp Med* **184**, 627-637 (1996).

47.   Nordenfelt, P. & Tapper, H. Phagosome dynamics during phagocytosis by neutrophils. *J Leukoc Biol* **90**, 271-284 (2011).

48.   Mayadas, T.N., Cullere, X. & Lowell, C.A. The multifaceted functions of neutrophils. *Annu Rev Pathol* **9**, 181-218 (2014).

49.   Jaconi, M.E.*, et al.* Cytosolic free calcium elevation mediates the phagosome-lysosome fusion during phagocytosis in human neutrophils. *J Cell Biol* **110**, 1555-1564 (1990).

50.   Williams, R. Killing controversy. *J Exp Med* **203**, 2404 (2006).

51.   Mulay, S.R., Linkermann, A. & Anders, H.J. Necroinflammation in Kidney Disease. *J Am Soc Nephrol* **27**, 27-39 (2016).

52.   Brinkmann, V.*, et al.* Neutrophil extracellular traps kill bacteria. *Science* **303**, 1532-1535 (2004).

53. Desai, J., Mulay, S.R., Nakazawa, D. & Anders, H.J. Matters of life and death. How neutrophils die or survive along NET release and is "NETosis" = necroptosis? *Cell Mol Life Sci* **73**, 2211-2219 (2016).

54. Yousefi, S.*, et al.* Catapult-like release of mitochondrial DNA by eosinophils contributes to antibacterial defense. *Nat Med* **14**, 949-953 (2008).

55. Chow, O.A.*, et al.* Statins enhance formation of phagocyte extracellular traps. *Cell Host Microbe* **8**, 445-454 (2010).

56. von Kockritz-Blickwede, M.*, et al.* Phagocytosis-independent antimicrobial activity of mast cells by means of extracellular trap formation. *Blood* **111**, 3070-3080 (2008).

57. Vorobjeva, N.V. & Pinegin, B.V. Neutrophil extracellular traps: mechanisms of formation and role in health and disease. *Biochemistry (Mosc)* **79**, 1286-1296 (2014).

58. Wartha, F. & Henriques-Normark, B. ETosis: a novel cell death pathway. *Sci Signal* **1**, pe25 (2008).

59. Fuchs, T.A.*, et al.* Novel cell death program leads to neutrophil extracellular traps. *J Cell Biol* **176**, 231-241 (2007).

60. Yipp, B.G. & Kubes, P. NETosis: how vital is it? *Blood* **122**, 2784-2794 (2013).

61. Hakkim, A.*, et al.* Activation of the Raf-MEK-ERK pathway is required for neutrophil extracellular trap formation. *Nat Chem Biol* **7**, 75-77 (2011).

62. Rohm, M.*, et al.* NADPH oxidase promotes neutrophil extracellular trap formation in pulmonary aspergillosis. *Infect Immun* **82**, 1766-1777 (2014).

63. Metzler, K.D., Goosmann, C., Lubojemska, A., Zychlinsky, A. & Papayannopoulos, V. A myeloperoxidase-containing complex regulates neutrophil elastase release and actin dynamics during NETosis. *Cell Rep* **8**, 883-896 (2014).

64. Papayannopoulos, V., Metzler, K.D., Hakkim, A. & Zychlinsky, A. Neutrophil elastase and myeloperoxidase regulate the formation of neutrophil extracellular traps. *J Cell Biol* **191**, 677-691 (2010).

65. Metzler, K.D.*, et al.* Myeloperoxidase is required for neutrophil extracellular trap formation: implications for innate immunity. *Blood* **117**, 953-959 (2011).

66. Pilsczek, F.H.*, et al.* A novel mechanism of rapid nuclear neutrophil extracellular trap formation in response to Staphylococcus aureus. *J Immunol* **185**, 7413-7425 (2010).

67. Clark, S.R.*, et al.* Platelet TLR4 activates neutrophil extracellular traps to ensnare bacteria in septic blood. *Nat Med* **13**, 463-469 (2007).

68. Buchanan, J.T.*, et al.* DNase expression allows the pathogen group A Streptococcus to escape killing in neutrophil extracellular traps. *Curr Biol* **16**, 396-400 (2006).

69. Urban, C.F., Reichard, U., Brinkmann, V. & Zychlinsky, A. Neutrophil extracellular traps capture and kill Candida albicans yeast and hyphal forms. *Cell Microbiol* **8**, 668-676 (2006).

70. McCormick, A.*, et al.* NETs formed by human neutrophils inhibit growth of the pathogenic mold Aspergillus fumigatus. *Microbes Infect* **12**, 928-936 (2010).

71. Saitoh, T.*, et al.* Neutrophil extracellular traps mediate a host defense response to human immunodeficiency virus-1. *Cell Host Microbe* **12**, 109-116 (2012).

72. Xu, J., Zhang, X., Monestier, M., Esmon, N.L. & Esmon, C.T. Extracellular histones are mediators of death through TLR2 and TLR4 in mouse fatal liver injury. *J Immunol* **187**, 2626-2631 (2011).

73. Young, R.L.*, et al.* Neutrophil extracellular trap (NET)-mediated killing of Pseudomonas aeruginosa: evidence of acquired resistance within the CF airway, independent of CFTR. *PLoS One* **6**, e23637 (2011).

74. Parker, H., Albrett, A.M., Kettle, A.J. & Winterbourn, C.C. Myeloperoxidase associated with neutrophil extracellular traps is active and mediates bacterial killing in the presence of hydrogen peroxide. *J Leukoc Biol* **91**, 369-376 (2012).

75. Jenne, C.N.*, et al.* Neutrophils recruited to sites of infection protect from virus challenge by releasing neutrophil extracellular traps. *Cell Host Microbe* **13**, 169-180 (2013).

76. Urban, C.F.*, et al.* Neutrophil extracellular traps contain calprotectin, a cytosolic protein complex involved in host defense against Candida albicans. *PLoS Pathog* **5**, e1000639 (2009).

77. Kumar, S.V.*, et al.* Neutrophil Extracellular Trap-Related Extracellular Histones Cause Vascular Necrosis in Severe GN. *J Am Soc Nephrol* **26**, 2399-2413 (2015).

78. Hakkim, A.*, et al.* Impairment of neutrophil extracellular trap degradation is associated with lupus nephritis. *Proc Natl Acad Sci U S A* **107**, 9813-9818 (2010).

79. Villanueva, E.*, et al.* Netting neutrophils induce endothelial damage, infiltrate tissues, and expose immunostimulatory molecules in systemic lupus erythematosus. *J Immunol* **187**, 538-552 (2011).

80. Mahajan, A., Herrmann, M. & Munoz, L.E. Clearance Deficiency and Cell Death Pathways: A Model for the Pathogenesis of SLE. *Front Immunol* **7**, 35 (2016).

81. Khandpur, R.*, et al.* NETs are a source of citrullinated autoantigens and stimulate inflammatory responses in rheumatoid arthritis. *Sci Transl Med* **5**, 178ra140 (2013).

82. Dwivedi, N. & Radic, M. Citrullination of autoantigens implicates NETosis in the induction of autoimmunity. *Ann Rheum Dis* **73**, 483-491 (2014).

83. Schorn, C.*, et al.* Bonding the foe - NETting neutrophils immobilize the pro-inflammatory monosodium urate crystals. *Front Immunol* **3**, 376 (2012).

84. Schorn, C.*, et al.* Monosodium urate crystals induce extracellular DNA traps in neutrophils, eosinophils, and basophils but not in mononuclear cells. *Front Immunol* **3**, 277 (2012).

85. Schett, G., Schauer, C., Hoffmann, M. & Herrmann, M. Why does the gout attack stop? A roadmap for the immune pathogenesis of gout. *RMD Open* **1**, e000046 (2015).

86. Hultqvist, M.*, et al.* Enhanced autoimmunity, arthritis, and encephalomyelitis in mice with a reduced oxidative burst due to a mutation in the Ncf1 gene. *Proc Natl Acad Sci U S A* **101**, 12646-12651 (2004).

87. Olofsson, P.*, et al.* Positional identification of Ncf1 as a gene that regulates arthritis severity in rats. *Nat Genet* **33**, 25-32 (2003).

88. Farrera, C. & Fadeel, B. Macrophage clearance of neutrophil extracellular traps is a silent process. *J Immunol* **191**, 2647-2656 (2013).

89. Galluzzi, L., Kepp, O., Krautwald, S., Kroemer, G. & Linkermann, A. Molecular mechanisms of regulated necrosis. *Semin Cell Dev Biol* **35**, 24-32 (2014).

90. van Loo, G.*, et al.* The serine protease Omi/HtrA2 is released from mitochondria during apoptosis. Omi interacts with caspase-inhibitor XIAP and induces enhanced caspase activity. *Cell Death Differ* **9**, 20-26 (2002).

91. Van Loo, G.*, et al.* A matrix-assisted laser desorption ionization post-source decay (MALDI-PSD) analysis of proteins released from isolated liver mitochondria treated with recombinant truncated Bid. *Cell Death Differ* **9**, 301-308 (2002).

92. Vanden Berghe, T., Kaiser, W.J., Bertrand, M.J. & Vandenabeele, P. Molecular crosstalk between apoptosis, necroptosis, and survival signaling. *Mol Cell Oncol* **2**, e975093 (2015).

93. Linkermann, A., Stockwell, B.R., Krautwald, S. & Anders, H.J. Regulated cell death and inflammation: an auto-amplification loop causes organ failure. *Nat Rev Immunol* **14**, 759-767 (2014).

94. Holler, N.*, et al.* Fas triggers an alternative, caspase-8-independent cell death pathway using the kinase RIP as effector molecule. *Nat Immunol* **1**, 489-495 (2000).

95. Degterev, A.*, et al.* Chemical inhibitor of nonapoptotic cell death with therapeutic potential for ischemic brain injury. *Nat Chem Biol* **1**, 112-119 (2005).

96.   Linkermann, A. & Green, D.R. Necroptosis. *N Engl J Med* **370**, 455-465 (2014).

97.   Zhou, W. & Yuan, J. SnapShot: Necroptosis. *Cell* **158**, 464-464 e461 (2014).

98.   Su, L*., et al.* A plug release mechanism for membrane permeation by MLKL. *Structure* **22**, 1489-1500 (2014).

99.   Sun, L*., et al.* Mixed lineage kinase domain-like protein mediates necrosis signaling downstream of RIP3 kinase. *Cell* **148**, 213-227 (2012).

100.   Dixon, S.J*., et al.* Ferroptosis: an iron-dependent form of nonapoptotic cell death. *Cell* **149**, 1060-1072 (2012).

101.   Yang, W.S*., et al.* Regulation of ferroptotic cancer cell death by GPX4. *Cell* **156**, 317-331 (2014).

102.   Izzo, V., Bravo-San Pedro, J.M., Sica, V., Kroemer, G. & Galluzzi, L. Mitochondrial Permeability Transition: New Findings and Persisting Uncertainties. *Trends Cell Biol* (2016).

103.   Elrod, J.W. & Molkentin, J.D. Physiologic functions of cyclophilin D and the mitochondrial permeability transition pore. *Circ J* **77**, 1111-1122 (2013).

104.   Baines, C.P*., et al.* Loss of cyclophilin D reveals a critical role for mitochondrial permeability transition in cell death. *Nature* **434**, 658-662 (2005).

105.   Vanden Berghe, T., Linkermann, A., Jouan-Lanhouet, S., Walczak, H. & Vandenabeele, P. Regulated necrosis: the expanding network of non-apoptotic cell death pathways. *Nat Rev Mol Cell Biol* **15**, 135-147 (2014).

106.   Brennan, M.A. & Cookson, B.T. Salmonella induces macrophage death by caspase-1-dependent necrosis. *Mol Microbiol* **38**, 31-40 (2000).

107.   Case, C.L*., et al.* Caspase-11 stimulates rapid flagellin-independent pyroptosis in response to Legionella pneumophila. *Proc Natl Acad Sci U S A* **110**, 1851-1856 (2013).

108.   Lamkanfi, M. & Dixit, V.M. Mechanisms and functions of inflammasomes. *Cell* **157**, 1013-1022 (2014).

109.   Doitsh, G*., et al.* Cell death by pyroptosis drives CD4 T-cell depletion in HIV-1 infection. *Nature* **505**, 509-514 (2014).

110.   Andrabi, S.A., Dawson, T.M. & Dawson, V.L. Mitochondrial and nuclear cross talk in cell death: parthanatos. *Ann N Y Acad Sci* **1147**, 233-241 (2008).

111.   Curtin, N.J. & Szabo, C. Therapeutic applications of PARP inhibitors: anticancer therapy and beyond. *Mol Aspects Med* **34**, 1217-1256 (2013).

112. Arai, Y., *et al.* Serum neutrophil extracellular trap levels predict thrombotic microangiopathy after allogeneic stem cell transplantation. *Biol Blood Marrow Transplant* **19**, 1683-1689 (2013).

113. Mori, Y., *et al.* alpha-Enolase of Streptococcus pneumoniae induces formation of neutrophil extracellular traps. *J Biol Chem* **287**, 10472-10481 (2012).

114. Kessenbrock, K., *et al.* Netting neutrophils in autoimmune small-vessel vasculitis. *Nat Med* **15**, 623-625 (2009).

115. Nakazawa, D., *et al.* Enhanced formation and disordered regulation of NETs in myeloperoxidase-ANCA-associated microscopic polyangiitis. *J Am Soc Nephrol* **25**, 990-997 (2014).

116. Sayah, D.M., *et al.* Neutrophil extracellular traps are pathogenic in primary graft dysfunction after lung transplantation. *Am J Respir Crit Care Med* **191**, 455-463 (2015).

117. Li, P., *et al.* PAD4 is essential for antibacterial innate immunity mediated by neutrophil extracellular traps. *J Exp Med* **207**, 1853-1862 (2010).

118. Huang, H., *et al.* Damage-associated molecular pattern-activated neutrophil extracellular trap exacerbates sterile inflammatory liver injury. *Hepatology* **62**, 600-614 (2015).

119. Knight, J.S., *et al.* Peptidylarginine deiminase inhibition is immunomodulatory and vasculoprotective in murine lupus. *J Clin Invest* **123**, 2981-2993 (2013).

120. Knuckley, B., *et al.* Substrate specificity and kinetic studies of PADs 1, 3, and 4 identify potent and selective inhibitors of protein arginine deiminase 3. *Biochemistry* **49**, 4852-4863 (2010).

121. Causey, C.P., *et al.* The development of N-alpha-(2-carboxyl)benzoyl-N(5)-(2-fluoro-1-iminoethyl)-l-ornithine amide (o-F-amidine) and N-alpha-(2-carboxyl)benzoyl-N(5)-(2-chloro-1-iminoethyl)-l-ornithine amide (o-Cl-amidine) as second generation protein arginine deiminase (PAD) inhibitors. *J Med Chem* **54**, 6919-6935 (2011).

122. Narasaraju, T., *et al.* Excessive neutrophils and neutrophil extracellular traps contribute to acute lung injury of influenza pneumonitis. *Am J Pathol* **179**, 199-210 (2011).

123. Neeli, I. & Radic, M. Opposition between PKC isoforms regulates histone deimination and neutrophil extracellular chromatin release. *Front Immunol* **4**, 38 (2013).

124. Köcktritz-Blickwede, M.V., Chow, O., Ghochani, M. & Nizet, V. Visualization and Functional Evaluation of Phagocyte Extracellular Traps. in *Methods in Microbiology*, Vol. 37 (eds. Kabelitz, D. & Kaufmann, S.H.E.) I39-I60 (Elsevier Ltd., 2010).

125. Sayah, D.M.*, et al.* Neutrophil extracellular traps are pathogenic in primary graft dysfunction after lung transplantation. *American journal of respiratory and critical care medicine* **191**, 455-463 (2015).

126. Shi, J.*, et al.* Cleavage of GSDMD by inflammatory caspases determines pyroptotic cell death. *Nature* **526**, 660-665 (2015).

127. Zhao, W., Fogg, D.K. & Kaplan, M.J. A novel image-based quantitative method for the characterization of NETosis. *J Immunol Methods* **423**, 104-110 (2015).

128. Yipp, B.G.*, et al.* Infection-induced NETosis is a dynamic process involving neutrophil multitasking in vivo. *Nature medicine* **18**, 1386-1393 (2012).

129. Byrd, A.S., O'Brien, X.M., Johnson, C.M., Lavigne, L.M. & Reichner, J.S. An extracellular matrix-based mechanism of rapid neutrophil extracellular trap formation in response to Candida albicans. *J Immunol* **190**, 4136-4148 (2013).

130. Peschel, A. & Hartl, D. Anuclear neutrophils keep hunting. *Nature medicine* **18**, 1336-1338 (2012).

131. Yousefi, S., Mihalache, C., Kozlowski, E., Schmid, I. & Simon, H.U. Viable neutrophils release mitochondrial DNA to form neutrophil extracellular traps. *Cell death and differentiation* **16**, 1438-1444 (2009).

132. Parker, H., Dragunow, M., Hampton, M.B., Kettle, A.J. & Winterbourn, C.C. Requirements for NADPH oxidase and myeloperoxidase in neutrophil extracellular trap formation differ depending on the stimulus. *Journal of leukocyte biology* **92**, 841-849 (2012).

133. Mulay, S.R., Kumar, S.V., Lech, M., Desai, J. & Anders, H.J. How Kidney Cell Death Induces Renal Necroinflammation. *Semin Nephrol* **36**, 162-173 (2016).

134. Galluzzi, L.*, et al.* Molecular definitions of cell death subroutines: recommendations of the Nomenclature Committee on Cell Death 2012. *Cell Death Differ* **19**, 107-120 (2012).

135. Jorgensen, I. & Miao, E.A. Pyroptotic cell death defends against intracellular pathogens. *Immunol Rev* **265**, 130-142 (2015).

136. Syed, F., Mena-Gutierrez, A. & Ghaffar, U. A case of iced-tea nephropathy. *N Engl J Med* **372**, 1377-1378 (2015).

137. Karaolanis, G., Lionaki, S., Moris, D., Palla, V.V. & Vernadakis, S. Secondary hyperoxaluria: a risk factor for kidney stone formation and renal failure in native kidneys and renal grafts. *Transplant Rev (Orlando)* **28**, 182-187 (2014).

138. Janoudi, A., Shamoun, F.E., Kalavakunta, J.K. & Abela, G.S. Cholesterol crystal induced arterial inflammation and destabilization of atherosclerotic plaque. *Eur Heart J* (2015).

139. Huang, D., Zhou, H. & Gao, J. Nanoparticles modulate autophagic effect in a dispersity-dependent manner. *Sci Rep* **5**, 14361 (2015).

140. Shen, H., Kreisel, D. & Goldstein, D.R. Processes of sterile inflammation. *J Immunol* **191**, 2857-2863 (2013).

141. Chen, G.Y. & Nunez, G. Sterile inflammation: sensing and reacting to damage. *Nat Rev Immunol* **10**, 826-837 (2010).

142. Desai, J.*, et al.* PMA and crystal-induced neutrophil extracellular trap formation involves RIPK1-RIPK3-MLKL signaling. *Eur J Immunol* **46**, 223-229 (2016).

143. Desai, J.*, et al.* Neutrophil extracellular trap formation can involve RIPK1-RIPK3-MLKL signalling. *European journal of immunology* (2015).

144. Amini, P.*, et al.* NET formation can occur independently of RIPK3 and MLKL signaling. *European journal of immunology* (2015).

145. Mulay, S.R.*, et al.* Cytotoxicity of crystals involves RIPK3-MLKL-mediated necroptosis *Nat Commun* **in press**(2016).

146. Linkermann, A. & Green, D. Mechanisms of disease: Necroptosis. *N Engl J Med* **370**, in press (2014).

147. Linkermann, A.*, et al.* Synchronized renal tubular cell death involves ferroptosis. *Proc Natl Acad Sci U S A* **111**, 16836-16841 (2014).

148. Kearney, C.J., Cullen, S.P., Clancy, D. & Martin, S.J. RIPK1 can function as an inhibitor rather than an initiator of RIPK3-dependent necroptosis. *FEBS J* **281**, 4921-4934 (2014).

149. Ng, G.*, et al.* Receptor-independent, direct membrane binding leads to cell-surface lipid sorting and Syk kinase activation in dendritic cells. *Immunity* **29**, 807-818 (2008).

150. Orlowski, G.M.*, et al.* Correction: Multiple Cathepsins Promote Pro-IL-1beta Synthesis and NLRP3-Mediated IL-1beta Activation. *J Immunol* **196**, 503 (2016).

151. McComb, S.*, et al.* Cathepsins limit macrophage necroptosis through cleavage of Rip1 kinase. *J Immunol* **192**, 5671-5678 (2014).

152. Mulay, S.R.*, et al.* Cytotoxicity of crystals involves RIPK3-MLKL-mediated necroptosis. *Nat Commun* **7**, 10274 (2016).

153. Strowig, T., Henao-Mejia, J., Elinav, E. & Flavell, R. Inflammasomes in health and disease. *Nature* **481**, 278-286 (2012).

154. Duewell, P.*, et al.* NLRP3 inflammasomes are required for atherogenesis and activated by cholesterol crystals. *Nature* **464**, 1357-1361 (2010).

155. Mulay, S.R.*, et al.* Calcium oxalate crystals induce renal inflammation by NLRP3-mediated IL-1beta secretion. *J Clin Invest* **123**, 236-246 (2013).

156. Ea, H.K., So, A., Liote, F. & Busso, N. Basic calcium phosphate crystals induce NLRP3 inflammasome activation: the in vitro and in vivo face to face. *Proc Natl Acad Sci U S A* **108**, E1361; author reply E1362 (2011).

157. Diamantopoulos, A.P., Brodin, C., Hetland, H. & Haugeberg, G. Interleukin 1beta blockade improves signs and symptoms of chronic calcium pyrophosphate crystal arthritis resistant to treatment. *J Clin Rheumatol* **18**, 310-311 (2012).

158. Prencipe, G.*, et al.* Inflammasome activation by cystine crystals: implications for the pathogenesis of cystinosis. *J Am Soc Nephrol* **25**, 1163-1169 (2014).

159. Hornung, V.*, et al.* Silica crystals and aluminum salts activate the NALP3 inflammasome through phagosomal destabilization. *Nat Immunol* **9**, 847-856 (2008).

160. Dostert, C.*, et al.* Innate immune activation through Nalp3 inflammasome sensing of asbestos and silica. *Science* **320**, 674-677 (2008).

161. Pauwels, N.S.*, et al.* Role of IL-1alpha and the Nlrp3/caspase-1/IL-1beta axis in cigarette smoke-induced pulmonary inflammation and COPD. *Eur Respir J* **38**, 1019-1028 (2011).

162. Baron, L.*, et al.* The NLRP3 inflammasome is activated by nanoparticles through ATP, ADP and adenosine. *Cell Death Dis* **6**, e1629 (2015).

163. Winter, M.*, et al.* Activation of the inflammasome by amorphous silica and TiO2 nanoparticles in murine dendritic cells. *Nanotoxicology* **5**, 326-340 (2011).

164. Palomaki, J.*, et al.* Long, needle-like carbon nanotubes and asbestos activate the NLRP3 inflammasome through a similar mechanism. *ACS Nano* **5**, 6861-6870 (2011).

165. Lunov, O.*, et al.* Amino-functionalized polystyrene nanoparticles activate the NLRP3 inflammasome in human macrophages. *ACS Nano* **5**, 9648-9657 (2011).

166. Fink, S.L. & Cookson, B.T. Caspase-1-dependent pore formation during pyroptosis leads to osmotic lysis of infected host macrophages. *Cell Microbiol* **8**, 1812-1825 (2006).

167.   von Moltke, J., Ayres, J.S., Kofoed, E.M., Chavarria-Smith, J. & Vance, R.E. Recognition of bacteria by inflammasomes. *Annu Rev Immunol* **31**, 73-106 (2013).

168.   Rock, K.L., Latz, E., Ontiveros, F. & Kono, H. The Sterile Inflammatory Response. *Annual Review of Immunology, Vol 28* **28**, 321-342 (2010).

169.   Franklin, B.S., Mangan, M.S. & Latz, E. Crystal Formation in Inflammation. *Annu Rev Immunol* (2016).

170.   An, L.L., *et al.* Complement C5a potentiates uric acid crystal-induced IL-1beta production. *Eur J Immunol* **44**, 3669-3679 (2014).

171.   Samstad, E.O., *et al.* Cholesterol crystals induce complement-dependent inflammasome activation and cytokine release. *J Immunol* **192**, 2837-2845 (2014).

7. Abbrevations

A	
ACPAs	anticitrullinated peptide antibodies
ANAs	antibodies against histones
ANCAs	anti-neutrophil cytoplasmic antibodies
C	
CGD	chronic granulomatous disease
COPD	chronic obstructive pulmonary disease
CPP	calcium pyrophosphate dihydrate
CYPD	cyclophilin D
D	
DAMPs	danger associated molecular patterns
DC	dendritic cells
E	
ELISA	enzyme-linked immunosorbent assay
G	
GAS	group A *Streptococcus*
G-CSF	Granulocyte-colony stimulating factor
GPX4	glutathione peroxidase 4
H	
HIV-1	human immunodeficiency virus 1
I	
IF	immunofluorescence
IFN-α	interferon α
IL	interleukin

L	
LPS	lipopolysaccharide
M	
MCP-1	monocyte chemoattractant protein
MLKL	mixed lineage kinase domain-like
MOMP	mitochondrial outer membrane permeabilization
MPO	myeloperoxidase
MPT	Mitochondrial permeability transition
N	
NADPH	Nicotinamide adenine dinucleotide phosphate
NET	Neutrophil extracellular trap
NE	neutrophil elastase
P	
PAD4	peptidyl-arginine deiminase 4
PARP1	poly ADP-ribose plymerase 1
PMA	phorbol 12-myristate 13-acetate
PMN	polymorphonuclear leukocytes
PRR	pattern recognition receptors
PSGL1	P-selectin glycoprotein ligand 1
R	
RA	Rheumatoid arthritis
RCD	regulated cell death
RIPK	receptor-interacting protein kinase
RN	regulated necrosis
RNP	ribonucleoproteins

ROS	reactive oxygen species
S	
SEM	scanning electron microscopy
SF	synovial fluids
SLE	Systemic lupus erythematosus
SOCS	suppressors of cytokine signaling
STATs	signal transducers and activators of transcription
T	
TGF	transforming growth factor
TLR	toll-like receptor
TNF	Tumour necrosis factor

8. Appendix

Composition of buffers used

FACS buffer :

Sterile DPBS	500 ml
Na Azide	500 mg (0.1 %)
BSA	1 g (0.2 %)

10X HBSS (Hank's Balanced Saline Solution) with Ca, Mg:

For 1000 ml

KCl	4 g
KH_2PO_4	0.6 g
NaCl	80 g
$Na_2HPO_4.2H_2O$	0.621 g
$NaHCO_3$	3.5 g
$CaCl_2$	1.4 g (or $CaCl_2.2H_2O$ 1.854 g)
$MgCl_2.6H_2O$	1 g
$MgSO_4.7H_2O$	1 g
D-Glucose	10 g

Dissolve in 900 ml of distilled water and adjust to pH 7.4 with 1N HCl or 1N NaOH.
Make up the volume with distilled water to 1000 ml.

10X HBSS (Hank's Balanced Saline Solution) without Ca, Mg:

For 1000 ml

KCl	4 g
KH_2PO_4	0.6 g

NaCl   80 g

$Na_2HPO_4.2H_2O$ 0.621 g

Dissolve in 1000 ml and autoclave.

50 % Glycerol in 20 mM Tris-HCl (pH 7.5), 1 mM $MgCl_2$:

      a. 0.48 g of Tris-HCl in 100 ml of distilled water, adjust pH to 7.4 (= 40 mM)

      b. 50 ml of Glycerol 100 % + 50 ml of 40 mM Tris-HCl (20 mM)

      c. Add 100 ul of 1M $MgCl_2$ solution.

EDTA 2 mM:

EDTA 7.44 mg in 10 ml HBSS (without Ca, Mg)

To be preheated in 37 0C water bath before use.

Citrate buffer 10X:

      110 mM Sodiumcitrate in ddH2O

      with 2N NaOH to pH 6

PBS:

      2.74 M NaCl

      54 mM KCl

      30 mM KH2PO4

      130 mM Na2HPO4

      in ddH2O

Adjust pH to 7.5 with HCl

Gel Running Buffer (10x):

        Tris   30g

        Glycine   144g

        SDS   5g

Make up volume to 1000ml (pH 8.3)

Transfer Buffer (1x):

        Tris   1.5g

        Glycine   7.2g

Make up volume to 500ml

TBS (10x):

        Tris   24.23g

        NaCl   80.06g

        Conc. HCL   around 17.5ml

Make up volume to 1000ml (pH 7.6)

TBS-T (1x):

        TBS (1x)   1000ml

        Tween 20   1ml

Sample buffer:

        Milipore water   3,8 ml

        0,5 M Tris HCl, pH 6,8   1 ml

        Glycerol   0,8 ml

        10% SDS   1,6 ml

2- mercaptoehanol   0,4 ml

1% (w/v) bromophenol blue 0,4 ml

Total 8 ml

Separating Buffer (1x):

Tris (1.5mM)   18,2g

SDS   400mg

Make up volume to 100ml (pH 8.8)

Stacking Buffer (1x):

Tris (0.5mM)   6,05g

SDS   400mg

Make up volume to 100ml (pH 6.8)

Staining solution:

Methanol   500ml

Acetic acid   100ml

Water   400ml

Coomasie Brilliant blue R : 2.5 g (0.25%)

Destaining solution:

Methanol   150ml

Acetic acid   100ml

Water   750ml

9. Acknowledgement

I would like to acknowledge some important people, who have helped, cared, taught and inspired me to keep going on. My sincere gratitude to all of you with the deepest of my conscious being!

I would like to thank my PhD mentor **Prof. Hans-Joachim Anders**. He taught, encouraged, supported, guided with patience and inspired me. Thank you for accepting me as your student and instilling the confidence in me and assistance with the transition to a new professional perspective. I would also like to thank my immediate supervisor and dearest friend **Dr. Shrikant Ramesh Mulay**. Your expertise, advice, support and care have uplifted my spirits and have inspired me a lot. As a dear one, you are the one that has made everything possible so far in Munich. Thanks for being by my side, always. I would sincerely like to acknowledge and thank Dr.Andreas Linkermann for his support and enthusiastic zeal towards my scientific work. I also thank Volker Vielhauer, Dr. Bruno Luckow and Dr. Peter Nelson for constructive discussions and our collaborators Dr. Bastian Popper and Professor Helen Liapis for their valuable support for this thesis.

My sincere gratitude to my **lab mates** Santhosh, Julian, Sathish, Daigo, Mohsen, Maceij, Lukas R., Lukas K., Steffi, Simone, Marc, Jonny, Melissa, Nuru, Orestes, Dana, Tomo, Xie, Bea, Anais, Heny, Martrez, Jana, Dan, Kathy, Jenny, Yutian, Que yu, Shanqing & Ewa for the wonderful time and memories. It would be unfinished without Onkar 'bhai' and Supriya 'didi' who have helped me in every situation. Thank you for everything bhai and didi. I am also indebted to my violin teacher Anwar and other friends, Hari raj, Nilay, Rupa, Anar, Munjal, Krishna, Rupak, Jaini, Preethi didi, Sneha, Prajakta, Priyanka, Jaydeep, Itika, Dhawal, Urjita & others for the great time in Munich. My sincere thanks to Pavan for making it possible to dance on my PhD project. I also say thank you to my friends Shishir, Jui, Sneha, Astha, Gayatri ma'am, Aditi, Palak, Roby, Harsh, Devanshi, Bhoomi, Dhruvi and Aashini for their forever love and care.

There are no words to express my feeling, love and affectionate gratitude to **my family**, my beloved fathers: Bhagirath Desai, Rajiv Gandhi and Mayur Vashee ; my mothers: Milka Desai, Beena Gandhi and Ila Vashee and all my beloved grandparents for their love, care and unconditional sacrifices. My gratitude to my sister Bhuyasi and my brothers Saurabh and Anshumaan for their constant support. Lastly, it would have not been possible without one ever smiling man who has been there for me and continues to support and encourage me in my endeavours. Ashutosh, thanks a lot for giving me not only the wings but also the whole sky to wonder and a limitless horizon to dream for. **Thank you very much!**

It is my duty to express my tearful acknowledgement to the animals, which have been sacrificed for the betterment of human kind.

Date: …………….. Jyaysi Bhagirath Desai

Curriculum Vitae

Jyaysi Desai (MSc Neuroscience)

Doctoral Research Fellow Nephrologisches Zentrum,

Educational Qualification:

- **2013-till date : Doctoral Research Fellow, Ludwig Maximillian University**,AG Prof. Dr. HJ Anders, Nephrology centre, Munich, Germany

- **2010-2011:   M.Sc. Neuroscience** (Neuro-developmental Biology),   Institute of Psychiatry, King's College London (grade: Merit)

- **2007-2010:   B.Sc. Biochemistry** (vocational Biotechnology), St. Xavier's college, Ahmedabad, India (grade: First)

- **2005-2007   Higher Secondary School**, Gujarat higher secondary board, India (grade: First)

Research Experience:

- **Doctoral research:** *´Molecular mechanisms of crystal induced neutrophil cell death'* under guidance of Prof. Dr. HJ Anders at LMU klinikum Munich.

A combined biochemical and various imaging approach to dissect the exact molecular mechanism of a unique neutrophil cell death called NETosis (neutrophil extracellular traps) to define the precise role of neutrophils in immunity. Model system: Mouse and Human neutrophils.

- **Research assistant:** 'Tissue *specific chromatin adaptation upon the influence of environment'* at the faculty of medicine, LMU Munich.

A combined Biochemical and Genomic approach to develop cell type specific tools to study chromatin plasticity in order to study the changes in transcription process upon outer environmental stimuli. Model system: *Drosophila melanogaster*

- **Master's Project:** '*Transcriptional and epigenetic signatures defining neural stem cells and astrocyte potential'* under guidance of Dr. Angela Bithell at Centre for Cellular Basis of Behaviour (CCBB), King's College London.

Research publications:

- Mulay SR, Kumar VRS, Lech M, **Desai J**, Anders HJ. Semin Nephrol. 2016 May;36(3):162-73. How kidney cell death induces renal necroinflammation.

- Mulay SR, Romoli S, **Desai J**, Kumar VRS, Anders HJ, Thomasova D, Am J Pathol. 2016 Jun;186(6):1442-53. Murine double minute-2 inhibition ameliorates established crescentic glomerulonephritis.

- **Desai J**, Mulay SR, Nakazawa D, Anders HJ: Matters of life and death. Cell Mol Life Sci. 2016 Jun;73(11-12):2211-9. How neutrophils die or survive along NET release and is "NETosis" = necroptosis?

- Mulay SR, **Desai J**, Kumar SVR, Eberhard JN, Thomasova D, Romoli S, Grigorescu M, Kulkarni OP, Popper B, Vielhauer V, Zuchtriegel G, Reichel C, Bräsen JH, Romagnani P, Bilyy R, Munoz LE, Herrmann M, Liapis H, Krautwald S, Linkermann A, Anders HJ. Nat Commun. 2016 Jan 28;7:10274. Cytotoxicity of crystals involves RIPK3-MLKL-mediated necroptosis.

- Mulay SR, Eberhard JN, Pfann V, Marschner J, Romoli S, **Desai J**, Grigorescu M, Kumar SVR, Rathkolb B, Wolfgang H, Herrmann M, Bilyy R, Bäuerle T, Asplin J, Aronson PS, Knauf F, Anders HJ. Am J Physiol Renal Physiol. 2016 Jan 13:ajprenal.00488.2015. Oxalate-induced chronic kidney disease with its uremic and cardiovascular complications in C57BL/6 mice.

- **Desai J***, Kumar VRS*, Mulay SR, Konrad L, Romoli S, Schauer C, Herrmann M, Bilyy R, Müller S, Popper B, Thomasova D, Krautwald S, Linkermann A, Anders HJ. Eur J Immunol. 2016 Jan;46(1):223-9. Monosodium urate crystal-induced cell death and neutrophil extracellular trap formation involve RIPK1-RIPK3-MLKL signaling.

- Michelucci A, Bithell A, Burney MJ, Johnston CE, Wong KY, Teng SW, **Desai J**, Gumbleton N, Anderson G, Stanton LW, Williams BP, Buckley NJ. Mol Neurobiol. 2015 Jul 4. The Neurogenic Potential of Astrocytes Is Regulated by Inflammatory Signals.

- Lorenz G, **Desai J**, Anders HJ. Curr Opin Nephrol Hypertens. 2014 May;23(3):211-7. Lupus nephritis: update on mechanisms of systemic autoimmunity and kidney immunopathology.

Oral Presentations:

- 'DAMP-induced NET formation is mediated by RIPK3-MLKL pathway of necroptosis' at 7th DAMPs HMGB1 meeting at Bonn, Germany (September 2015)

- 'The role of H3.3 in cell type specific gene expression' at Elite Network Bavaria summer retreat (July 2012)

Poster Presentations:

- The RIPK3-MLKL pathway of necroptosis mediates formation of neutrophil extracellular traps' at Cell death meeting at Cold Spring Harbor Laboratory, Long Islands, New York, USA (September 2015)

- 'DAMP-induced NET formation is mediated by RIPK3-MLKL pathway of necroptosis' at 7th DAMPs HMGB1 meeting at Bonn, Germany (September 2015)

- 'Transcriptional and epigenetic signatures defining neural stem cells and astrocyte potential' at Institute of Psychiatry (IoP), King's College London (September 2011)

Co-curricular activities:

- Participated in the 'Dance you PhD' competition by 'science' journal to explain my PhD research project through performing art
  video:https://www.youtube.com/watch?v=SeX0YW1TxP4

- My scientific drawings are published in below research articles (2014):

  i)   Trends Mol Med. 2014 Mar;20(3):154-65. doi: 10.1016/j.molmed.2013.12.002. Epub 2014 Jan 14

  ii)   Semin Immunopathol. 2014 Jan 9. PMID:24402709

- Organized a Nobel Laureate talk of late Sir Herald Kroto at Gene centre Munich (July 2013)

- Network: Graduate program of Protein dynamics in Health and disease, Elite Network of Bavaria, Germany (2012-13)

Honors and Awards:

- Cold Spring Harbor Laboratory travel award for cell death meeting (2015)

- 'Dance your PhD 2015': Best dance video in Chemistry category and Audience choice award (2015).

- Biological research studentship and membership, Elite Network Bavaria (ENB), Germany (2012-13)

- Biological Sciences Undergraduate Research Award, St. Xavier's College(2009-10)

- M. Kamut and R. Froehlich fellowship for Biochemistry and Biotechnology (2009-10)

- Principal's prize for all round excellence, St. Xavier's College. (2010)

References:

Professor Hans-Joachim Anders   2. Dr. Angela Bithell

Nephrologisches Zentrum   Lecturer in Stem Cell Biology

Medizinische Klinik und Poliklinik IV   and Regenerative medicine

Ludwig Maximilians Universität München   School of Pharmacy

 Ziemssenstr. 1, D-80336 München   University of Reading

                                                                 Reading RG5 6AP UK

hans-joachim.anders@med.uni-muenchen.de   a.bithell@reading.ac.uk